SYNTHETIC APPROACHES TO CYCLOPROPYL PEPTIDOMIMETICS AS 20S PROTEASOME INHIBITORS

By

Avraz F. Anwar

A Thesis Submitted in Partial Fulfillment

of the Requirements for the Degree of

Master of Science in Chemistry

Middle Tennessee State University

May 2021

Thesis Committee:

Dr. Norma Dunlap

Dr. Kevin Bicker

Dr. Scott Handy

ACKNOWLEDGEMENTS

It is with my utmost honor and pleasure to begin my acknowledgements by thanking Dr. Norma Dunlap. I could never express my appreciation towards Dr. Dunlap enough as she has undoubtably been the most influential person I have been fortunate to meet. Dr. Dunlap has significantly changed my life in many ways by inspiring me to pursue a career in organic chemistry as well as mentoring me to expand my skills and knowledge as a chemist. I am and will always be thankful that Dr. Dunlap accepted me as her last graduate student.

I would like to thank all MTSU's chemistry and biology faculty for everything they have done to develop me as a student. I especially thank both Dr. Kevin Bicker and Dr. Scott Handy for not only their commitment to serve as committee members for my thesis, but also demonstrating admirable qualities as both educators and chemists. Similarly to Dr. Dunlap, Dr. Bicker and Dr. Handy have inspired me to pursue a career in academics.

Throughout my career as both an undergraduate and a graduate student I have been extremely fortunate to meet all the friends I have as they have been greatly supportive, encouraging, motivating, and simply wonderful people to have in my life. A very deserving and honorable mention goes to my best friend, Wesley Riley, as he has always been truly selfless to help and encourage me in every way.

I am pleased to conclude my acknowledgements by thank my family for all the love, support, and guidance they have given me throughout my entire life. I am sincerely thankful and blessed to have such amazing people in my life that have supported me to accomplish all my goals thus far!

ABSTRACT

Proteasome inhibitors are a relatively new class of chemotherapeutics with only three drugs currently on the market. Belactosin A, a natural product found in *Streptomyces sp.*, possesses anti-tumor effects due to its proteasome inhibition properties, however it is not used clinically due to its toxicity. This led to several syntheses of belactosin A analogs in hopes of similar efficacy and lower toxicity. Most reported syntheses require a substantial number of steps to synthesize the cyclopropyl backbone and the β-lactone warhead of belactosin A. An efficient stereoselective cyclopropanation of amino acid enones that undergo a Michael-induced ring closure is reported here with the use of cinchona alkaloids as a catalysts, and lactonization of L-threonine to afford the α-substituted β-lactone warhead. The proposed synthetic route of the L-threonine-derived β-lactone analog of belactosin A is significantly more efficient compared to alternative analogs reported in literature.

TABLE OF CONTENTS

LIST OF FIGURES

LIST OF TABLES

LIST OF SCHEMES

CHAPTER ONE: INTRODUCTION

There is a high interest in cancer therapy in the scientific community as cancer is the second most common cause of death worldwide. [1] Common cancer therapies include chemotherapy, radiation therapy, and surgery. Chemotherapy is one of the most common treatments in late stages of cancer. [2] Most chemotherapeutics cause DNA damage, which potentially leads to severe side effects. Examples include but are not limited to, cisplatin, 5-fluorouracil, and doxorubicin, which correspond to alkylating agents, antimetabolites, and anthracyclines, respectively. A relatively new class of chemotherapeutics is proteasome inhibitors. Since proteasome inhibitors have a unique mechanism of action that does not damage DNA and has anti-tumor properties, many labs around the world are interested in the synthesis of these new potential therapeutics. There are three proteasome inhibitors on the market and several more promising compounds in clinical trials. For example, marizomib is a β-lactone natural product in phase II clinical trials. Belactosin A is also a β-lactone natural product with a unique cyclopropyl peptide backbone that is a potent inhibitor of the 26 Svedberg unit (S) proteasome, but is not used clinically due to its skeletal muscle wasting side effects. [3] The primary goal of this project is to synthesize an analog of belactosin A that can inhibit the 26S proteasome with relatively low toxic effects. A secondary goal is to improve stereoselectivity in the synthetic route using cinchona catalysts.

A. 26S Proteasome: structure, function, and mechanism of action.

Structure:

The 26S eukaryotic proteasome is a 2.4 megadalton (MDa) multi-subunit complex that resides in the nucleus and cytoplasm. [4] The proteasome is comprised of

two 19S terminal regulatory particles (RP) and a 20S catalytic core particle (CP). The 19S RP are comprised of two major units, the base and lid. The base is comprised of four non-ATPase regulatory particles (Rpn), Rpn 1, 2, 10, and 13, and six ATPase regulatory particles (Rpt), Rpt 1-6. The lid is comprised of nine Rpn 3, 5-9, 11, 12, 14, and 15. The 20S CP is comprised of four stacked heptameric rings, two outer α_{1-7} and two inner β_{1-7} subunits, forming a barrel-shaped structure (**Figure 1**). In each β_{1-7} ring there are three active sites, β_1, β_2, and β_5, which correspond to caspase-like (C-L), trypsin-like (T-L), and chymotrypsin-like (CT-L) activities, respectively. The C-L region cleaves acidic residues, T-L cleaves basic residues, and CT-L cleaves hydrophobic residues, and each site contains a catalytically active *N*-terminal threonine (NTT). [5]

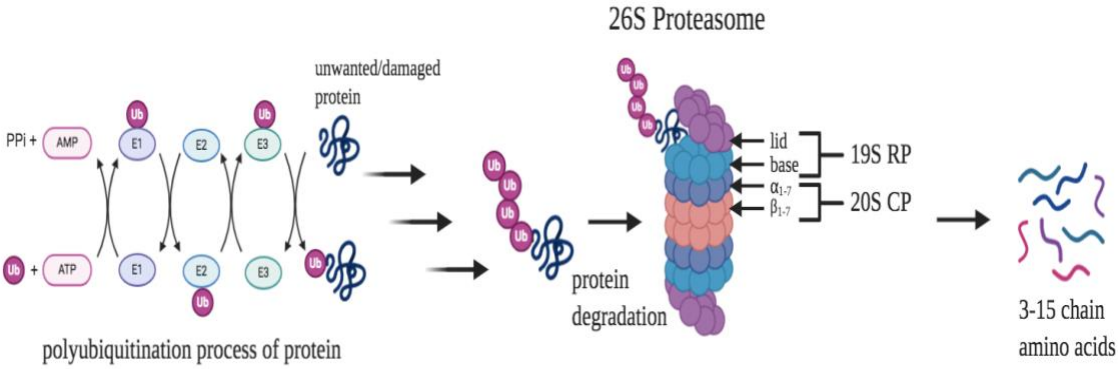

Figure 1: Process of the ubiquitin-protease pathway: the unwanted or damaged protein is polyubiquitinated, which is then degraded into small amino acid chains by the 26S proteasome.

Function/Mechanism of Action:

The proteasome is responsible for the hydrolysis/degradation of proteins that are damaged or not needed *via* the ubiquitin-protease pathway (UPP), which is an adenosine triphosphate (ATP) dependent pathway. As seen in **Figure 1**, the UPP starts with ATP being used, which is converted to adenosine monophosphate (AMP) and pyrophosphate (PPi), to create a thioester bond between ubiquitin (Ub) and the ubiquitin activating enzyme (E1). The E1 from the Ub-E1 complex is replaced by a Ub-conjugating enzyme (E2) *via* a transacylation reaction. Ub-ligase (E3) then utilizes the Ub-E2 complex to create an amide isopeptide bond between Ub and protein (**Figure 1**). [6]

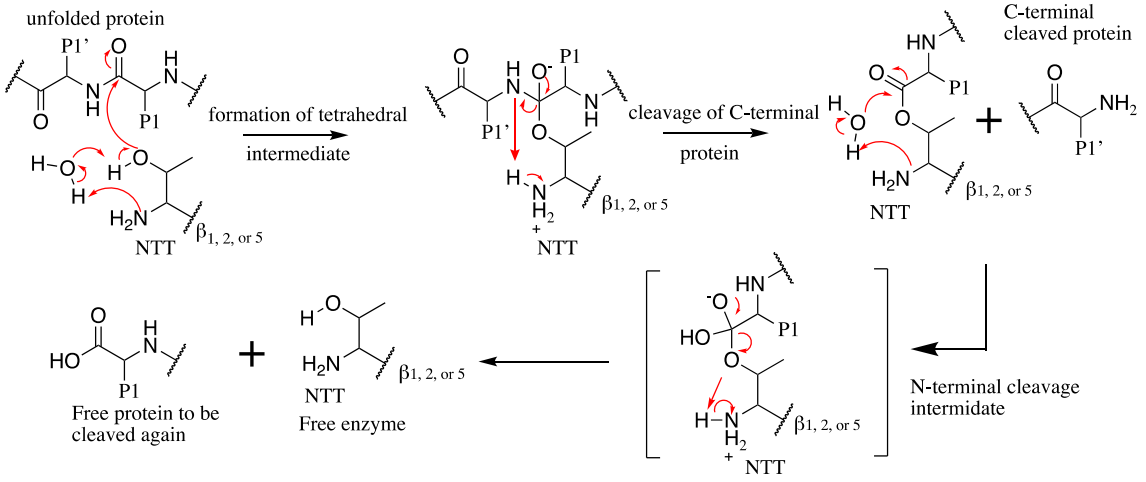

Figure 2: General mechanism of protein hydrolysis.

This process is repeated several times until the protein is polyubiquitinated. Once the polyubiquitinated protein interacts with the 19S RP it becomes de-ubiquitinated and unfolded. When the unfolded protein enters the 20S CP through 19S RP it becomes

hydrolyzed by the $\beta_{1, 2, \text{ or } 5}$ active sites. Hydrolysis happens when a water molecule acts as a base to deprotonate the NTT, making it a strong nucleophile. A covalent bond is formed between the unfolded protein's carbonyl group and the ionized hydroxyl group of the NTT *via* a nucleophilic attack, which forms an oxazolidine intermediate (**Figure 2**). [7] The amide bond from the intermediate is cleaved when the scissile bond, the bond that the proteasome cleaves, shifts to the ester, which creates a new *N*-terminal the on C-terminal protein and a NTT-*N*-terminal protein ester complex. After this process has taken place multiple times, the products are multiple 3-15 chain amino acids and Ub.

B. Proteasome inhibition: purpose, examples, and mechanism of action.

Purpose:

In the past two decades, inhibition of the 26S proteasome has been of high interest in the scientific community. The reason is that the inhibition of the 26S proteasome has proven to show anti-tumor effects as cancer/malignant cells express far more proteasomes than normal healthy cells. [8][9] Normal cells undergo cell cycle arrest, while cancerous cells undergo apoptosis when proteasome inhibitors are present. [10] Unlike most chemotherapeutics, the inhibition of the 26S proteasome does not inadvertently damage DNA, *ergo* it does not induce the same side effects and is generally very specific. [11] Proteasome inhibitors have been shown to treat multiple myeloma (MM), and clinical trials show promising results for certain types of leukemia, lymphoma, and solid tumors. [12] Most proteasome inhibitors target the 20S CP active sites while having a variety of active site specificity. Recent research has reported that there is less resistance towards 20S CP inhibitors and allow for lower dosages of 20S CP inhibitors when used in conjunction with 19S RP inhibitors. [13]

Examples of inhibitors:

There are currently three FDA approved proteasome inhibitors clinically used, bortezomib, carfilzomib, and ixazomib, approved in 2003, 2012, and 2015, respectively (**Figure 3**). Some notable proteasome inhibitors in Phase II clinical trials are marizomib, oprozomib, and delanzomib, as well as the first synthetic proteasome inhibitor, MG-132 (**Figure 3**).

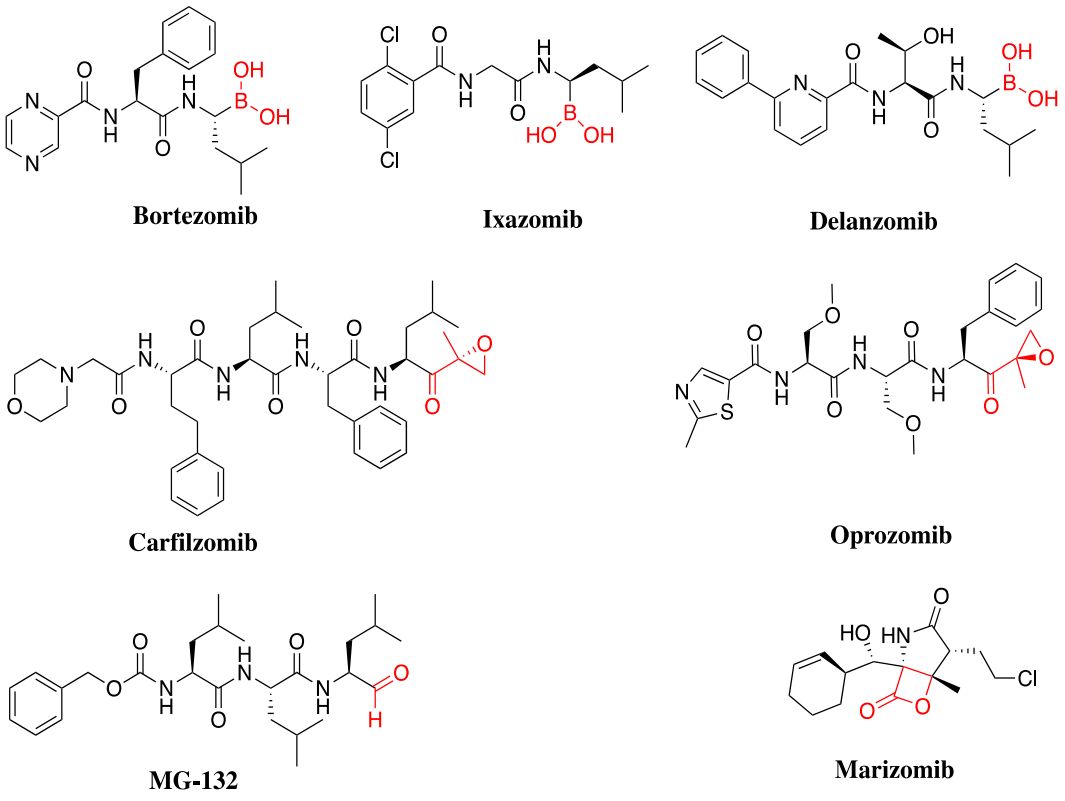

Figure 3: Structures of proteasome inhibitors with highlighted warheads.

Proteasome inhibitors have a variety of electrophilic functional groups that can covalently bond to the nucleophilic NTT. These functional groups are referred to as warheads. The most common warheads are highlighted in red in **Figure 3**, boronates (top row), epoxyketones (middle row), aldehydes (bottom left), and β-lactones (bottom right). β-lactams, nitriles, and α-ketoaldehydes are also electrophilic functional groups that possess potential inhibition activity.

There are two methods of inhibition, reversible and irreversible (**Figure 4**).

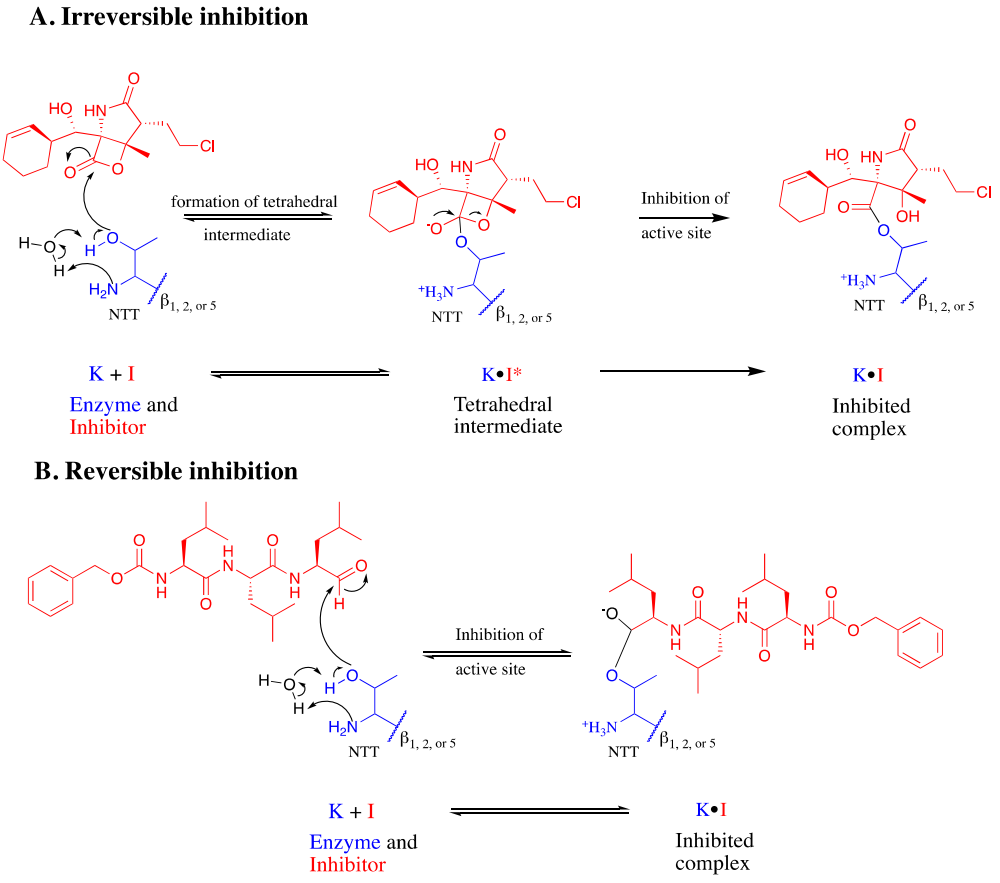

Figure 4: Proteasome inhibition: A) irreversible inhibition *via* marizomib. B) reversible inhibition *via* MG-132.

Both boronates and aldehydes inhibit the proteasome reversibly, while epoxyketones and β-lactones inhibit the proteasome irreversibly. A reversible inhibitor binds to the enzyme and can be dissociated back into its original form, while an irreversible inhibitor creates a tetrahedral intermediate, followed by a covalent bond. [10]

Boronates (specifically bortezomib) are considered the first generation of proteasome inhibitors. There are currently two boronate proteasome inhibitors on the market, and one that is in Phase II clinical trials, bortezomib, ixazomib, and delanzomib, respectively. Boronates are in a specific category of reversible inhibitors called slow tight-binding inhibitors, which have a very slow dissociation rate such that they are nearly irreversible. Boronates are specifically selective for serine/threonine proteases and are resistant to metabolic oxidation. [10] Boronates tend to target the CT-L active site in the proteasome and create a slowly reversible, covalently bonded tetrahedral intermediate at a low nanomolar (nM) concentration (**Table 1**).

Table 1: The half maximal inhibitory concentration (IC_{50}) and administration route of proteasome inhibitors *in vitro* peptidase activity. [15]

	CT-L IC_{50} (nM)	C-L IC_{50} (nM)	T-L IC_{50} (nM)	Administration
Bortezomib	7.9	53	59	Intravenous
Ixazomib	3.4	31	3500	Oral
Carfilzomib	6	2400	3600	Intravenous
Marizomib	3.5	430	28	Intravenous
MG-132	68	1400	4500	N/A

Currently, bortezomib is used to treat MM and is administered intravenously, but delanzomib and ixazomib have been shown to treat other malignant cancers *via* oral administration. [14] Overall, boronates are currently the most successful family of proteasome inhibitors.

Epoxyketones (specifically carfilzomib) are considered the second generation of proteasome inhibitors. Carfilzomib and oprozomib are both tripeptide epoxyketone proteasome inhibitors. Both bind irreversibly, as oprozomib is an orally administered analog of carfilzomib. The idea of epoxyketones, as proteasome inhibitors, originated from epoxomicin (**Figure 5)**, a natural product proteasome inhibitor. Epoxomicin was discovered and isolated at Bristol-Myers Squibb when scientists noticed *in vivo* anti-tumor activity from an unidentified *Actinomycetes* strain. [16] Epoxyketones are very selective towards the CT-L active site relative to other proteasome inhibitors (**Table 1**). Epoxyketones create a six membered morpholine adduct that targets both the amine and the hydroxyl group of NTTs.

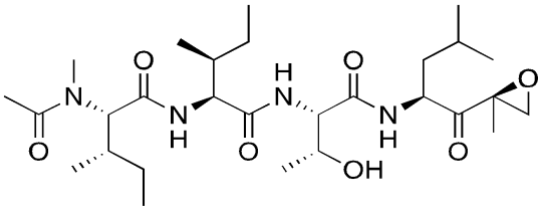

Figure 5: Structure of epoxomicin.

Synthetic aldehydes (specifically MG-132) are the first known proteasome inhibitors. [14] Although there are no aldehyde proteasome inhibitors in the market, they are still widely used for *in vitro* and *in vivo* biochemical research, because they can easily enter cells and the effects may be reversed. Aldehydes slowly bind to NTTs, which forms a hemiacetal (**Figure 4B**). The main issues with aldehydes are that they easily oxidize and they inhibit serine and cysteine proteases, which cause off target effects.

β-Lactones are also a promising warhead for proteasome inhibition. β-Lactones form an irreversible ester adduct with NTTs (**Figure 4A**), but are slowly hydrolyzed by water. β-Lactones are of high interest because they are more selective and potent than aldehydes, as they do not inhibit most serine or cysteine proteases. [14] Another reason why β-lactones are of interest is because changes in the structure can lead to drastic change in efficacy, and they occur in some biologically active natural products. For example, in omuralide (**Figure 6**), a natural compound isolated from *Streptomyces*, changing the methyl group on the lactam to longer aliphatic chains enhanced its inhibitory potency 2 to 3-fold. [14]

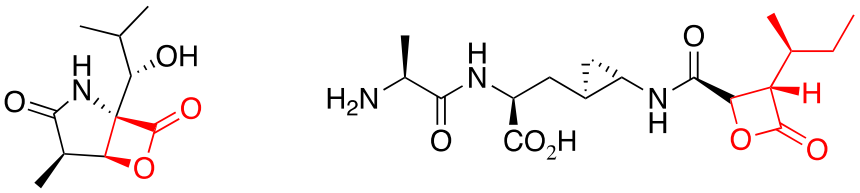

Omuralide **Belactosin A**

Figure 6: Structures of natural product proteasome inhibitors, omuralide and belactosin A, with a β-lactone warhead highlighted in red.

Similarly, stereochemical changes in belactosin A (**Figure 6**), a natural product isolated from *Streptomyces sp.*, led to enhanced proteasome inhibitory properties. [17][18]

There are several ways of synthesizing β-lactones, with the two most common methods being either a 2+2 cycloaddition or cyclization of an activated β-hydroxy-acid. A synthetic route used in Daniel Romo's lab reacts aldehydes and thiopyridyl ketene acetals *via* a $ZnCl_2$-mediated tandem Mukaiyama aldol lactonization (TMAL). [19] This method is referred to as a 2+2 cycloaddition, and yields diastereoselective products of *cis*-1,2-disubstituted β-lactones. Armin De Meijere's lab synthesizes β-lactones by reacting thioacids with a hydroxyl group *via* an intramolecular cyclization of an activated β-hydroxy-acid (*vida supra*). [20] A reported method by the John Vederas lab seems to be the most efficient synthetic route (**Figure 7**). [21]

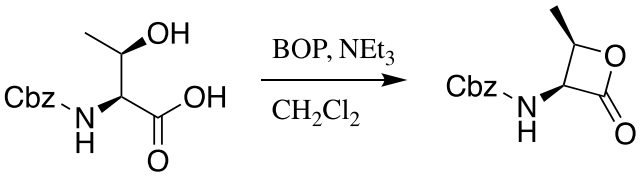

Figure 7: Synthesis of β−lactone *via* Vederas' method.

This method uses a strong coupling reagent (BOP) to cyclize the hydroxyl and the carboxylic acid of threonine. The main advantages of this method are stereoselective formation of the lactone, simple reaction conditions, and commercially available starting materials.

The methyl substituent on the lactone can increase the half-life of the lactone by up to 5-fold or greater as compared to the unsubstituted β-lactone. [22] The cyclization process does not interfere with the stereochemistry, so the stereochemistry of the lactone can be predicted by starting with a specific stereoisomer of threonine. Overall, this synthetic route is efficient in every aspect, as stereoselective synthesize a lactone can be obtained within roughly three hours.

Marizomib (originally known as Salinosporamide A) is a naturally occurring bicyclic γ-lactam-β-lactone isolated from the marine actinomycete *Salinispora tropica* and is currently in clinical trials for the treatment of multiple myeloma and other cancers. [14] [15] Marizomib inhibits all three proteasome active sites and is slowly excreted from cells due to irreversible binding. Pharmacodynamical assays indicate that marizomib is a potent proteasome inhibitor (**Table 1**), while pharmacokinetic assays indicate a short half-life. [15] Marizomib is 35 times more potent than omuralide, and is at least 1000-times less potent against other proteases like chymotrypsin, trypsin, cathepsin A and cathepsin B. The NTT reacts with the β-lactone to form an ester adduct, but the chloride acts as a leaving group and forms a cyclic ether product. [14] Overall, marizomib has shown very promising results, and the community should expect β-lactones to be the new generation of proteasome inhibitors.

Mechanism of Action:

There are several proposed mechanisms of action of how proteasome inhibitors treat malignant/cancerous cells. Examples include but are not limited to the downregulation of cell growth factors, upregulation of apoptotic proteins, and inhibition of angiogenesis (**Figure 8**). Although these mechanisms are not novel to treat cancerous

cells, it is relatively novel that the inhibition of the 26S proteasome cause these effects. It is also important to note that these mechanisms do not cause damage to DNA as most chemotherapeutics do.

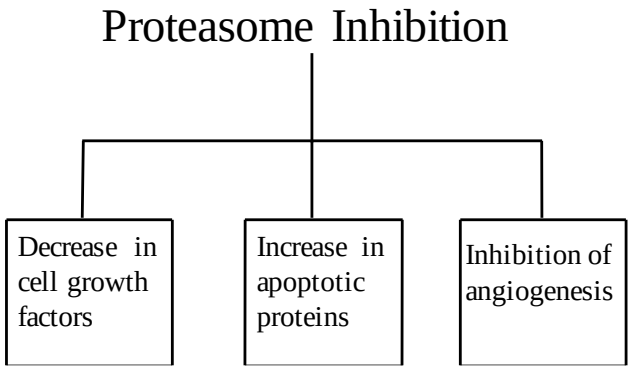

Figure 8: Effects of proteasome inhibition.

It is important for cells to maintain the proper amount of growth factors or else the cells can proliferate at an uncontrollable rate, or not proliferate at all. Molecules such as p27, a tumor suppressor, cause cell cycle regulation by inhibiting cyclin dependent kinases (CDKs). CDKs, when activated by cyclins, cause cells to overcome the cell cycle check points, which leads to cell proliferation. The ubiquitin ligase S-phase kinase protein 2 (Skp-2) targets p27 for proteasomal degradation. It has been reported that high expression of the ubiquitin ligase S-phase kinase protein 2 (Skp-2) has been seen in several types of cancer. [23] Therefore, it is vital that cancerous cells are treated with proteasome inhibitors so that p27 is not degraded so that the cells can maintain proper growth factors.

Malignant cells are able to proliferate at an uncontrollable rate by preventing apoptosis. Apoptosis can be prevented by an increased rate in proteasomal degradation of tumor suppressant p53. P53 causes an upregulation of several pro-apoptotic proteins such as, NOXA, PUMA, and Bax. Increased levels of p53 also cause a downregulation of anti-apoptotic proteins such as the Bcl-2 protein family. [11][12] Proteasome inhibitors have been proven to induce p53-dependent apoptosis in malignancies such as renal cell carcinoma cell, colon cancer, melanoma, and multiple myeloma. [12]

Studies have also shown that bortezomib has anti-angiogenesis effects by decreasing the secretion of vascular endothelial growth factor. [24] When cancerous cells are not able to undergo angiogenesis it results in cell death due to the lack of nutrients, oxygen, and waste disposal. This mechanism is especially effective since most tumors are dependent on undergoing angiogenesis.

C. Cyclopropyl Peptidomimetics: examples, stereoselectivity of cyclopropanation, and approach to belactosin A analogs.

Examples:

The discovery and development of peptidomimetics has significantly advanced modern medicine. Peptidomimetics, compared to native peptides, have shown better efficacy, bioavailability, and stability. [25] In particular, cyclopropyl peptidomimetics have been reported to have anti-tumor, antiviral, and antidepressant activity. [26] The cyclopropane moiety increases the stability and decreases flexibility without having the reactivity of a π bond. [27] Examples of cyclopropyl peptidomimetics include Steven Martin's HIV-1 protease inhibitor, Peter Wipf's cyclopropyl tripeptide isosteres, and Norma Dunlap's three-step synthesis of cyclopropyl peptidomimetics (**Figure 9**). [26-29]

Belactosin A, although it is not a peptidomimetic, is a natural product tripeptide that has a cyclopropyl ring in its peptide backbone. Belactosin A also has anti-tumor activity due to its proteasome inhibition abilities, but is not used clinically.

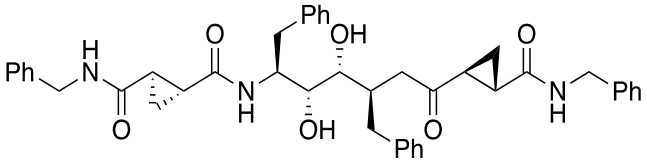

Martin's HIV protease inhibitor

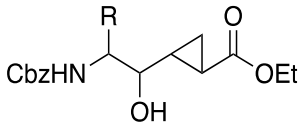

Dunlap's cyclopropyl peptidomimetics

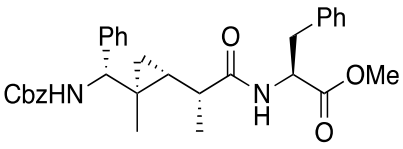

Wipf's cyclopropyl tripeptide isostere

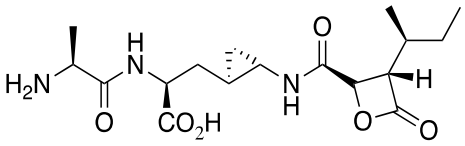

Belactosin A

Figure 9: Examples of compounds with the cyclopropane moiety.

Martin's lab was one of the first to utilize the cyclopropane moiety in peptide backbones. Cyclopropanation was done through heating a *syn* allylic diazoester carbenoid in the presence of a chiral rhodium catalyst, which affords high stereoselectivity for one stereoisomer. This led to the novel HIV-1 protease inhibitor that is effective at subnanomolar concentrations. [28] The purpose of including the cyclopropane moiety was to reduce the flexibility of linear pseudopeptides and to help enforce the biologically active conformation of ligands.

Wipf's lab introduced a novel synthetic route of cyclopropyl tripeptide isosteres. The synthesis is a one-pot, three-component aldimine addition. This method is a cascade reaction of an alkyne, zirconocene, and an aldimine, which is followed by a Simmons-Smith cyclopropanation. The synthetic route is not stereospecific as it affords an inseparable 1:1 mixture of stereoisomers. The purpose of synthesizing the cyclopropyl ring was to promote β-turn effects in the peptidomimetic. [29]

Dunlap's lab developed a very efficient three-step synthesis of cyclopropyl peptidomimetics from Cbz-protected amino acid Weinreb amides. Cbz-protected amino acid Weinreb amides are treated with vinylmagnesium bromide to afford amino acid enones. The enones are then treated with ethyl-(dimethylsulfuranylidene)-acetate (EDSA) or bromonitromethane, which will then undergo a Michael-induced ring closure (MIRC) to afford the cyclopropyl keto-esters or nitrocyclopropyl compounds, respectively. These compounds are then reduced to afford the cyclopropyl peptidomimetic backbone (**Figure 10**). [26][30] This synthetic route is not stereoselective, as most products yield a 1:1 mixture of *syn* and *anti* diastereomers. These cyclopropyl peptidomimetics were synthesized as precursors to belactosin A analogs.

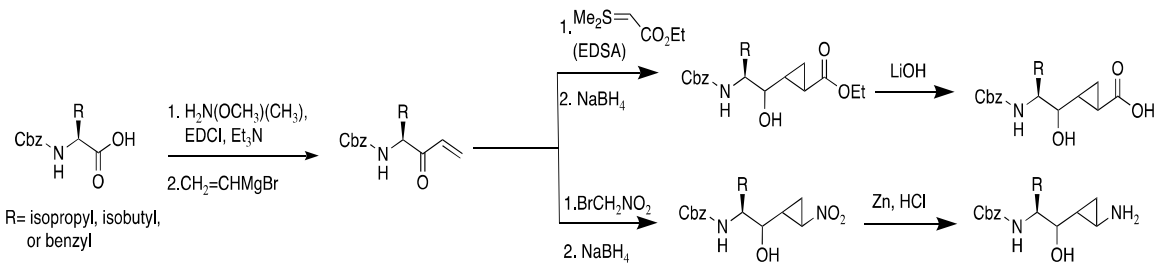

Figure 10: Dunlap's synthetic route to cyclopropyl peptidomimetics as belactosin A precursors.

Stereoselectivity of Cyclopropanation:

The reported syntheses can efficiently afford cyclopropyl peptidomimetics, but each lack complete stereoselective control of the cyclopropane ring. There are many reports in literature of stereoselective cyclopropanations that undergo a MIRC mechanism. Examples include but are not limited to, Varinder Aggarwal's camphor catalysts, Steven Ley's tetrazole catalyst, and Matthew Gaunt's cinchona catalysts (**Figure 11**). [31-33] Each catalyst affords stereoselective cyclopropanations of enones.

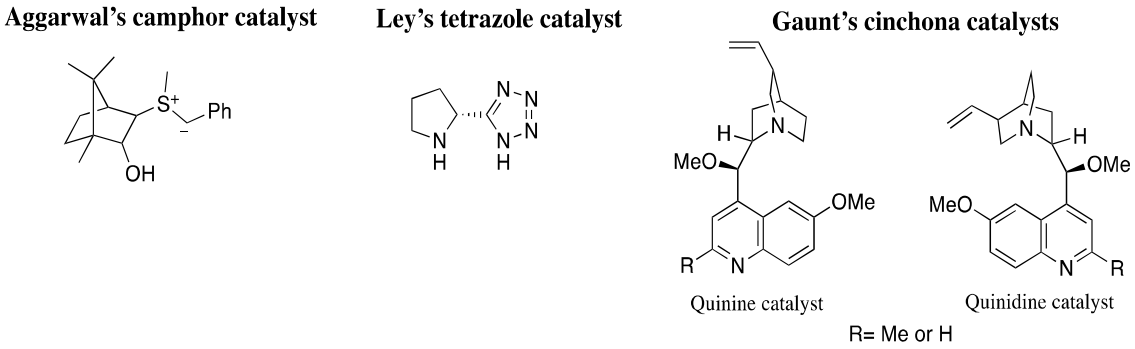

Figure 11: Catalysts used for stereoselective cyclopropanations of enones.

Aggarwal's group has developed camphor-derived sulfur ylide catalysts from camphor sulfonyl chlorides in four steps. These catalysts afford high enantioselectivity, >90% enantiomeric excess (*e.e.*) and diastereomeric ratio (*d.r.*), for both enones and α,β unsaturated esters. [31] Aggarwal's catalysts are highly selective for only one stereoisomer, which is a limitation if the other stereoisomer is desired.

Ley's group has developed a tetrazole catalysts derived from proline in four steps. This catalyst affords high enantioselectivity for nitro-cyclopropanations from enones. [32]

Similarly to Aggarwal's camphor catalysts, Ley's tetrazole catalyst affords high selectivity for only one enantiomer.

Gaunt's group utilizes the cinchona alkaloids analogs, quinine and quinidine methyl ether, to afford highly stereoselective cyclopropyl compounds. The catalysts form a transient asymmetric ammonium ylide with the chiral amine and the α-bromo acetates, which will then undergo a MIRC to form the cyclopropane with either α, β unsaturated esters or enones. [33] Gaunt's cinchona catalysts are especially effective as either enantiomer can be synthesized.

Approach to Belactosin A Analogs:

Asai's lab discovered and isolated the natural product, belactosin A, from *Streptomyces sp.* with intentions of testing it for antitumor and antibiotic activity. There was no antimicrobial activity, however when tested against HeLa S3 cells antitumor activity was observed with a IC_{50} value of 51 μm. [17] It was later discovered that the antitumor activity was a result of irreversible binding of the β-lactone and the NTT at the CT-L β-subunit. [34] Labs have developed total synthesis, core structures and derivatives of belactosin A since the discovery. [18][35-37]

De Meijere and Romo's lab developed two novel synthetic routes for belactosin A and C, respectively. De Meijere's synthetic route comprises of an acylation/β-lactonization reaction with the ability to modify any substituent, which allows flexibility for derivatives (**Figure 12 A**). [35] On the other hand, Romo's synthetic route comprises of the previously mention TMAL method. As seen in **Figure 12 B,** Romo uses two approaches: one involves a distal double diastereoselective distal TMAL reaction (in red)

with a dipeptide glyoxamide, while the other approach involves amide coupling of a dipeptide with a β-lactone carboxylic acid (in blue). [36]

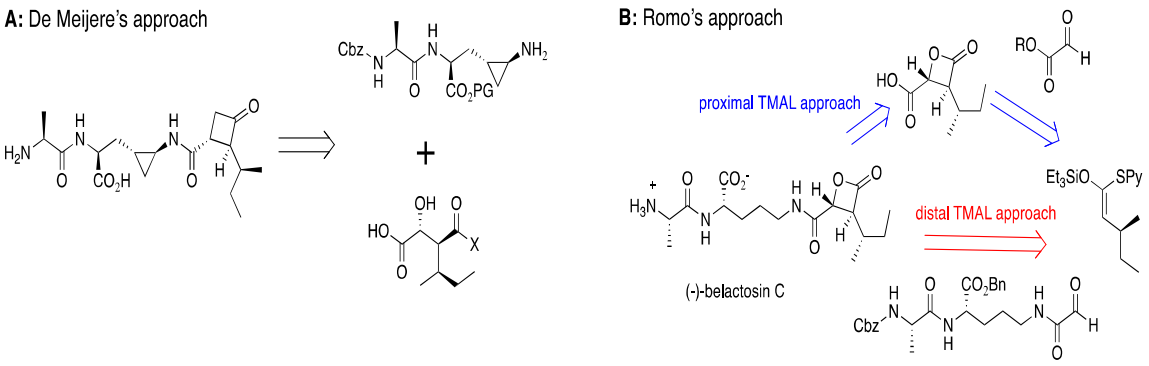

Figure 12: A) De Meijere's synthetic method for belactosin A derivatives. B) Romo's synthetic route for (-)-belactosin C (distal TMAL approach in red, proximal TMAL approach in blue).

Charette's lab developed an efficient diastereoselective synthetic route to the cyclopropyl core of belactosin A from an α-nitrocyclopropyl lactone unit. The synthesis utilizes rhodium catalysts to afford an α-nitrocyclopropyl lactone unit from an α-diazo unsaturated ester, which undergoes an intramolecular cyclopropanation. [37]

Shuto's lab has progressed the most in developing belactosin A derivatives. The initial goal was to discover which configuration provided the highest efficacy. The results have shown that compared to the natural configuration, trans/L-*anti* (trans refers to the configuration of the cyclopropyl ring, L refers to the configuration of the carboxylic acid, and *anti* refers to the configuration of the cyclopropyl ring to the carboxylic acid), the trans/L-*syn* isomer shows the highest potency when tested against the CT-L 20S human proteasome. [18] When replacing the carboxylic acid with a vinyl group, adding a

carboxybenzyl group (Cbz) to the free amine, and a *cis* cyclopropyl ring the potency is increased 20-fold relative to the natural product (**Table 2**). [18]

Table 2: IC_{50} of belactosin A and derivatives for peptidase activity of the 20S human proteasome.

Inhibitor	IC_{50} (nM)
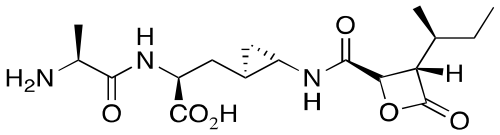 Belactosin A	304
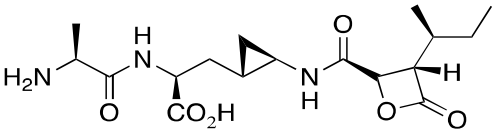 Belactosin A syn isomer	145
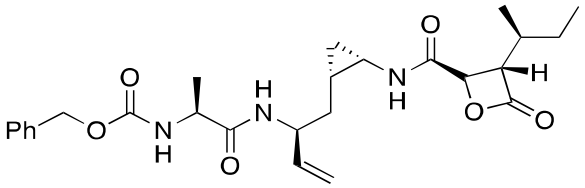 Belactosin A cis derivative	15

A few labs are attempting to synthesize derivatives of belactosin A, as it is a promising lead compound that possesses anti-tumor activity. Although none have reached clinical trials to date, the scientific community should expect these compounds to be a new generation of anti-tumor proteasome inhibitors.

D. Goals of Project: stereoselective cyclopropanation and β–lactone coupling to cyclopropyl peptidomimetics.

The overall goal of this project is to synthesize analogs of belactosin A (**Scheme 1**). This goal has two objectives; one objective is to utilize quinine and quinidine benzyl ethers to improve stereoselectivity in synthesis of the cyclopropane moiety, while the other objective is to synthesize and couple a L-threonine derived β-lactone to the cyclopropyl peptidomimetic. After the belactosin A analogs are synthesized, they will be assayed for biological activity.

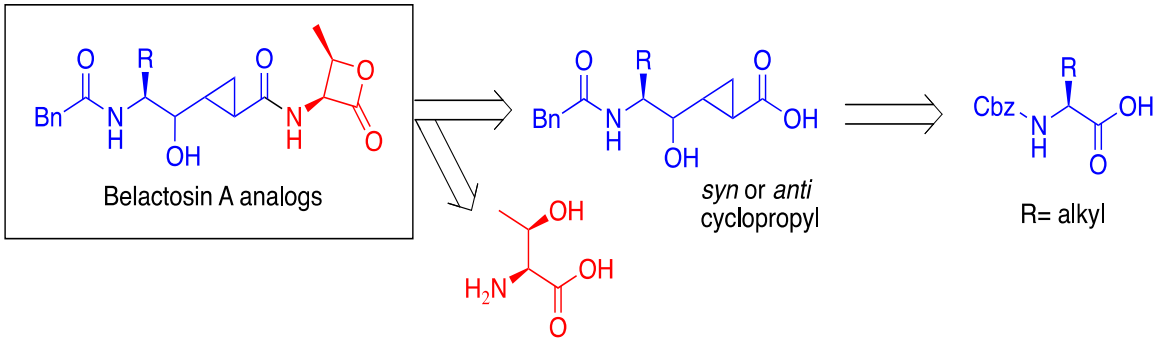

Scheme 1: Proposed retrosynthesis of belactosin A analogs.

Stereoselective Cyclopropanation:

As previously mentioned, Dunlap's group has developed an efficient four-step synthesis of cyclopropyl peptidomimetics, but the syntheses lack stereoselective control of the cyclopropyl moiety. Similarly to Gaunt's research in stereoselective cyclopropanations of enones, Dunlap's group has investigated stereoselective cyclopropanations of Cbz-protected amino acid enones using quinine methyl ether.

Quinine methyl ether only affords *syn* selectivity for α-branched amino acids (valine, isoleucine, and the unnatural *tert*-butyl R group analog). The pseudo-enantiomer quinidine methyl ether afforded no selectivity in any case. [30] To extend the investigation of cinchona catalysts, this project will focus on utilizing quinine and quinidine benzyl ether for both the cyclopropyl keto-esters and the cyclopropyl Weinreb amides.

β-Lactone Formation and Coupling to Cyclopropyl Peptidomimetics:

After the cyclopropyl peptidomimetic backbone is synthesized, the β-lactone warhead must be coupled to the *C*-terminus. Vederas' method will be used to synthesize the β-lactone moiety, as it affords high yields of a stereospecific lactone in few steps from commercially available materials. Two synthetic routes will be attempted to couple the β-lactone to the cyclopropyl peptidomimetic backbone. The coupling attempts will be performed on model compounds to develop ideal conditions and preserve the valuable precursor materials. After ideal conditions are determined they will be applied to the cyclopropyl peptidomimetics that were derived from the cyclopropyl keto-esters to afford belactosin A analogs. After the belactosin A analogs are synthesized, they will be assayed for proteasome inhibition activity and cancer cell cytotoxicity.

CHAPTER 2: METHODS AND MATERIALS

A. Instruments, materials, and reagents used

NMR data were obtained on either a 500 MHz FT-NMR model ECA-500 JEOL or a 300MHz FT-NMR model ECA-300 JEOL (Peabody, MA) purchased with funding provided by the National Science Foundation. Splitting patterns are reported by the following: s (singlet), d (doublet), t (triplet), q (quartet), m (multiplet), dd (doublet of doublets) and AB (AB multiplet). Coupling constants (J values) are recorded in hertz (Hz). All signal assignments are based on ^{1}H, ^{13}C, COSY, HMQC and $DEPT_{135}$. Polarimetry was performed using an Autopol III polarimeter (Rudolph Research, Fairfield, NJ). FT-IR spectra were recorded using an Agilent Cary 630 FTIR spectrometer (Agilent Technologies, Santa Clara, California). High resolution ESI-MS was performed at Notre Dame University, Notre Dame, Indiana. Purifications of all compounds except the catalysts were done on a pre-packed silica gel column using a Teledyne Isco Combiflash system, eluting with a gradient of 100% hexanes to 100% ethyl acetate. Reactions were monitored by analytical thin-layer chromatography (TLC) on silica gel 60 F254 pre-coated on glass plates (Merck). Where indicated, catalytic hydrogenation was performed on a Parr hydrogenation apparatus (Mod# A16CA, Moline, IL) using a GE Motor (Mod# 5KH35LNB1645X, RPM 1725). Observation of TLC was conducted by using a UV lamp ($\lambda MAX = 254$ nm) and either ninhydrin or phosphomolybdic acid stain. HPLC was performed using a Breeze Waters System with a normal phase Waters Spherisorb column (10 x 250 mm). All isomers were analyzed by HPLC with an initial solvent ratio of 80/20 hexane-ethyl acetate (5.0 min), 70/30 over 20.0 min. for a total run time of 25.0 min. with a flow rate of 2.0 mL/min.

All chemical reagents and solvents were commercially available from Sigma-Aldrich and used without further purification; (2-(1H-benzotriazol-1-yl)-1,1,3,3tetramethyl uronium hexafluorophosphate (HBTU), 1-Ethyl-3-(3-dimethylaminopropyl) carbodiimide (EDCI), hydroxybenzotriazole (HOBt), (benzotriazol-1-yloxy)tris (dimethylamino)phosphonium hexafluorophosphate (BOP), triethylamine (NEt_3), *N*-hydroxysuccinimide (NHS), ethyl acetate (EA), hexanes (Hex), dichloromethane (DCM), tetrahydrofuran (THF), MeOH (methanol), dimethyl formamide (DMF), benzyl alcohol (BnOH), p-toluenesulfonic acid (TsOH). Solvent extractions were performed using ethyl acetate or methylene chloride where indicated and washed with 1 M HCl, saturated sodium bicarbonate, and brine (reagent grade, Fisher Scientific, Pittsburgh, PA).

B. Compounds synthesized: model compounds and stereoselective cyclopropanations

Model Compounds:

Model compounds were used to determine optimal conditions for the synthesis of the β-lactone warhead, as well as preserving the valuable cyclopropyl peptidomimetic backbone material. Two approaches were pursued for lactone formation. The first approach was lactonization followed by coupling to a model system. **Scheme 2** shows conditions used to afford an amino β-lactone (**3**) derived from the lactonization of Cbz-protected L-threonine (**1**). Compound **1** was treated with BOP or HBTU then NEt_3 to afford **2** *via* an intramolecular lactonization reaction. The Cbz group of **2** was then removed with H_2 and Pd/C to deprotect the amine and afford the free amino β-lactone (**3**), which was then immediately carried forward to the next reaction.

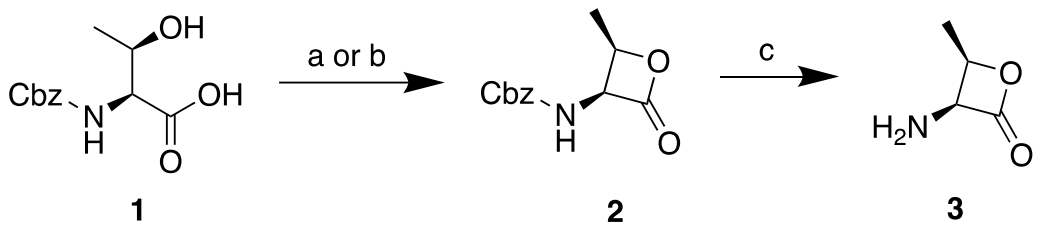

Reaction conditions: (a) BOP, NEt_3; (b) HBTU, NEt_3; (c) H_2, Pd/C.

Scheme 2: Synthesis of a β-lactone derived from Cbz-protected L-threonine.

The other approach was to couple threonine to an acid and then lactonize. **Scheme 3** shows the synthetic route using a model compound, cyclopropane carboxylic acid (**4**), to determine optimal lactonization conditions.

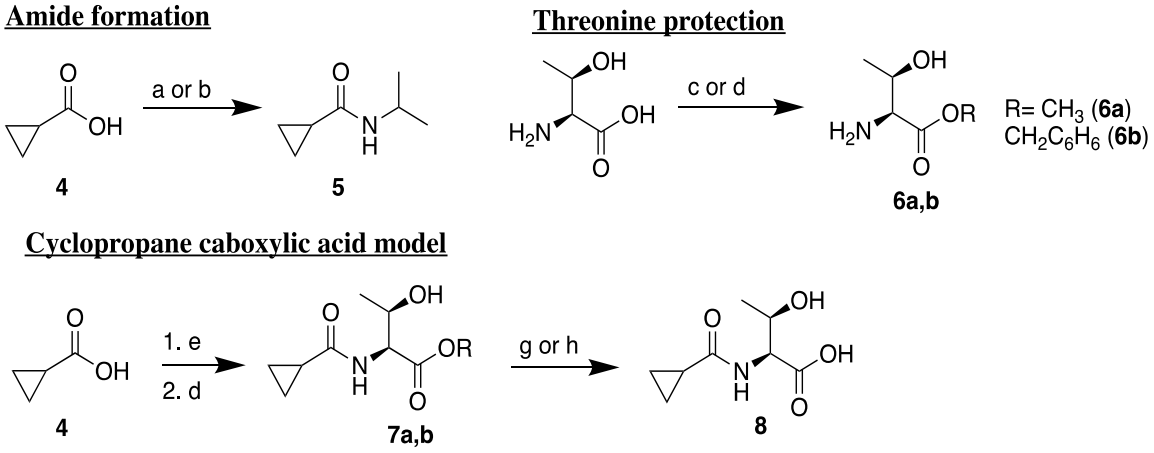

Reaction conditions: (a) NHS, EDCI, $NH_2CH(CH_3)_2$; (b) $Cl_2(CO)_2$, DMF, $NH_2CH(CH_3)_2$; (c) $SOCl_2$, MeOH; (d) BnOH, p-TsOH; (e) EDCI, HOBt; (f) **6a,b**, NEt_3; (g) LiOH; (h) Pd/C, ammonium formate.

Scheme 3: Model coupling using cyclopropyl acid.

Compound **4** was treated with EDCI and NHS, or oxalyl chloride and DMF to activate the acid and was then coupled with isopropyl amine to afford an amide (**5**). Threonine

was protected to form the methyl and benzyl esters **6a or 6b**, respectively, for amide coupling to **4** when treated with EDCI, HOBt, and NEt_3, which afforded **7a** or **7b**. Compound **7a** was saponified with LiOH to afford the hydroxyacid (**8**). The benzyl ester (**7b**) was treated with Pd/C and NH_4HCO_2 in a transfer hydrogenation to afford **8**.

An alternative model is shown in **Scheme 4**, using Fmoc protected phenylalanine (**9**), to determine optimal lactonization conditions. Compound **9** was treated with EDCI and HOBt to activate the acid and was then treated with **6b** and NEt_3 to afford the amide (**10**). The benzyl ester of **10** was removed with Pd/C and ammonium formate to afford **11**, where H_2 and Pd/C afforded **12**, maintaining the Fmoc protecting group.

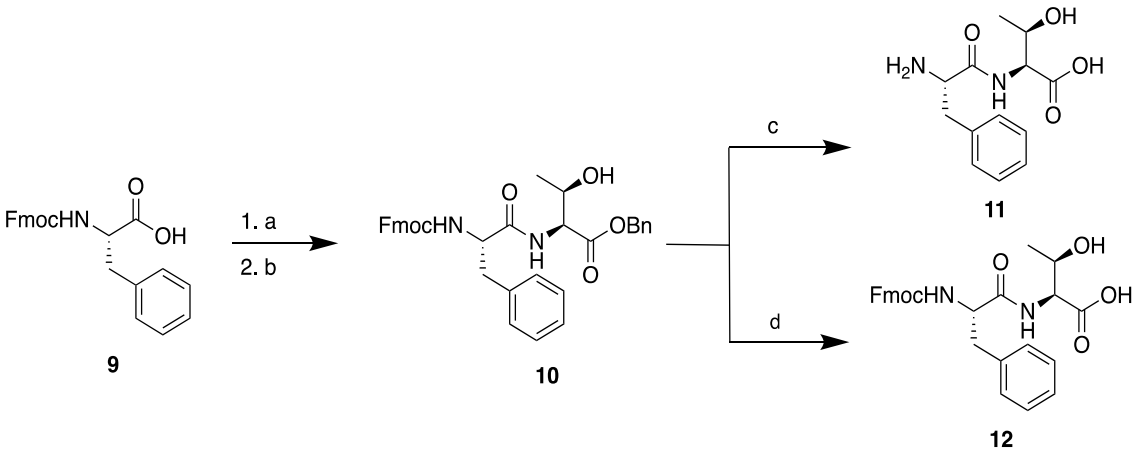

Reaction conditions: (a) EDCI; (b) **6b**; (c) Pd/C, ammonium formate; (d) H_2, Pd/C.

Scheme 4: Model coupling using Fmoc-protected phenylalanine.

A final model system is shown in **Scheme 5**, using ibuprofen (**13**), to determine optimal lactonization conditions. Compound **13** was treated with EDCI and HOBt to activate the acid and was then treated with **6b** and NEt_3 to afford the amide (**14**).

Deprotection of the benzyl ester (**14**) with Pd/C and ammonium formate afforded **15**. The acid (**15**) was then treated with BOP and NEt_3 to afford both **16** and **17**, the β-lactone and an α,β unsaturated acid product, respectively.

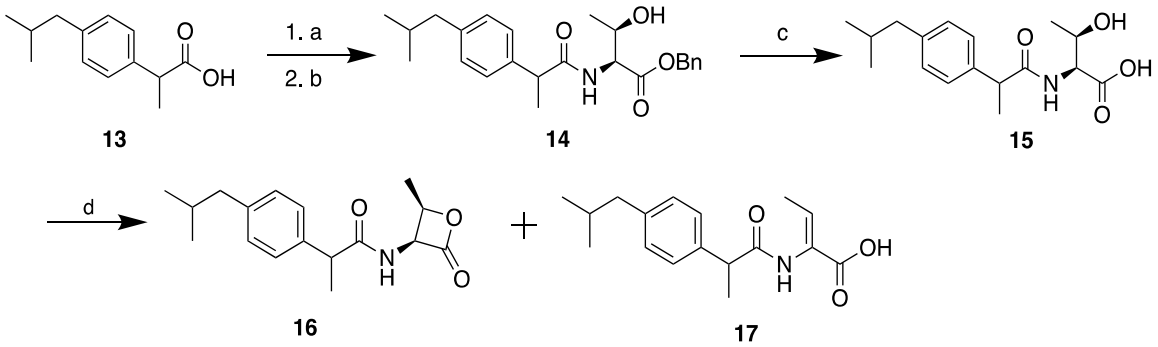

Reaction conditions: (a) EDCI, HOBt; (b) **6b**, NEt_3; (c) Pd/C, ammonium formate; (d) BOP and NEt_3.

Scheme 5: Model coupling using ibuprofen.

Stereoselective cyclopropanations:

To synthesize the cyclopropyl peptidomimetic backbone from amino acid-derived enones four key reagents can be used (**Figure 13**).

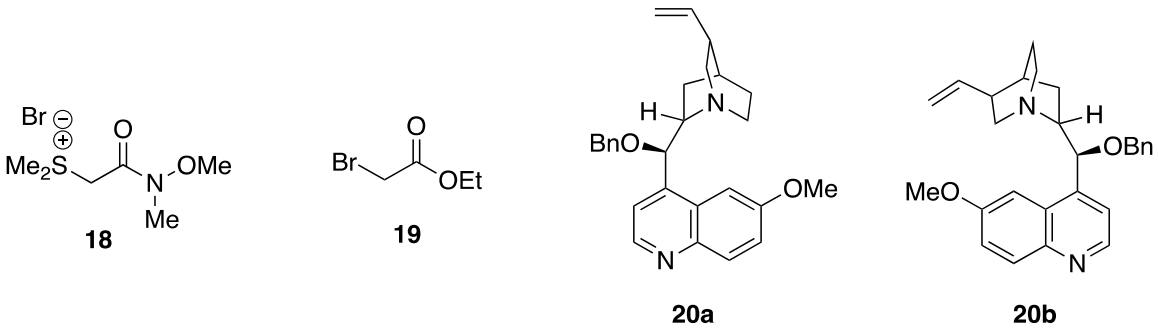

Figure 13: Key reagents used in cyclopropanation of amino acid-derived enones.

The salt (**18**) and bromoethyl acetate (**19**) are used to afford the Weinreb amide and the ester cyclopropyl series, respectively. Quinine and quinidine benzyl ether catalysts, **20a** and **20b**, are used to enhance stereoselectivity.

Scheme 6 shows the stereoselective cyclopropanation of two L-amino-acid derived enones to afford cyclopropyl esters. To afford the *syn* product (**22** and **25**), the enones (**21** and **24**) are treated with **19**, **20a**, and K_2CO_3. To afford the *anti* product (**23** and **26**), the enones (**21** and **24**) are treated with **19**, **20b**, and K_2CO_3.

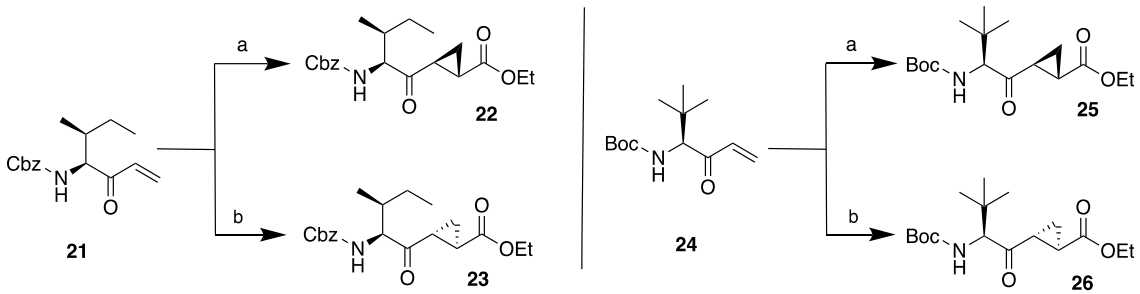

Reaction conditions: (a) **19**, **20a**, K_2CO_3; (b) **19**, **20b**, K_2CO_3.

Scheme 6: Stereoselective cyclopropanations of Cbz-L-isoleucine and Boc-*tert*-L-leucine enones.

To gain insight into the stereoselectivity, the D-enone (**29**) from Cbz-D-valine (**27**) was prepared. **Scheme 7** shows the synthetic route of stereoselective cyclopropanations starting from the commercially available Cbz-D-valine (**27**) to afford cyclopropyl esters. The acid (**27**) was treated with EDCI, NEt_3, and $NH(OCH_3)CH_3$ to afford the Weinreb amide (**28**). Compound **28** was then treated with vinylmagnesium bromide to afford the enone (**29**). The enone (**29**) was then treated with **19**, K_2CO_3, and either **20a** or **20b** to afford the *anti* (**30**) or *syn* (**31**) product, respectively.

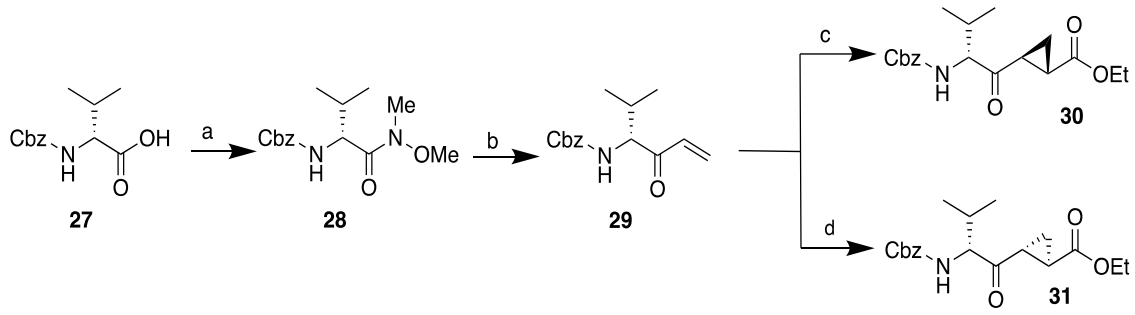

Reaction conditions: (a) EDCI, NEt_3, $NH(OCH_3)CH_3$; (b) $CH_2CHMgBr$; (c) **19**, **20a**, K_2CO_3; (d) **19**, **20b**, K_2CO_3.

Scheme 7: Synthetic route to Cbz-D-valine cyclopropyl esters.

Scheme 8 shows the cyclopropanation of two L-amino-acid derived enones to afford cyclopropyl Weinreb amides. Cbz-valine (**32a**) and Cbz-phenylalanine (**32b**) enones are treated with **18**, K_2CO_3, and either **20a** or **20b** to afford a mixture of the *syn* (**33a,b**) or the *anti* (**34a,b**) cyclopropyl Weinreb amides, respectively.

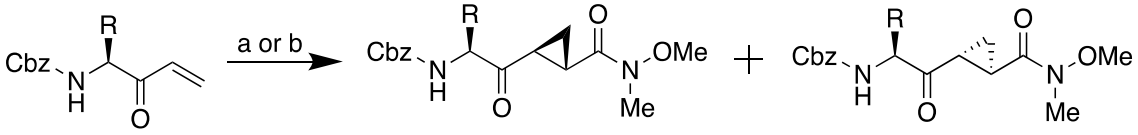

R= $CH(CH_3)_2$ (**32a**)
$CH_2C_6H_6$ (**32b**)

33a,b

34a,b

Reaction conditions: (a) **18**, **20a**, K_2CO_3; (b) **18**, **20b**, K_2CO_3.

Scheme 8: Synthesis of cyclopropyl Weinreb amides from L-amino-acid derived enones.

C. Experimentals

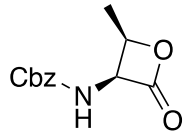

Benzyl ((2R, 3S)-2-methyl-4-oxooxetan-3-yl)carbamate (2): To a stirred solution of **1** (126 mg, 0.5 mmol) in DCM (20 mL), NEt_3 (0.20 mL, 1.5 mmol) and BOP (265 mg, 0.60 mmol) were added at 0° C. The solution stirred for one hour at 0° C and room temperature for four hours, under an argon atmosphere. The solvent was evaporated and the crude product was purified by CombiFlash to afford 59 mg (50%) as a white solid. Rf 0.86 [EA/Hex 4:1]; FT-IR: 3283, 1815 (C=O lactone), 1698 (C=O Cbz), 1551 cm^{-1} $[\alpha]_D$= +8.1° (c 0.021, acetone); ^{1}H NMR (500 MHz, $CDCl_3$): δ 1.40 (d, J= 6.30 Hz, 3H, C<u>H</u>$_3$), 4.79 (q, J= 5.73Hz, 1H, C<u>H</u>CH$_3$), 5.10 (s, 2H, OC<u>H</u>$_2$), 5.42 (d, J= 2.86, 1H, NC<u>H</u>), 6.25 (d, J= 8.59 Hz, 1H, N<u>H</u>), 7.31 (m, 5H, aryl); ^{13}C NMR (125 MHz, $CDCl_3$): δ 14.95 (<u>C</u>H$_3$), 60.39 (N<u>C</u>H), 67.88 (O<u>C</u>H$_2$), 75.06 (<u>C</u>HCH$_3$), 128.32-128.73 (aryl), 135.68 (4° aryl), 155.68 (Cbz <u>C</u>=O), 169.29 (lactone <u>C</u>=O); mass spectrum (ESI-MS) *m/z* ($C_{12}H_{13}NaNO_4$) calculated for (M+Na) 258.0736, found 258.0739.

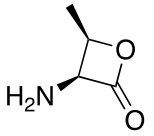

(3S,4R)-3-amino-4-methyloxetan-2-one (3): 2 was transferred to a Parr bottle with EA (20 mL). 10% Pd/C (74 mg) was added to the solution and shaken under H_2 (35 psi) for 4 hours. The solution was filtered through celite, and the crude product was instantly used in the next reaction.

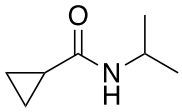

N-isopropylcyclopropanecarboxamide (5): Method A: To a stirred solution of **4** (172 mg, 2 mmol) in DCM (10 mL), N-hydroxysuccinimide (230 mg, 2 mmol) and EDCI (384 mg, 2 mmol) were added at room temperature. After 2 hours, isopropyl amine (0.16 mL, 1.86 mmol) was added to the stirred solution. After 22 hours, the solution was poured into 1 M HCl and extracted with EA. The organic layer was dried with anhydrous magnesium sulfate, filtered, and the solvent was evaporated. The crude product was purified by CombiFlash, and the fractions were followed by TLC. Fractions were collected and evaporated to afford 191 mg (80%) of a white solid.

Method B: To a stirred solution of **4** (172 mg, 2 mmol) in DCM (10 mL), oxalyl chloride (0.2 mL, 2.3 mmol) and DMF (4 drops) were added at room temperature. After 2 hours, isopropyl amine (0.16 mL, 1.86 mmol) was added to the stirred solution at room temperature. After 21 hours, the solution was poured into 1 M HCl and extracted with DCM. The organic layer was dried with anhydrous magnesium sulfate, filtered, and the solvent was evaporated. The crude product was purified by CombiFlash to afford 125 mg (53%) of a white solid. Rf 0.70 [EA/Hex 5:1]; ^{1}H NMR (500 MHz, $CDCl_3$): δ 0.69 (m, 2H, one of C$\underline{H}_2$ cpyl), 0.92 (m, 2H, one of C$\underline{H}_2$ cpyl), 1.14 (d, J= 6.87 Hz, 6H, CH(C$\underline{H}_3$)$_2$), 1.37 (m, 1H, C$\underline{H}$ cpyl), 4.08 (septet, J= 6.30 Hz, 1H, NC$\underline{H}$), 6.07 (s, 1H, N$\underline{H}$); ^{13}C NMR (125 MHz, $CDCl_3$): δ 6.82 ($\underline{C}H_2$), 14.65 ($\underline{C}$H cypl), 22.81 ($\underline{C}H_3$), 41.35 ($\underline{C}$HN), 172.77 ($\underline{C}$=O).

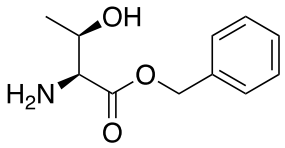

Benzyl L-threoninate (6b): L-Threonine (3.75 g, 31.34 mmol) was suspended in a solution of 4:1 benzene/ benzyl alcohol (6.5 mL, 62.69 mmol), and p-TsOH (6.47 g, 37.61 mmol) was added. The solution was then fitted with a Dean-Stark trap filled with benzene, and the solution was heated to reflux. After 22 hours, the solution was poured into water and extracted two times with EA. Solid KOH was added to the aqueous layer to reach a pH of 9.0 and then extracted four times with EA. The organic layer was dried with anhydrous magnesium sulfate, filtered, and the solvent was evaporated to afford 2.78 g (42.5%) as a yellow syrup.

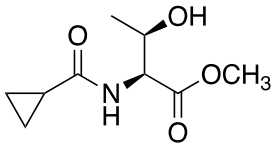

Methyl (cyclopropanecarbonyl)-L-threoninate (7a): To a stirred solution of **4** (92 mg, 1.07 mmol) in DCM (5 mL), EDCI (205 mg, 1.07 mmol) and HOBt (15 mg, 0.107 mmol) was added. After 30 minutes, **6a** (180 mg, 1.07 mmol) and NEt_3 (0.15 mL, 1.07 mmol) were added. After 21 hours, the solution was poured into 1 M HCl and extracted three times with EA. The organic layer was dried with anhydrous magnesium sulfate, filtered, and the solvent was evaporated to afford 104 mg (23.3%) as a white solid. ^{1}H NMR (500 MHz, $CDCl_3$): δ 0.75 (m, 2H, one of C$\underline{H}_2$ cpyl), 0.94 (m, 2H, one of C$\underline{H}_2$ cpyl), 1.18 (d, J= 6.30 Hz, 3H, CHC$\underline{H}_3$), 1.53 (m, 1H, C$\underline{H}$ cpyl), 3.73 (s, 3H, OC$\underline{H}_3$), 4.30 (dq, J= 2.57, 6.30, 1H, C$\underline{H}$OH), 4.58 (dd, J= 2.86, 8.59, 1H, NC$\underline{H}$), 6.87 (d,

J= 8.59, 1H, NH); ^{13}C NMR (125 MHz, $CDCl_3$): δ 7.69 ($\underline{C}H_2$), 14.61 ($\underline{C}H$ cypl), 19.93 ($CH\underline{C}H_3$), 52.63 ($O\underline{C}H_3$), 57.64 ($N\underline{C}H$), 68.15 ($\underline{C}HOH$), 171.89 ($N\underline{C}$=O), 174.90 ($O\underline{C}$=O).

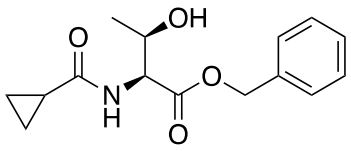

Benzyl (cyclopropanecarbonyl)-L-threoninate (7b): To a stirred solution of **4** (221 mg, 2.57 mmol) in DCM (15 mL), EDCI (493 mg, 2.57 mmol) and HOBt (35 mg, 0.257 mmol) were added. After one hour, **6b** (537 mg, 2.57 mmol) and NEt_3 (0.36 mL, 2.57 mmol) were added. After 20 hours, the solution was poured into 1 M HCl and extracted three times with EA, and then the organic layer was washed with 1 M NaOH. The organic layer was dried with anhydrous magnesium sulfate, filtered, and the solvent was evaporated. The crude product was purified by manual flash column chromatography, eluting with 1:1 EA/Hex to afford 132 mg (19%) as a white solid. Rf 0.32 [EA/Hex 2:1]; ^{1}H NMR (500 MHz, $CDCl_3$): δ 0.79 (m, 2H, one of $C\underline{H}_2$ cpyl), 0.99 (m, 2H, one of $C\underline{H}_2$ cpyl), 1.21 (d, J= 6.30 Hz, 3H, $CHC\underline{H}_3$), 1.50 (m, 1H, $C\underline{H}$ cpyl), 4.35 (dq, J= 2.57, 6.30 Hz, 1H, $C\underline{H}OH$), 4.66 (dd, J= 2.29, 9.16 Hz, 1H, $NC\underline{H}$), 5.19 (ABq, J_{AB}= 10.31 Hz, 2H, $OC\underline{H}_2$), 6.53 (d, J= 8.59 Hz, 1H, $N\underline{H}$) 7.26-7.36 (m, 5H, aryl); ^{13}C NMR (125 MHz, $CDCl_3$): δ 7.74 ($\underline{C}H_2$), 14.78 ($\underline{C}H$ cypl), 20.07 ($CH\underline{C}H_3$), 57.53 ($N\underline{C}H$), 67.43 ($O\underline{C}H_2$), 68.36 ($\underline{C}HOH$), 128.29-128.72 (aryl), 134.11 (4° aryl), 171.05 ($N\underline{C}$=O), 174.53 ($O\underline{C}$=O); mass spectrum (ESI-MS) *m/z* ($C_{15}H_{20}NO_4$) calculated for (M+1) 278.1387, found 278.1390.

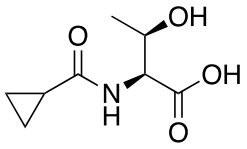

(cyclopropanecarbonyl)-L-threonine (8): Method A: To a stirred solution of **6a** (84 mg, 0.418 mmol) in 1:2 THF (4 mL)/ H_2O (8 mL), lithium hydroxide monohydrate (265 mg, 6.31 mmol) was added. After 2 hours, the solution was poured into water and extracted with EA. The aqueous layer was acidified to a pH of 2 and was extracted three times with EA. The organic layer was dried with anhydrous magnesium sulfate, filtered, and the solvent was evaporated then triturated with hexane to afford 54 mg (69%) as a white solid.

Method B: To a stirred solution of **6b** (130 mg, 0.469 mmol) in MeOH (20 mL), ammonium formate (296 mg, 4.69 mmol) and 10% Pd/C (100 mg) were added. After 1.5 hours, the solution was filtered through celite, and pour into water (20 mL) and extracted three times with EA. The aqueous layer was lyophilized to afford 80 mg (90%). Rf 0.50 [EA/Hex 4:1]; ^{1}H NMR (500 MHz, D_2O): δ 0.86 (m, 4H, both of C$\underline{H}_2$ cpyl), 1.19 (d, J= 6.30 Hz, 3H, CHC$\underline{H}_3$), 1.77 (m, 1H, C$\underline{H}$ cpyl), 4.20 (m, 1H, C$\underline{H}$OH), 4.27 (m, 1H, NC$\underline{H}$); ^{13}C NMR (125 MHz, D_2O): δ 7.48 (C$\underline{H}_2$), 14.08 (C$\underline{H}$ cypl), 19.07 (CH$\underline{C}H_3$), 58.32 (N$\underline{C}$H), 67.44 ($\underline{C}$HOH), 174.23 (N$\underline{C}$=O), 178.11 (O$\underline{C}$=O).

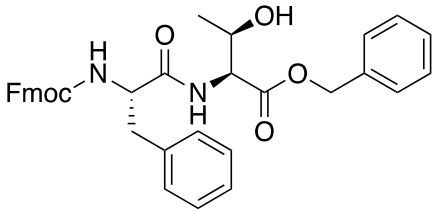

Benzyl (((9H-fluoren-9-yl)methoxy)carbonyl)-L-phenylalanyl-L-threoninate (10): To a stirred solution of **9** (387 mg, 1.0 mmol) in DCM (20 mL), EDCI (192 mg, 1.0 mmol) was added. After 30 minutes, **6b** (209 mg, 1.0 mmol) was added. After 20 hours, the solution was poured into 1 M HCl and extracted three times with EA. The organic layer was dried with anhydrous magnesium sulfate, filtered, and the solvent was evaporated. The crude product was purified by CombiFlash to afford 385 mg (66.8%) as a pale-yellow foam. Rf 0.63 [EA/Hex 1:1]; $[\alpha]_D$= -14.6° (c 0.00915, acetone); ^{1}H NMR (500 MHz, $CDCl_3$): 1.11 (d, J= 6.30 Hz, 3H, CHC<u>H</u>$_3$), 3.08 (m, 2H, C<u>H</u>$_2$Ph), 4.12 (t, J= 6.87 Hz, 1H, C<u>H</u> Fmoc), 4.20-4.37 (m, 2H, OC<u>H</u>$_2$ Fmoc), 4.28 (dq, J= 2.86, 6.30 Hz, 1H, C<u>H</u>OH), 4.57 (m, J= 6.87 Hz, 1H, NC<u>H</u> Phe), 4.62 (dd, J= 2.58, 8.98 Hz, 1H, NC<u>H</u> Thr), 5.13 (s, 2H, OC<u>H</u>$_2$ Ph), 5.62 (d, J= 8.02 Hz, 1H, N<u>H</u> Thr), 7.02 (d, J= 8.59 Hz, 1H, N<u>H</u> Phe), 7.15-7.75 (m, aryl); ^{13}C NMR (125 MHz, acetone-D_6): δ 19.75 (CH<u>C</u>H$_3$), 37.87 (<u>C</u>H$_2$ Phe), 47.07 (<u>C</u>H Fmoc), 56.31 (N<u>C</u>H Fmoc), 57.94 (N<u>C</u>H Thr), 66.32 (O<u>C</u>H$_2$ Fmoc), 66.40 (O<u>C</u>H$_2$ Ph), 67.23 (<u>C</u>HOH), 119.89-144.14 (aryl), 155.98 (O<u>C</u>=ON), 170.38 (O<u>C</u>=O), 171.82 (N<u>C</u>=O); mass spectrum (ESI-MS) *m/z* ($C_{35}H_{34}N_2NaO_6$) calculated for (M+Na) 601.2309, found 601.2320.

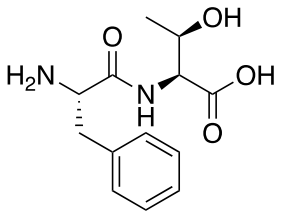

L-phenylalanyl-L-threonine (11): To a stirred solution of **10** (210 mg, 0.363 mmol) in MeOH (20 mL), ammonium formate (229 mg, 3.64 mmol) and 10% Pd/C (170 mg) were added. After 22 hours, the solution was filtered through a pad of celite. The filtered solution was poured into water and extracted three times with EA. The aqueous layer was lyophilized to afford 78 mg (80.4%).

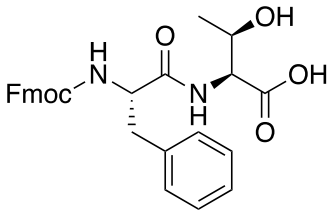

(((9H-fluoren-9-yl)methoxy)carbonyl)-L-phenylalanyl-L-threonine (12): To a stirred solution of **10** (132 mg, 0.23 mmol) in MeOH (30 mL), 10% Pd/C (128 mg) was added to the solution and shaken under H_2 (40 psi) for 3.5 hours. The solution was filtered through celite and evaporated to afford 98 mg (88.3%).

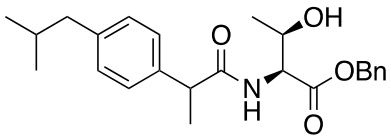

Benzyl (2-(4-isobutylphenyl)propanoyl)-L-threoninate (14): To a stirred solution of **13** (206 mg, 1.0 mmol) in DCM (10 mL), EDCI (192 mg, 1.0 mmol) and HOBt (13.5 mg, 0.1 mmol) were added. After 40 minutes **6b** (209 mg, 1.0 mmol) and

NEt_3 (0.14 mL, 1.0 mmol). After 24 hours, the solution was poured into 1 M HCl and extracted three times with EA. The organic layer was dried with anhydrous magnesium sulfate, filtered, and the solvent was evaporated. The crude product was purified by CombiFlash to afford 103 mg (25.9%). Rf 0.20 [EA/Hex 1:3]; $[\alpha]_D$= +1.95° (c 0.0390, $CHCl_3$); ^{1}H NMR (500 MHz, $CDCl_3$): δ 0.87 (d, J= 6.30 Hz, 6H, CH($C\underline{H}_3$)$_2$), 1.10 (d, J= 6.30 Hz, 3H, CHC$\underline{H}_3$ Thr), 1.49 (d, J= 7.45 Hz, 3H, CHC$\underline{H}_3$ ibuprofen), 1.81 (m, J= 6.87 Hz, 1H, C$\underline{H}$(CH_3)$_2$), 2.41 (d, J= 7.45 Hz, 2H, CHC$\underline{H}_2$), 3.64 (q, J= 6.87 Hz, 1H, C$\underline{H}CH_3$ ibuprofen), 4.30 (dq, J= 2.29, 6.30 Hz, 1H, C$\underline{H}$OH), 4.58 (dd, J= 2.29, 9.16 Hz, 1H, NC$\underline{H}$), 5.07 (ABq, J_{AB}= 12.03 Hz, 2H, OC$\underline{H}_2$), 6.42 (d, J= 8.59 Hz, 1H, N$\underline{H}$), 7.04 (d, J= 8.02 Hz, 2H, aryl ibuprofen), 7.18 (d, J= 8.02 Hz, 2H, aryl ibuprofen), 7.24-7.31 (m, 5H, aryl Bn ester); ^{13}C NMR (125 MHz, $CDCl_3$): δ 18.39 (CH$\underline{C}H_3$ ibuprofen), 19.74 (CH$\underline{C}H_3$ Thr), 22.25 (CH($\underline{C}H_3$)$_2$), 30.02 ($\underline{C}$H(CH_3)$_2$), 44.89 (CH$\underline{C}H_2$), 46.39 ($\underline{C}HCH_3$ ibuprofen), 57.35 (N$\underline{C}$H), 67.05 (O$\underline{C}H_2$), 67.74 ($\underline{C}$HOH), 127.29-129.38 (aryl), 135.51(4° aryl Bn ester), 137.91 (4° aryl ibuprofen), 140.51 (4° aryl ibuprofen), 170.64 (O$\underline{C}$=O), 175.19 (N$\underline{C}$=O); mass spectrum (ESI-MS) *m/z* ($C_{24}H_{32}NO_4$) calculated for (M+H) 398.2326, found 398.2332.

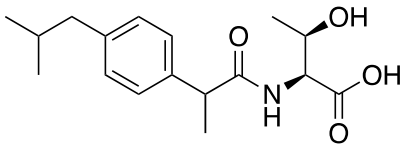

(2-(4-isobutylphenyl)propanoyl)-L-threonine (15): To a stirred of **14** (68.6 mg, 0.173 mmol) in MeOH (15 mL), ammonium formate (108.8 mg, 1.73 mmol) and 10% Pd/C (69 mg) were added. After 4 hours, the solution was filtered through a pad of celite. The filtered solution was poured into 1M HCl and extracted two times with EA. The

organic layer was dried with anhydrous magnesium sulfate, filtered, and the solvent was evaporated to afford 49 mg (93%) as a pale-yellow oil. ^{1}H NMR (500 MHz, $CDCl_3$): δ 0.85 (d, J= 6.30 Hz, 6H, $CH(C\underline{H}_3)_2$), 1.10 (d, J= 6.30 Hz, 3H, $CHC\underline{H}_3$ Thr), 1.48 (d, J= 6.87 Hz, 3H, $CHC\underline{H}_3$ ibuprofen), 1.81 (m, J= 6.87 Hz, 1H, $C\underline{H}(CH_3)_2$), 2.41 (d, J= 7.45 Hz, 2H, $CHC\underline{H}_2$), 3.68 (q, J= 6.87 Hz, 1H, $C\underline{H}CH_3$ ibuprofen), 4.32 (d, J= 5.15 Hz, 1H, C<u>H</u>OH), 4.49 (d, J= 7.45 Hz, 1H, NC<u>H</u>), 6.80 (d, J= 8.02 Hz, 1H, N<u>H</u>), 7.07 (d, J= 8.02 Hz, 2H, aryl ibuprofen), 7.18 (d, J= 8.02 Hz, 2H, aryl ibuprofen); ^{13}C NMR (125 MHz, $CDCl_3$): δ 18.21 ($CH\underline{C}H_3$ ibuprofen), 18.98 ($CH\underline{C}H_3$ Thr), 22.40 ($CH(\underline{C}H_3)_2$), 30.24 ($\underline{C}H(CH_3)_2$), 45.06 ($CH\underline{C}H_2$), 46.34 ($\underline{C}HCH_3$ ibuprofen), 57.44 (N<u>C</u>H), 67.59 (<u>C</u>HOH), 127.24, 129.6260 (aryl), 138.24 (4° aryl ibuprofen), 140.86 (4° aryl ibuprofen), 174.01 (N<u>C</u>=O), 176.50 (O<u>C</u>=O); mass spectrum (ESI-MS) *m/z* ($C_{17}H_{25}NO_4$) calculated for (M+H) 308.1856, found 308.1853.

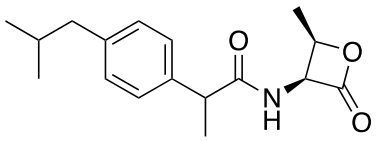

2-(4-isobutylphenyl)-N-((2R,3S)-2-methyl-4-oxooxetan-3-yl)propanamide (16): To a stirred solution of **15** (50.4 mg, 0.164 mmol) in DCM (10 mL), NEt_3 (0.0690 mL, 0.493 mmol) and BOP (87 mg, 0.197 mmol) were added at 0°C for one hour, then room temperature for one hour under an argon atmosphere. After 2 hours, the solution was poured into 1 M HCl and extracted 3 times with DCM. The organic layer was dried with anhydrous magnesium sulfate, filtered, and the solvent was evaporated. The crude product was purified by CombiFlash to afford 13.0 mg (28.7%) of a pale-yellow oil. Rf 0.77 [EA/Hex 1:1]; ^{1}H NMR (500 MHz, $CDCl_3$): δ 0.83 (dd, J= 1.99, 6.30 Hz, 6H,

CH(C<u>H</u>$_3$)$_2$), 1.11 (d, J= 6.30 Hz, 3H, CHC<u>H</u>$_3$ Thr), 1.51 (d, J= 5.73 Hz, 3H, CHC<u>H</u>$_3$ ibuprofen), 1.79 (m, 1H, C<u>H</u>(CH$_3$)$_2$), 2.37 (d, J= 7.45 Hz, 2H, CHC<u>H</u>$_2$), 3.68 (q, J= 6.87 Hz, 1H, C<u>H</u>CH$_3$ ibuprofen), 4.38 (q, J= 6.30 Hz, 1H, C<u>H</u>OH), 4.70 (d, J= 8.02 Hz, 1H, NC<u>H</u>), 6.68 (d, J= 8.02 Hz, 1H, N<u>H</u>), 7.02 (d, J= 6.30 Hz, 2H, aryl ibuprofen), 7.17 (d, J= 6.30 Hz, 2H, aryl ibuprofen); ^{13}C NMR (125 MHz, CDCl$_3$): δ 18.36 (CH<u>C</u>H$_3$ ibuprofen), 19.14 (CH<u>C</u>H$_3$ Thr), 22.39 (CH(<u>C</u>H$_3$)$_2$), 30.97 (<u>C</u>H(CH$_3$)$_2$), 45.05 (CH<u>C</u>H$_2$), 46.49 (<u>C</u>HCH$_3$ ibuprofen), 57.66 (N<u>C</u>H), 67.16 (<u>C</u>HOH), 127.29, 129.38 (aryl), 137.40 (4° aryl ibuprofen), 141.01 (4° aryl ibuprofen), 172.84 (N<u>C</u>=O), 176.85 (O<u>C</u>=O); mass spectrum (ESI-MS) *m/z* (C$_{17}$H$_{23}$NO$_4$) calculated for (M+H) 290.1750, found 290.1711.

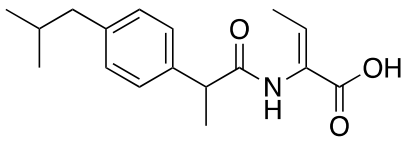

(Z)-2-(2-(4-isobutylphenyl)propanamido)but-2-enoic acid (17): To a stirred solution of **15** (123 mg, 0.40 mmol) in DCM (25 mL), NEt$_3$ (0.17 mL, 1.2 mmol) and BOP (213 mg, 0.48 mmol) were added at 0°C for one hour, then room temperature for 18 hours under an argon atmosphere. The solution was poured into 1 M HCl and extracted 3 times with EA. The organic layer was dried with anhydrous magnesium sulfate, filtered, and the solvent was evaporated. The crude product was purified by CombiFlash to afford 52.6 mg of a pale-yellow oil. Rf 0.77 [EA/Hex 1:1]; FT-IR: 3300 (vinyl), 1702 (acid C=O), 1655 (amide C=O) cm^{-1}; ^{1}H NMR (500 MHz, CDCl$_3$): δ 0.88 (dd, J= 1.99, 6.30 Hz, 6H, CH(C<u>H</u>$_3$)$_2$), 1.53 (d, J= 6.30 Hz, 3H, CHC<u>H</u>$_3$ Thr), 1.65 (d, J= 5.73 Hz, 3H, CHC<u>H</u>$_3$ ibuprofen), 1.84 (m, 1H, C<u>H</u>(CH$_3$)$_2$), 2.45 (d, J= 7.45 Hz, 2H, CHC<u>H</u>$_2$), 3.71 (q, J= 6.87 Hz, 1H, C<u>H</u>CH$_3$ ibuprofen), 6.79 (d, J= 8.02 Hz, 1H, N<u>H</u>), 6.84 (m, 1H, vinyl),

7.25 (d, J= 6.30 Hz, 2H, aryl ibuprofen), 7.13 (d, J= 6.30 Hz, 2H, aryl ibuprofen); ^{13}C NMR (125 MHz, $CDCl_3$): δ 14.80 ($CH\underline{C}H_3$ ibuprofen), 18.36 ($CH\underline{C}H_3$ Thr), 22.43 ($CH(\underline{C}H_3)_2$), 30.25 ($\underline{C}H(CH_3)_2$), 45.09 ($CH\underline{C}H_2$), 46.92 ($\underline{C}HCH_3$ ibuprofen), 125.81 (vinyl $\underline{C}H$), 127.29, 129.38 (aryl), 136.32 (vinyl $\underline{C}N$), 138.05 (4° aryl ibuprofen), 141.08 (4° aryl ibuprofen), 165.90 ($HO\underline{C}=O$), 173.38 ($N\underline{C}=O$); mass spectrum (ESI-MS) *m/z* ($C_{17}H_{23}NO_3$) calculated for (M+H) 290.1, found 290.1711.

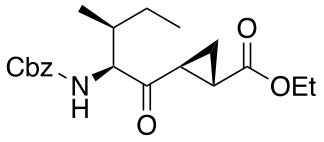

Ethyl (1*S*,2*S*)-2-(((benzyloxy)carbonyl)-*L*-isoleucyl)cyclopropane-1-carboxylate (**22**):To a stirred solution of **21** (53.3 mg, 0.19 mmol) in 1.0 mL anhydrous acetonitrile, was added freshly ground potassium carbonate (35 mg, 0.25 mmol), along with a solution of **20a** (25 mg, 0.060 mmol) in 0.5 mL anhydrous acetonitrile. **19** (32 μL, 0.19 mmol) was added and the solution was heated to reflux. After two hours, another portion of **19** (32 μL, 0.19 mmol) was added, and after four hours a final portion of **19** (32 μL, 0.19 mmol) was added. After 26 hours, the solution was poured into brine and extracted three times with EA. The organic layer was dried with anhydrous magnesium sulfate, filtered, and evaporated. The crude was purified by CombiFlash to afford 54 mg (77%) of a pale yellow oil. The isomers were analyzed by HPLC to identify a 82:18 *syn:anti* ratio. Rf 0.63 [EA/Hex 1:1]; $[\alpha]_D$ = +81.4˚ (c = 0.017, $CHCl_3$); ^{1}H-NMR (500 MHz, $CDCl_3$): δ 0.90 (t, J= 7.45 Hz, 3H, $CHCH_2C\underline{H}_3$), 1.01 (d, J= 6.87 Hz, 3H, $CHC\underline{H}_3$), 1.10 (m, 2H $CHC\underline{H}_2$), 1.26 (t, J= 7.45 Hz, 3H $OCH_2C\underline{H}_3$), 1.39 (m, 1H one of the $C\underline{H}_2$

cp), 1.49 (m, 1H one of the C$\underline{H}_2$ cp), 2.07 (m, 1H, C$\underline{H}CH_3$), 2.25 (m, 1H, C1H), 2.53 (m, 1H, C2H), 4.14 (q, J= 7.45 Hz, 2H, OC$\underline{H}_2CH_3$), 4.61(dd, J= 4.01, 8.59 Hz, 1H, C$\underline{H}$N), 5.09 (s, 2H, OC$\underline{H}_2$Ph), 5.53 (d, J= 8.02 Hz, 1H N$\underline{H}$), 7.3 (m, 5H, aryl); ^{13}C-NMR (125 MHz, $CDCl_3$): δ 11.88 (CHCH$_2\underline{C}H_3$), 14.01 (OCH$_2\underline{C}H_3$), 16.01 (CH$\underline{C}H_3$), 17.71 (cp $\underline{C}H_2$), 24.14 (CH$\underline{C}H_2CH_3$), 24.72 (C1), 27.75 (C2), 36.98 ($\underline{C}HCH_3$), 61.13 (O$\underline{C}H_2CH_3$), 65.29 ($\underline{C}$HN), 66.90 (O$\underline{C}H_2$Ph), 127.96-128.39 (arylCH), 136.36 (4°aryl), 156.44 (Cbz $\underline{C}$=O), 171.77 (ester $\underline{C}$=O), 206.06 (ketone $\underline{C}$=O). Exact mass spectrum (ESI-MS) *m/z* ($C_{29}H_{29}NO_5$) calculated for (M+1) 362.1967, found 362.1961.

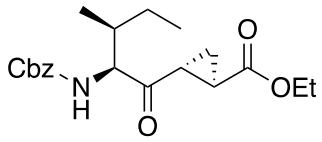

Ethyl (1*R*,2*R*)-2-(((benzyloxy)carbonyl)-*L*-isoleucyl)cyclopropane-1-carboxylate (22): To a stirred solution of **21** (50 mg, 0.18 mmol) in 1.0 mL anhydrous acetonitrile, was added freshly ground potassium carbonate (33 mg, 0.24 mmol), and a solution of **20b** (25 mg, 0.060 mmol) in 0.5 mL acetonitrile. **19** (20 μL, 0.18 mmol) was added and the solution was heated to reflux. After two hours, another portion of **19** (20 μL, 0.18 mmol) was added, and after four hours the final portion of **19** (20 μL, 0.18 mmol) was added. After 20 hours, the solution was poured into brine and extracted twice with EA. The organic layer was dried with anhydrous magnesium sulfate, filtered, and evaporated. The crude product was purified by CombiFlash to afford 46 mg (70%) of a pale yellow oil. The isomers were analyzed by HPLC to identify a 7:93 *syn:anti* ratio. Rf 0.45 [EA/Hex 1:2]; $[\alpha]_D$ = +21.5˚ (c= 0.016g/mL, $CHCl_3$); ^{1}H-NMR (500 MHz, $CDCl_3$):

δ 0.90 (t, J= 7.45 Hz, 3H, $CHCH_2C\underline{H}_3$), 1.01 (d, J= 6.30 Hz, 3H, $CHC\underline{H}_3$), 1.09 (m, J= 6.87 Hz, 2H, $CHC\underline{H}_2$), 1.26 (t, J= 7.45 Hz, 3H, $OCH_2C\underline{H}_3$), 1.51 (m, 2H $C\underline{H}_2$ cp), 2.01 (m, 1H, $C\underline{H}CH_3$), 2.12 (m, 1H, C1H), 2.52 (m, 1H, C2H), 4.16 (q, J= 6.87 Hz, 2H $OC\underline{H}_2CH_3$), 4.60 (dd, J= 4.01, 8.59 Hz, 1H, $C\underline{H}N$), 5.09 (s, 2H, $OC\underline{H}_2Ph$), 5.42 (d, J= 8.02 Hz, 1H, $N\underline{H}$), 7.3 (m, 5H, aryl); ^{13}C-NMR (125 MHz, $CDCl_3$): δ 11.16 ($CHCH_2\underline{C}H_3$), 13.59 ($OCH_2\underline{C}H_3$), 15.58 ($CH\underline{C}H_3$), 16.62 (cp $\underline{C}H_2$), 23.81 ($CH\underline{C}H_2CH_3$), 24.64 (C1), 27.25 (C2), 36.68 ($\underline{C}HCH_3$), 60.58 ($O\underline{C}H_2CH_3$), 64.71 ($\underline{C}HN$), 66.44 ($O\underline{C}H_2Ph$), 127.49-129.94 (aryl CH), 135.70 (4°aryl), 155.70 (Cbz $\underline{C}$=O), 170.91 (ester $\underline{C}$=O), 205.35 (ketone $\underline{C}$=O); mass spectrum (ESI-MS) *m/z* ($C_{20}H_{28}NO_5$) calculated for (M+1) 362.1967, found 362.1962.

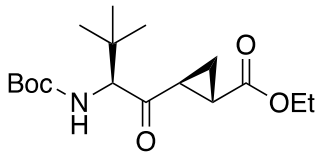

Ethyl (1*S*,2*S*)-2-((*S*)-2-((*tert*-butoxycarbonyl)amino)-3,3-dimethylbutanoyl) cyclopropane-1-carboxylate (25):To a stirred solution of **24** (55 mg, 0.21 mmol) in 1.0 mL anhydrous acetonitrile, was added freshly ground potassium carbonate (38 mg, 0.28 mmol), along with a solution of **20a** (25 mg, 0.060 mmol) in 0.5 mL anhydrous acetonitrile. **19** (23.6 μL, 0.21 mmol) was added and the solution was heated to reflux. After two hours, another portion of **19** (23.6 μL, 0.21 mmol) was added, and after four hours the final addition portion of **19** (23.6 μL, 0.21 mmol) was added. After 26 hours, the solution was poured into brine and extracted twice with EA. The organic layer was dried with anhydrous magnesium sulfate, filtered, and evaporated. The crude was purified

by CombiFlash to afford 44 mg (59%) of a pale yellow oil. The isomers were analyzed by NMR to identify a 91:9 *syn:anti* ratio. Rf 0.71 [EA/Hex 1:2]; $[\alpha]_D$= +105.6° (c 0.02, $CHCl_3$); ^{1}H-NMR (500 MHz, $CDCl_3$): δ 0.95 (s, 9H $CHC_4\underline{H}_9$), 1.23 (t, J= 6.87 Hz, 3H, $CH_2C\underline{H}_3$), 1.39 (s, 9H $OC_4\underline{H}_9$), 1.46 (m, 2H, cp $C\underline{H}_2$), 2.20 (m, 1H, C1H), 2.49 (m, 1H, C2H), 4.11 (q, J= 17.16 Hz , 2H $C\underline{H}_2CH_3$), 4.34 (d, J= 9.16 Hz, 1H $C\underline{H}N$), 5.22 (d, J= 9.16 Hz, 1H $N\underline{H}$); ^{13}C-NMR (125 MHz, $CDCl_3$): δ 14.2 ($CH_2\underline{C}H_3$), 18.2 (cp $\underline{C}H_2$), 26.2, C1), 26.9 ($CHC\underline{C}_3H_9$), 28.4 ($OC\underline{C}_3H_9$), 30.3 (C2), 35.2 ($CH\underline{C}C_3H_9$), 61.2 ($\underline{C}H_2CH_3$), 67.6 ($\underline{C}HN$), 79.8 ($O\underline{C}C_3H_9$), 155.6 (carbamate $\underline{C}$=O) 171.7 (ester $\underline{C}$=O), 207.5 (ketone $\underline{C}$=O). Exact mass spectrum (ESI-MS) *m/z* ($C_{17}H_{30}NO_5$) calculated for (M+1) 328.2124, found 328.2118.

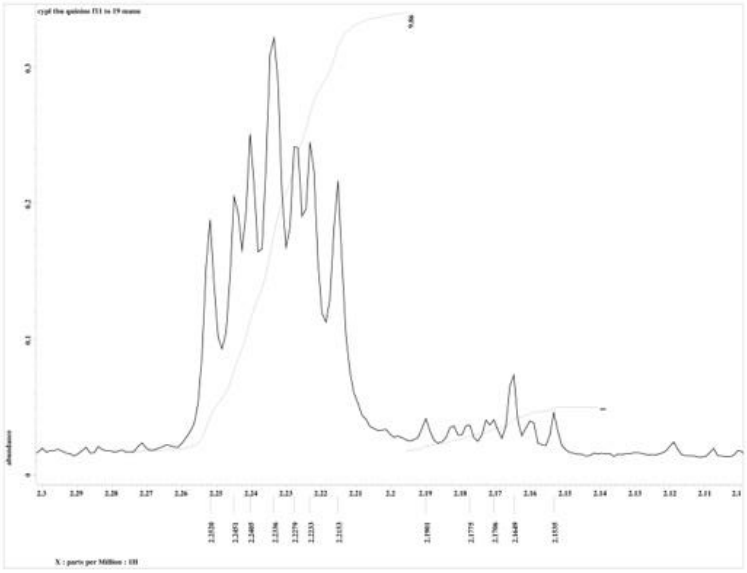

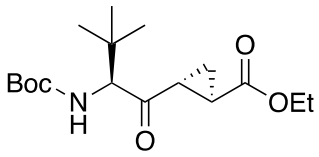

Ethyl (1*R*,2*R*)-2-((*S*)-2-((*tert*-butoxycarbonyl)amino)-3,3-dimethylbutanoyl) cyclopropane-1-carboxylate (26): To a stirred solution of **24** (55 mg, 0.21 mmol) in 1.0 mL anhydrous acetonitrile, was added freshly ground potassium carbonate (38 mg, 0.28 mmol), along with a solution of **20b** (25 mg, 0.060 mmol) in 0.5 mL anhydrous acetonitrile. **19** (23.6 μL, 0.21 mmol) was added and the solution was heated to reflux. After two hours, another portion of **19** (23.6 μL, 0.21 mmol) was added, and after four hours the final portion of **19** (23.6 μL, 0.21 mmol) was added. After 26 hours, the solution was poured into brine and extracted twice with EA. The organic layer was dried with anhydrous magnesium sulfate, filtered, and evaporated. The crude was purified by CombiFlash to afford 31 mg (42%) of a pale yellow oil. The isomers were analyzed by NMR to identify a 4:96 *syn:anti* ratio. Rf 0.68 [EA/Hex 1:2]; $[\alpha]_D$= -65.2° (c 0.02, $CHCl_3$); ^{1}H-NMR (500 MHz, $CDCl_3$): δ 0.98 (s, 9H, $CC_3\underline{H}_9$), 1.24 (t, J= 6.87 Hz, 3H $CH_2C\underline{H}_3$), 1.42 (s, 9H, $OCC_3\underline{H}_9$), 1.49 (m, J= 3.44 Hz, 2H cypl $C\underline{H}_2$), 2.17 (m, 1H, C1H), 2.55 (m, 1H, C2H), 4.13 (q, J= 7.45 Hz, 2H $C\underline{H}_2CH_3$), 4.32 (d, J= 9.16 Hz, 1H C<u>H</u>N), 5.20 (d, J= 8.59 Hz, 1H N<u>H</u>); ^{13}C-NMR (125 MHz, $CDCl_3$): δ 14.2 ($CH_2\underline{C}H_3$), 18.7 (cp $\underline{C}H_2$), 25.6 (C1), 26.8 ($CHC\underline{C}_3H_9$), 28.3 ($OC\underline{C}_3H_9$), 30.1 (C2), 35.0 ($CH\underline{C}C_3H_9$), 61.1 ($\underline{C}H_2CH_3$), 67.6 (<u>C</u>HN), 79.8 ($O\underline{C}C_3H_9$), 155.6 (carbamate <u>C</u>=O) 171.7 (ester <u>C</u>=O),

207.6 (ketone C=O). Exact mass spectrum (ESI-MS) *m/z* ($C_{17}H_{30}NO_5$) calculated for (M+1) 328.2124, found 328.2119.

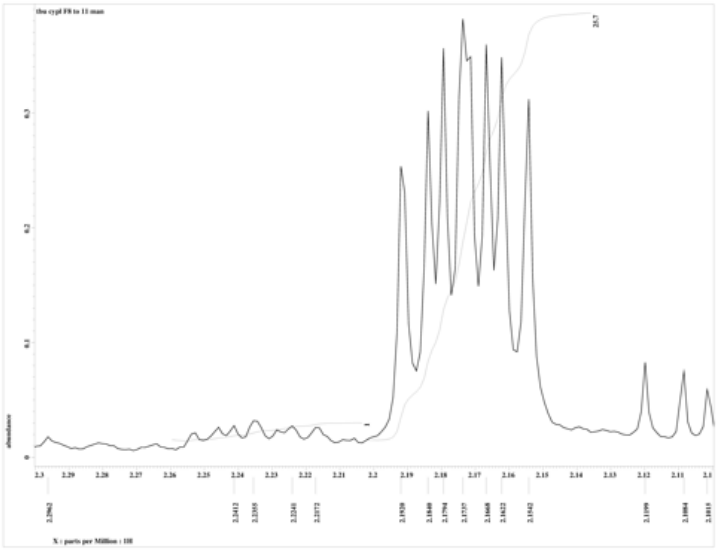

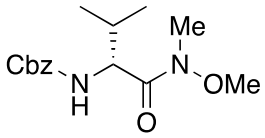

Benzyl (R)-(1-(methoxy(methyl)amino)-3-methyl-1-oxobutan-2-yl)carbamate (28): To a stirred solution of **27** (1000 mg, 3.98 mmol) in DCM (25mL), EDCI (763 mg, 3.98 mmol) was added, and after 15 minutes NEt_3 (0.60 mL, 4.2 mmol) and $NH(OCH_3)CH_3$ (388 mg, 3.98 mmol) were added. After 26 hours, the solution was poured into 1M HCl and extracted three times with DCM. The organic layer was collected and washed with aqueous $NaHCO_3$. The organic layer was collected, dried, and evaporated. The crude product was purified by CombiFlash to afford 811 mg (69%) of a pale-yellow oil. Rf 0.33 [EA-Hex 2:1]; $[\alpha]_D$= -3.36° (c 0.025, $CHCl_3$). ^{1}H-NMR (500

MHz, $CDCl_3$): δ 0.79 (dd, 6H, J=6.30, 14.89 Hz, CH($C\underline{H}_3$)$_2$)) 1.86 (septet, J=6.79 Hz, 1H, $C\underline{H}(CH_3)_2$), 2.97 (s, 3H, $NC\underline{H}_3$), 3.56 (s, 3H, $OC\underline{H}_3$), 4.50 (s, 1H, CH), 4.92 (dd, 2H, J=12.60, 40.09 Hz, $C\underline{H}_2$Cbz), 5.96 (d, 1H, J=9.16 Hz, N$\underline{H}$), 7.16-7.08 (m, 5H, aryl); ^{13}C-NMR (125 MHz, $CDCl_3$): δ 19.3, 17.7 (CH_3's), 31.2 ($\underline{C}H(CH_3)_2$), 31.6 ($N\underline{C}H_3$), 55.7 ($\underline{C}$HN), 61.4 ($O\underline{C}H_3$), 66.5 ($\underline{C}H_2$CBz), 128.3, 128.2, 127.9 (aryl), 136.6 (4° aryl $\underline{C}$),156.5 (Cbz $\underline{C}$=O), 172.5 (Weinreb $\underline{C}$=O).

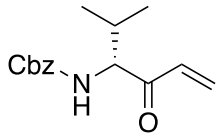

Benzyl (R)-(2-methyl-4-oxohex-5-en-3-yl)carbamate (29): To a solution of the **28** (300 mg, 1.02 mmol) in 2.6 mL anhydrous THF, at 0˚ C under an argon atmosphere, vinylmagnesium bromide (2.55 mL of a 1M solution in THF, 2.55 mmol) was added, and the solution was stirred for three hours, warming to room temperature. The mixture was poured into 1M HCl and extracted three times with EA. The organic layer was washed with aqueous sodium bicarbonate and then dried with anhydrous magnesium sulfate, filtered, and evaporated. The crude product was purified by CombiFlash to afford 168 mg (63%) of enone. Rf 0.60 [EA-Hex 1:1]; $[\alpha]_D$ = -66.6° (c 0.045, $CHCl_3$). ^{1}H-NMR (500 MHz, $CDCl_3$): δ 0.77, 1.00 (d, 3H each, J=6.88 Hz, CH($C\underline{H}_3$)$_2$), 2.15 (septet, J= 4.47 Hz, 1H, $C\underline{H}(CH_3)_2$), 4.64 (dd, J=4.12, 8.60 Hz, 1H, C$\underline{H}$N), 5.08 (s, 2H, $C\underline{H}_2$ Cbz), 5.69 (d, 1H, J=8.60 Hz, N$\underline{H}$), 5.83 (d, J=10.32 Hz, 1H, vinyl), 6.44 (m, J = 9.98 Hz, 2H, vinyl),7.33-7.25 (m, 5H, aryl); ^{13}C-NMR (125 MHz, $CDCl_3$): δ 16.7 ($\underline{C}H_3$), 19.9 ($\underline{C}H_3$), 30.7 ($\underline{C}$H isopropyl), 62.5 ($\underline{C}$HN), 70.0 ($C\underline{H}_2$ Cbz),128.6, 128.2, 128.1 (aryl), 130.1 ($\underline{C}H_2$ vinyl), 133.7 ($\underline{C}$H alkene), 136.5 (4° aryl C), 156.6 (Cbz $\underline{C}$=O), 198.4 (ketone $\underline{C}$=O).

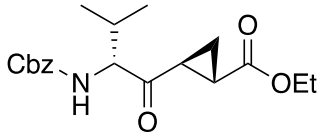

Ethyl (1S,2S)-2-(((benzyloxy)carbonyl)-D-valyl)cyclopropane-1-carboxylate (30): To a stirred **29** (80 mg, 0.31 mmol) in 2.0 mL anhydrous acetonitrile, freshly ground potassium carbonate (64 mg, 0.47 mmol) and a solution of quinine OBn (25 mg, 0.060 mmol) in 0.5 mL anhydrous acetonitrile were added. **19** (33.3 μL, 0.31 mmol) was added and the solution was heated to reflux. After two hours, another portion of **19** (33.3 μL, 0.31 mmol) was added, and after four hours the final portion of **19** (33.3 μL, 0.31 mmol) was added. After 20 hours, the solution was poured into brine and extracted twice with EA. The organic layer was dried with anhydrous magnesium sulfate, filtered, and evaporated. The crude was purified by CombiFlash to afford 53 mg (50%) of a yellow oil. The isomers were analyzed by HPLC to identify a 0:100 *syn*/*anti* ratio. Rf 0.77 [EA-Hex 1:1]; $[\alpha]_D$ = +5.4° (c 0.045, $CHCl_3$). ^{1}H-NMR (500 MHz, $CDCl_3$): δ 0.79 (d, 3H, J=6.87 Hz, CHC$\underline{H}_3$), 1.03 (d, 3H, J=6.87 Hz, CHC$\underline{H}_3$), 1.25 (t, 3H, J=76.87 Hz, $CH_2C\underline{H}_3$), 1.48 (t, J=6.30 Hz, 2H, C$\underline{H}_2$ cpyl), 2.14 (m, J= 2.86 Hz, 1H, CH cpyl), 2.29 (m, 1H, CH isopropyl), 2.52 (m, J= 1.72 Hz, 1H, CH cpyl), 4.15 (q, J=6.87 Hz, 2H, C$\underline{H}_2CH_3$), 4.58 (dd, J=8.60, 4.01 Hz, 1H, C$\underline{H}$N), 5.09 (AB, J_{AB}=12.0 Hz, 2H, CbzC$\underline{H}_2$), 5.45 (d, J=8.59 Hz, 1H, N$\underline{H}$), 7.34-7.31 (m, 5H, aryl); ^{13}C-NMR (125 MHz, $CDCl_3$): δ 205.9 (ketone $\underline{C}$=O), 171.6 (ester $\underline{C}$=O), 156.4 (Cbz $\underline{C}$=O), 136.3 (4˚ aryl), 128.6,128.2, 128.1 (aryl), 67.1 (Cbz $\underline{C}H_2$), 65.4 ($\underline{C}H_2CH_3$), 61.3 ($\underline{C}$HN), 30.3 (isopropyl $\underline{C}$H), 27.6 ($\underline{C}$H cpyl), 25.1 ($\underline{C}$H cpyl), 19.8 ($\underline{C}HCH_3$), 17.5 ($\underline{C}H_2$ cpyl), 16.8 (CH$\underline{C}H_3$), 14.2 ($CH_2\underline{C}H_3$).

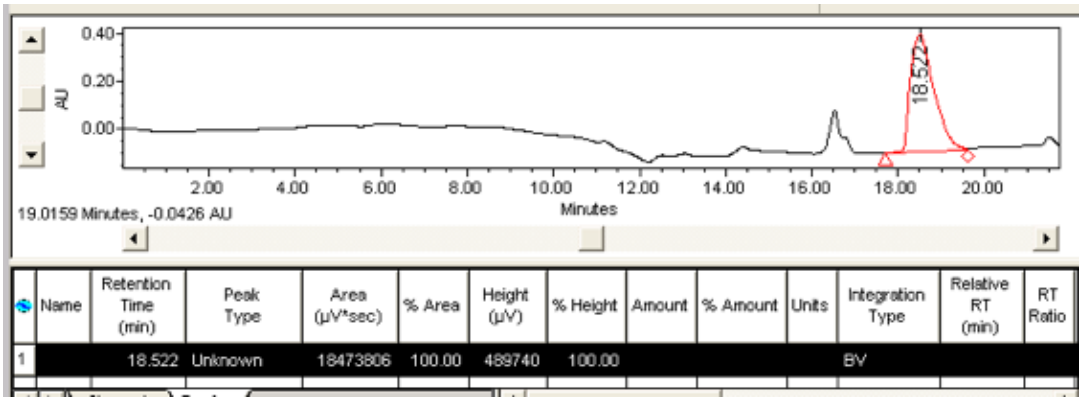

	Name	Retention Time (min)	Peak Type	Area (µV*sec)	% Area	Height (µV)	% Height	Amount	% Amount	Units	Integration Type	Relative RT (min)	RT Ratio
1		18.522	Unknown	18473806	100.00	489740	100.00				BV		

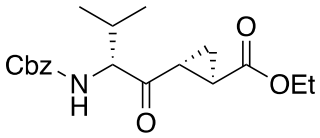

Ethyl (1R,2R)-2-(((benzyloxy)carbonyl)-D-valyl)cyclopropane-1-carboxylate (31):

To a stirred **29** (80 mg, 0.31 mmol) in 2.0 mL anhydrous acetonitrile, freshly ground potassium carbonate (64 mg, 0.47 mmol) and a solution of quinidine OBn (25 mg, 0.060 mmol) in 0.5 mL anhydrous acetonitrile were added. **19** (33.3 µL, 0.31 mmol) was added and the solution was heated to reflux. After two hours, another portion of **19** (33.3 µL, 0.31 mmol) was added, and after four hours the final portion of **19** (33.3 µL, 0.31 mmol) was added. After 20 hours, the solution was poured into brine and extracted twice with EA. The organic layer was dried with anhydrous magnesium sulfate, filtered, and evaporated. The crude was purified by CombiFlash to afford 60 mg (56%) of a yellow oil. The isomers were analyzed by HPLC to identify a 100:0 *syn*/*anti* ratio. Rf 0.77 [EA-Hex 1:1]; $[\alpha]_D$ = -11.0° (c 0.03, $CHCl_3$). ^{1}H-NMR (500 MHz, $CDCl_3$): δ 0.78 (d, 3H, J=6.87 Hz, CHC$\underline{H}_3$), 1.03 (d, 3H, J=6.87 Hz, CHC$\underline{H}_3$), 1.25 (t, 3H, J=76.87 Hz, $CH_2C\underline{H}_3$), 1.38, 1.48 (m, 2H, C$\underline{H}_2$ cpyl), 2.23 (m, J= 2.86 Hz, 1H, CH cpyl), 2.35 (m, 1H, CH isopropyl), 2.52 (m, J= 1.72 Hz, 1H, CH cpyl), 4.13 (q, J=6.87 Hz, 2H, C$\underline{H}_2CH_3$),

4.59 (dd, J=8.60, 4.01 Hz, 1H, CHN), 5.09 (s, 2H, CbzCH$_2$), 5.47 (d, J=8.59 Hz, 1H, NH), 7.34-7.30 (m, 5H, aryl); ^{13}C-NMR (125 MHz, $CDCl_3$): δ 205.9 (ketone C=O), 171.6 (ester C=O), 156.4 (Cbz C=O), 136.3 (4˚ aryl), 128.6, 128.2, 128.1 (aryl), 67.1 (Cbz CH_2), 65.4 (CH_2CH_3), 61.3 (CHN), 30.3 (isopropyl CH), 27.6 (CH cpyl), 25.1 (CH cpyl), 19.8 ($CHCH_3$), 17.5 (CH_2 cpyl), 16.8 ($CHCH_3$), 14.2 (CH_2CH_3).

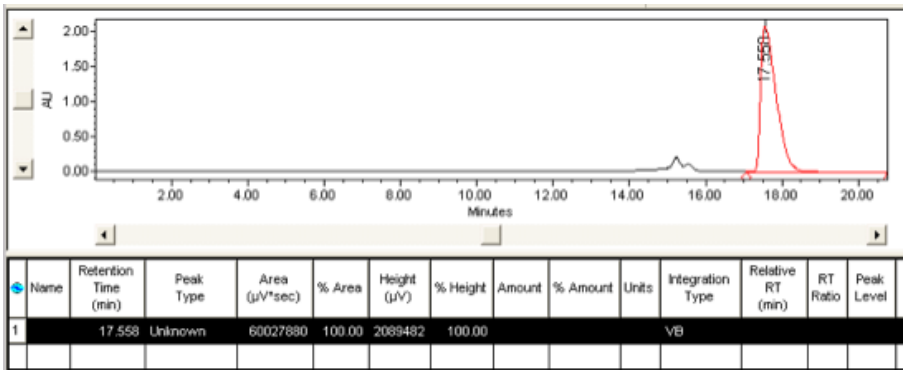

	Name	Retention Time (min)	Peak Type	Area (μV*sec)	% Area	Height (μV)	% Height	Amount	% Amount	Units	Integration Type	Relative RT (min)	RT Ratio	Peak Level
1		17.558	Unknown	60027880	100.00	2089482	100.00				VB			

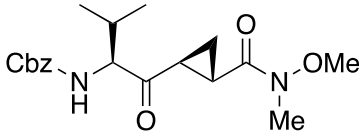

33a: To a stirred solution of **32a** (21 mg, 0.08 mmol) in 1.0 mL MeCN, freshly ground potassium carbonate (14 mg, 0.10 mmol), **20a** (25 mg, 0.060 mmol) dissolved in 0.5 mL MeCN, and **18** (43 mg, 0.18 mmol) were added and the solution was heated to reflux. After 21 hours, the solution poured into 1 M HCl and was extracted twice with EA after cooled to room temperature. The organic layer was collected and washed with brine then dried with anhydrous magnesium sulfate, filtered, and evaporated. The crude was purified by CombiFlash to afford 31 mg (100%) of a pale-yellow oil. The isomers were analyzed by HPLC to identify a 1:1 *syn*:*anti* ratio.

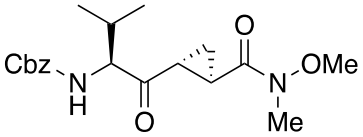

34a: To a stirred solution of **32a** (50.2 mg, 0.19 mmol) in 1.0 mL MeCN, freshly ground potassium carbonate (37 mg, 0.26 mmol), **20b** (25 mg, 0.060 mmol) dissolved in 0.5 mL MeCN, and **18** (102 mg, 0.42 mmol) were added and the solution was heated to reflux. After 23 hours, the solution poured into 1 M HCl and was extracted twice with EA after cooled to room temperature. The organic layer was collected and washed with brine then dried with anhydrous magnesium sulfate, filtered, and evaporated. The crude was purified by CombiFlash to afford 48 mg (70%) of a pale-yellow oil. The isomers were analyzed by HPLC to identify a 1:1 *syn*:*anti* ratio.

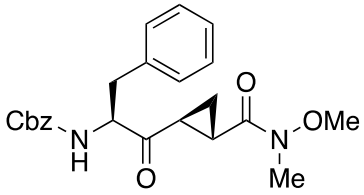

33b: To a stirred solution of **31b** (50 mg, 0.16 mmol) in 1.0 mL MeCN, freshly ground potassium carbonate (28 mg, 0.21 mmol), **20a** (25 mg, 0.060 mmol) dissolved in 0.5 mL MeCN, and **18** (85 mg, 0.35 mmol) were added and the solution was heated to reflux. After 28 hours, the solution poured into 1 M HCl and was extracted twice with EA after cooled to room temperature. The organic layer was collected and washed with brine then dried with anhydrous magnesium sulfate, filtered, and evaporated. The crude was purified by CombiFlash to afford 35 mg (53%) of a pale-yellow oil. The isomers were analyzed by NMR to identify a 1:1 *syn*:*anti* ratio.

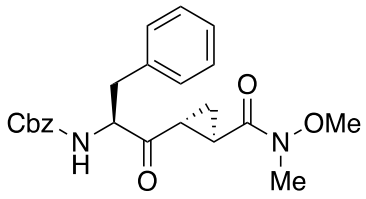

34b: To a stirred solution of **31b** (50 mg, 0.16 mmol), sodium hydride (14 mg, 0.35 mmol) in 1.0 mL DMSO, **18** (85 mg, 0.35 mmol), and **20b** (20 mg, 0.050 mmol) dissolved in 0.5 mL DMSO were added at room temperature under an argon atmosphere. After 15 minutes, the solution was poured into 1 M HCl and extracted three times with DCM. The organic layer was collected and washed with brine then dried with anhydrous magnesium sulfate, filtered, and evaporated. The crude was purified by CombiFlash to afford 47 mg (71%) of a pale-yellow oil. The isomers were analyzed by NMR to identify a 1:1 *syn:anti* ratio.

CHAPTER 3: RESULTS AND CONCLUSION

A. Synthetic rationale and results: cyclopropanation and lactonization

Cyclopropanation:

Cinchona catalysts were investigated to improve the stereoselectivity of the previously reported cyclopropanation of amino acid-derived enones. As previously mentioned, the use of Gaunt's quinine and quinidine methyl ethers resulted in limited diastereomeric selectivity. Thus, the use of bulkier quinine and quinidine benzyl ethers were investigated (**Scheme 2**). With quinine benzyl ether, the major product was the *syn* product, while using quinidine benzyl ether afforded the *anti* product for natural L-amino acids, which follows literature precedent. [33]

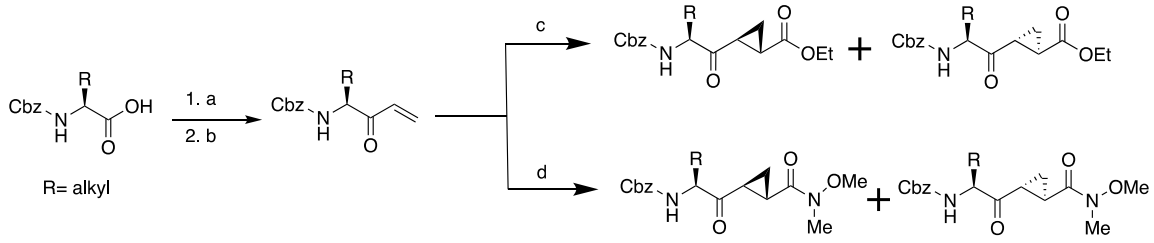

Reaction conditions: (a) EDCI, NEt_3, $NH(OCH_3)CH_3$; (b) $CH_2CHMgBr$; (c) **19**, **20a,b**, K_2CO_3; (d) **18**, **20a,b**, K_2CO_3.

Scheme 9: Stereoselective cyclopropanation route for keto-ester and Weinreb amide cyclopropyl peptidomimetics using quinine and quinidine benzyl ether.

The syntheses start with a Cbz-protected amino acid that was treated with $H_2N(OCH_3)(CH_3)$, EDCI, and triethylamine to afford the Weinreb amide amino acid. The Weinreb amide amino acid was then treated with vinylmagnesium bromide to afford the amino acid enone. The amino acid enone was then treated with either an

α–dimethylsulfide Weinreb amide or ethyl bromoacetate with potassium carbonate and the benzyl ether catalyst to afford the cyclopropyl Weinreb amides or the cyclopropyl keto-esters, respectively with stereoselectivity.

The cyclopropyl products were analyzed by integration of the cyclopropyl C1-H signal in the ^{1}H NMR or HPLC to determine the *syn:anti* ratio of the cyclopropane ring relative to the R group of the amino acid (**Table 3**).

Table 3: Cyclopropanation results using quinine and quinidine benzyl ether.

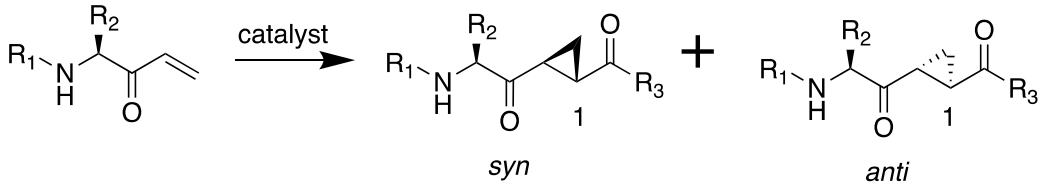

R_1	R_2	R_3	catalyst	*syn:anti ratio*
Cbz	*sec*-butyl	OEt	Quinine OBn	82:8
Cbz	*sec*-butyl	OEt	Quinidine OBn	7:93
Boc	*tert*-butyl	OEt	Quinine OBn	91:9
Boc	*tert*-butyl	OEt	Quinidine OBn	2:96
Cbz	isopropyl	$N(OCH_3)$ CH_3	Quinine OBn	50:50
Cbz	isopropyl	$N(OCH_3)$ CH_3	Quinidine OBn	50:50
Cbz	benzyl	$N(OCH_3)$ CH_3	Quinine OBn	50:50
Cbz	benzyl	$N(OCH_3)$ CH_3	Quinidine OBn	50:50

The *syn* and *anti* assignments were based on prior NMR and X-ray results. [26] The results indicated that quinine benzyl ether afforded high selectivity for the *syn* diastereomer, while quinidine benzyl ether afforded high selectivity for the *anti* diastereomer for the cyclopropyl keto-esters. No selectivity was observed in the cyclopropyl Weinreb amides.

Figure 14 shows a model to further investigate the mechanism of selectivity by using the unnatural Cbz-D-valine amino.

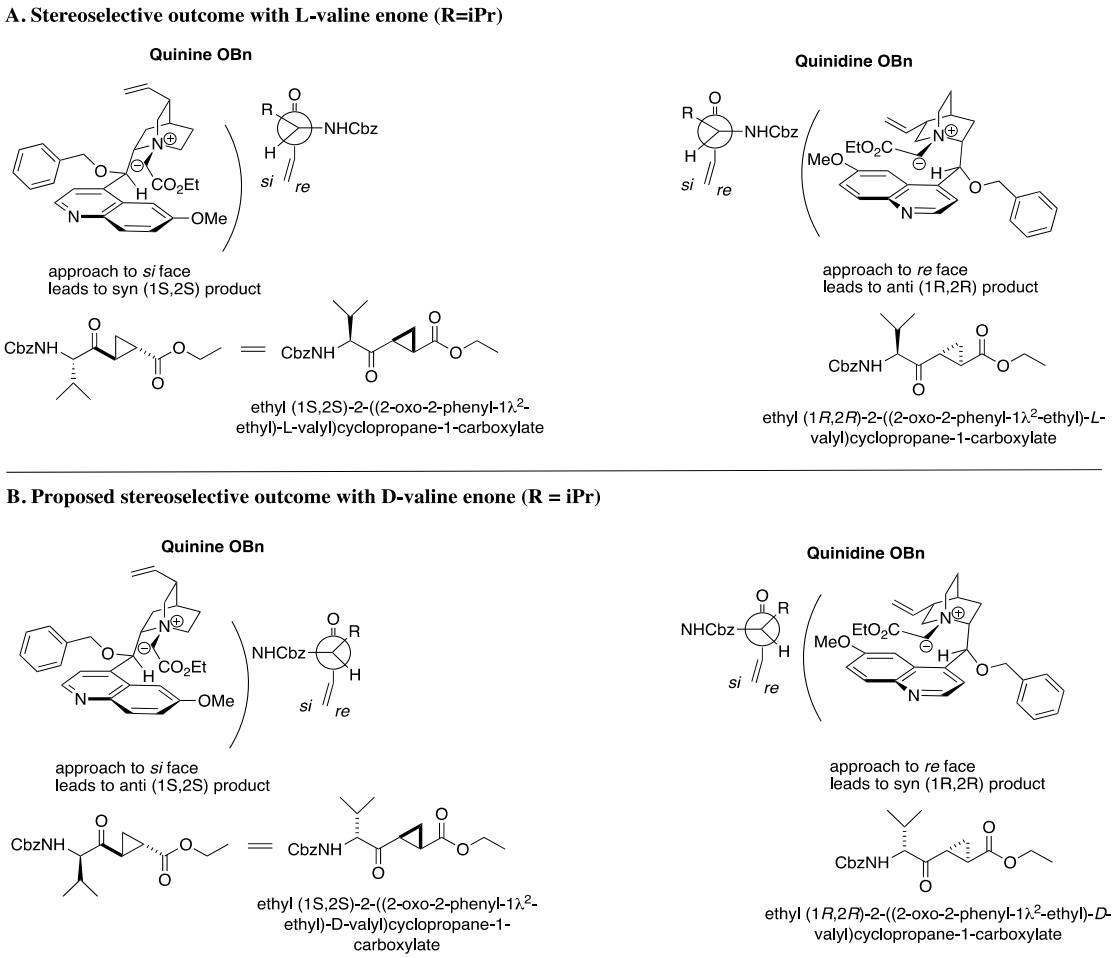

Figure 14: Proposed model for stereoselective cyclopropanation of natural (A) and unnatural (B) amino acid-derived enones.

The hypothesis, based on observed selectivity, was that the convex face of quinine OBn and quinidine OBn approached the amino acid-derived enone from the *si* face and the *re* of the alkene, respectively. For natural L-amino acids, addition to *si* face affords the *syn* product and addition to the *re* face affords the *anti* product. Thus, if the unnatural Cbz-D-valine amino acid was used, quinine OBn and quinidine OBn were expected to afford *anti* and *syn* addition, respectively. The model shows the enone in a Felkin-Anh conformation being approached by the catalysts' ylide intermediate from the convex side of the preferred *anti*-closed conformation where: anti refers to the orientation of the benzyl ether relative to the quinuclidine C-N bond and closed refers to the orientation of the quinuclidine ring over the bicyclic aryl system.[38-39]

The cyclopropanation of **29** provided evidence that the proposed model for stereoselective cyclopropanations seen in **Figure 14** was accurate. Treating **29** with quinine OBn afforded the *anti* product (**30**) while quinidine OBn afforded the *syn* product (**31**). HPLC and NMR analysis showed that the *syn:anti* ratio from quinine OBn was 0:100 and *vice versa* for quinidine OBn which showed a 100:0 ratio. These results are also consistent with Gaunt's work in stereoselective cyclopropanations using cinchona alkaloids (**Figure 15**).[33][40]

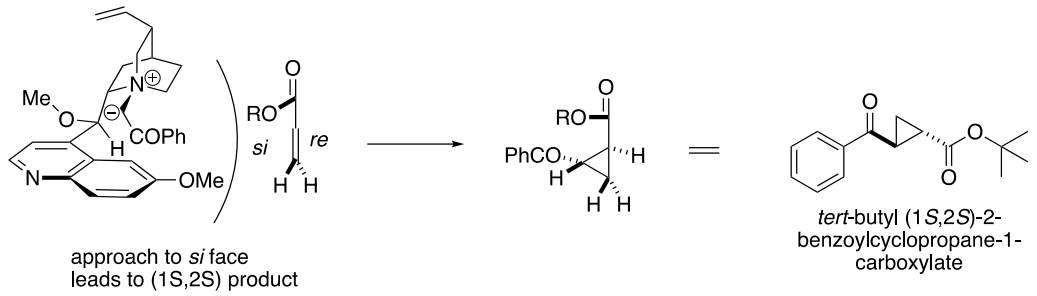

Figure 15: Gaunt's stereoselective cyclopropanation results of enone esters using the quinine methyl ether catalyst.

Figure 15 shows how the proposed model parallels Gaunt's original results of stereoselective cyclopropanations of enone esters using the quinine methyl ether catalyst, which affords addition to the *si* face as predicted.

The cyclopropyl keto-esters (**35**) were then reduced with $NaBH_4$ to afford the alcohols (**36**). The *N*-terminus was then deprotected *via* transfer hydrogenation and treated with phenylacetic acid and EDCI to replace the easily hydrolyzed carbamate group with the more stable amide bond (**37**). The *C*-terminus was then saponified with LiOH to afford the free acid (**38**), which can then be used to couple the β-lactone warhead (**Scheme 10**).

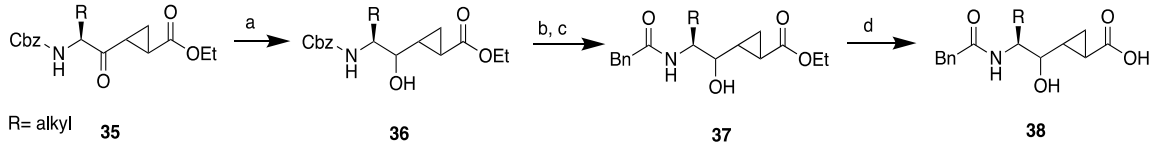

Reaction conditions: (a) $NaBH_4$; (b) Pd/C, ammonium formate; (c) phenylacetic acid, EDCI; (d) LiOH, H_2O.

Scheme 10: Synthesis of cyclopropyl peptidomimetic backbones from cyclopropyl keto-esters.

Lactonization:

Previous work in Dunlap's group concluded that reactive functional groups, such as β-lactones and β-lactams, were not easily coupled to the cyclopropyl peptidomimetics. For example, previous work using the un-substituted serine lactone has been unsuccessful.[41] However, current literature has shown that a 3-amino-4-methyl substituted β-lactone, derived from the lactonization of threonine, significantly increases the stability of the lactone.[21-22] This has developed interest in synthesizing a β-lactone warhead derived from threonine instead of the previously attempted serine-derived lactone.

Scheme 11 shows the proposed synthetic plan for lactone coupling. The rationale was to synthesize **2** from the intramolecular lactonization of **1** using BOP as an activating agent, which was then hydrogenated to afford the free amino β-lactone (**3**), which should then be immediately added to the *C*-terminus of the cyclopropyl peptidomimetic backbone (**39**).

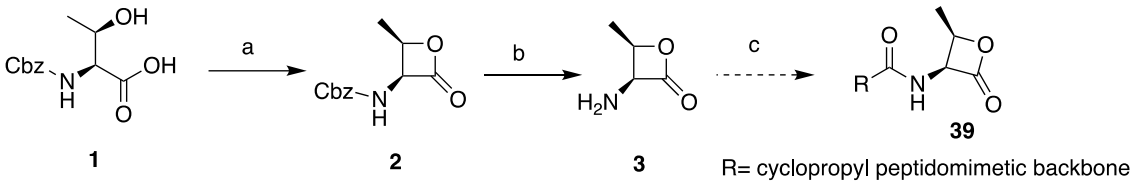

Reaction conditions: (a) BOP, NEt_3; (b) H_2, Pd/C; (c) Cyclopropyl peptidomimetic backbone, EDCI, NEt_3.

Scheme 11: Proposed method of direct lactone coupling to the cyclopropyl peptidomimetic backbone.

Due to limited supply of the cyclopropyl peptidomimetic backbones, model compounds were used to determine optimal coupling conditions. The first model compound used was cyclopropane carboxylic acid (**4**). In order to identify ideal coupling conditions for the cyclopropyl carboxylic acid and a 1˚ amine on a 2˚ carbon, several conditions were used with the acid and isopropylamine. Isopropylamine and **4** were used to help identify if the hindered amine or rigid acid was the issue in previous coupling attempts. Successful coupling of the model system using NHS and EDCI (80%) and oxalyl chloride and DMF (53%) determined that it is possible to couple a rigid cyclopropyl acid to a hindered amine.

Scheme 12 shows the conditions used for the coupling of **3** to the cyclopropyl carboxylic acid (**4**). The acid (**4**) was activated with either NHS and EDCI, or oxalyl chloride and DMF, and then the freshly prepared amino-lactone **3** was added to the solution.

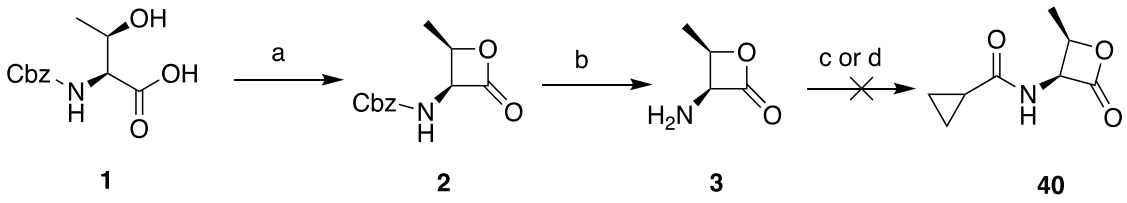

Reaction conditions: (a) BOP, NEt_3; (b) H_2, Pd/C; (c) **4**, EDCI, NHS; (d) **4**, $Cl_2(CO)_2$, DMF.

Scheme 12: Original synthetic conditions for lactone coupling using cyclopropane carboxylic acid as a model compound.

Unfortunately, both conditions failed as there was no amide coupling, indicating that instability of the amino-lactone is a problem, which is inconsistent with reports in literature. [42]

Since compound **3** is too unstable as a free amine, an alternative synthetic route was approached. **Scheme 13** shows the alternative synthesis of lactone coupling using the model acid **4**. This method couples the lactone precursor first (**6a,b**) to **4**, which was then saponified to afford **8**. The hydroxy-acid (**8**) then undergoes a intramolecular lactonization to obtain the cyclopropyl lactone amide (**40**). It was determined that **4** was not a good model system because **8** has poor solubility in organic solvents and was difficult to purify. Therefore, another model compound was used.

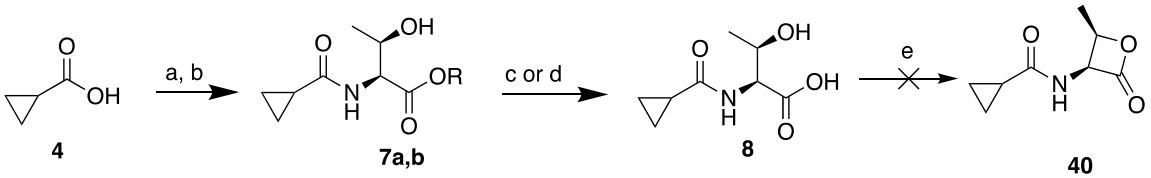

4 **7a,b** **8** **40**

Reaction conditions: (a) EDCI, HOBt; (b) **6a,b**, NEt_3; (c) LiOH; (d) Pd/C, ammonium formate; (e) BOP, NEt_3.

Scheme 13: Alternative synthetic conditions for lactone coupling using cyclopropane carboxylic acid as a model compound.

Fmoc-phenylalanine was used as an alternative model compound because it was readily available, it was a better representation of the peptide backbone relative to the simple acid (**4**), and it was expected to have better solubility. **Scheme 14** shows the alternative synthesis of lactone coupling using Fmoc-phenylalanine (**9**) as a model compound. This method couples the lactone precursor first (**6b**) to **9**, which was then saponified to **12**. Compound **12** would then undergo an intramolecular cyclization to

obtain the Fmoc-phenylalanine lactone amide (**41**). Unfortunately, the lactonization was unsuccessful due to the loss of the protecting group when using NEt_3, which afford an undesired product. Therefore a final model compound was investigated.

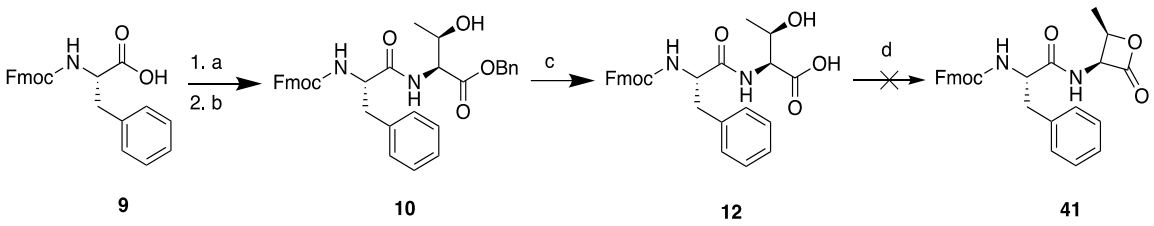

Reaction conditions: (a) EDCI; (b) **6b**; (c) H_2, Pd/C; (d) BOP, NEt_3

Scheme 14: Alternative synthetic conditions for lactone coupling using Fmoc-phenylalanine as a model compound.

Scheme 15 shows the same synthetic strategy using ibuprofen (**13**). Compound **13** was used because it was expected to be highly soluble in organic solvents and there was minimal risk of side reactions. As **Scheme 15** shows, the lactonization of **15** appeared to be successful on one attempt, but there was an equal amount of α,β unsaturated acid side product (**17**) formed. Unfortunately, when the same reaction conditions were repeated, it solely afforded **17**.

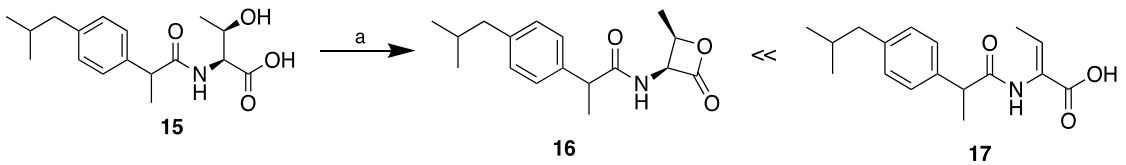

Reaction conditions: (a) BOP, NEt_3 (3, 2, 1, or 0 eq).

Scheme 15: Lactonization attempt of the ibuprofen model.

A series of conditions were tested for the ibuprofen model, varying NEt_3 equivalents, time, solvent, and temperature as variables in attempt to create a more selective reaction (**Table 4**). Every attempt yielded the unsaturated product or no product. Due to limited time and resources, more conditions were not tested.

Table 4: List of reaction conditions for the lactonization of the ibuprofen model compound.

	NEt_3 equivalents	Time	Solvent	Temperature ºC	Results
1	3 eq.	3 hours	DCM	1 hour at 0 2 hours at 25	50/50 lactone Unsaturated
2	3 eq.	19 hours	DCM	1 hour at 0 18 hours at 25	Unsaturated
3	3 eq.	2 hours	DCM	1 hour at 0 1 hours at 25	Unsaturated
4	3 eq.	6 hours	DCM	1 hour at 0 5 hours at 25	Unsaturated
5	2 eq.	2 hours	DCM	1 hour at 0 1 hour at 25	Unsaturated
6	2 eq.	24 hours	DMF	1 hours at 0 24 hours at 25	Unsaturated
7	1 eq.	3 hours	DCM	3 hours at 25	No product
8	0 eq.	5 hours	DMF	5 hours at 0	No product

B. Conclusions

Belactosin A, a natural product proteasome inhibitor, possesses promising efficacy as a chemotherapeutic due to its potent inhibitory effects of the proteasome. However, belactosin A is not used clinically due to its toxicity, which is why many labs globally are interested in synthesizing analogs with less toxic effects. There are many reported analogs of Belactosin A, but most syntheses required a substantial number of synthetic steps. The goals of this project were to develop a stereoselective cyclopropyl peptidomimetic backbone and couple a L-threonine-derived β-lactone warhead in a relatively low multi-step synthesis.

Previously, Dunlap's group has reported an efficient three-step synthesis of cyclopropyl peptidomimetics derived from amino acid Weinreb amides. Although the synthesis is substantially more efficient than most other reported cyclopropyl peptidomimetic syntheses, it lacks stereoselectivity of the cyclopropane moiety in regard to the amino acid R-group. This project has successfully developed highly selective cyclopropanations of amino acid-derived enones with the use of quinine and quinidine benzyl ether catalysts, as well as a model to accurately predict the stereochemistry. Quinine affords addition at the *si* face of the enone, while quinidine affords addition at the *re* face. Unfortunately, the use of cinchona catalysts only affords stereoselective control with the cyclopropyl keto-esters and not for the cyclopropyl Weinreb amides.

Coupling of the β-lactone warhead has proved to be the most challenging step of the synthesis. Previous work in literature has shown an efficient lactonization of β-hydroxy amino acids with the use of acid activating reagents. Literature has also shown that α-substituted β-lactones are significantly more stable than nonsubstituted lactones.

This information has inspired the synthesis of a β-lactone derived from L-threonine. Originally, the synthetic route for coupling the lactone was to first synthesize the *N*-Cbz-protected lactone, deprotect to get the free amine, and use acid activating reagents to form an amide bond between the acid and the free amine of the lactone. What seemed to be a trivial synthesis was unsuccessful. These results led to an alternative synthesis in which the acid protected amino acid was coupled to the backbone first, deprotected to give the free acid, and treated with acid activating reagents to afford the lactone. This synthetic route afforded a mixture of the lactone product and a α,β-unsaturated acid product once. When attempting to reproduce this data, only the unsaturated product was formed.

Scheme 16 shows the proposed full synthetic route of this project.

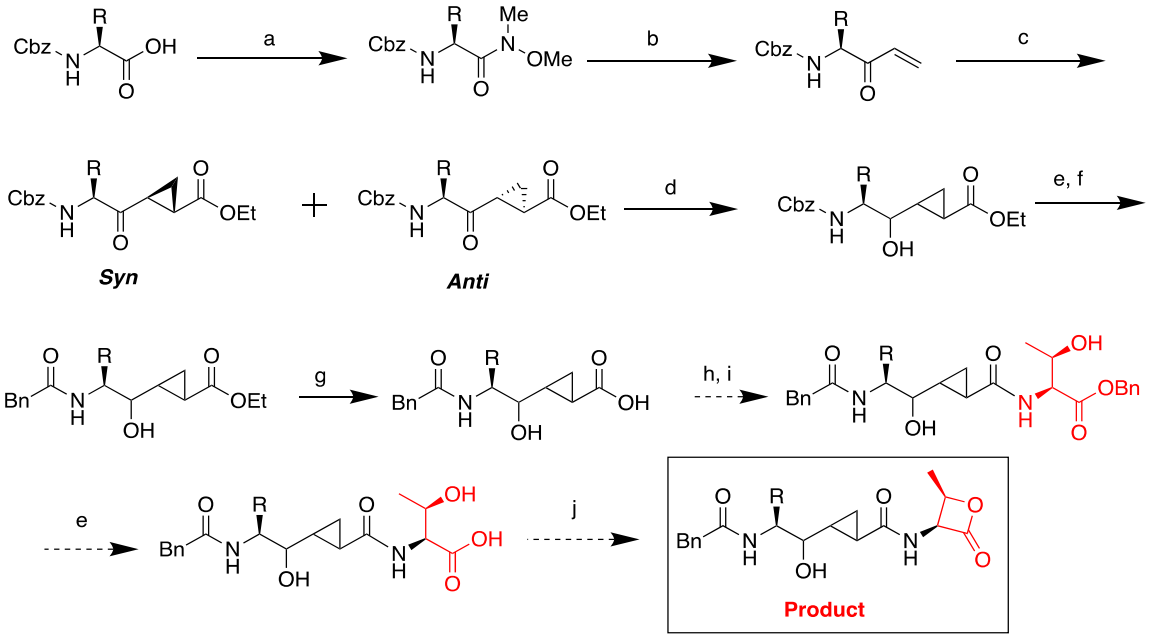

Reaction conditions: (a) EDCI, NEt_3, $NH(OCH_3)CH_3$; (b) $CH_2CHMgBr$; (c) **19**, **20a,b**, K_2CO_3; (d) $NaBH_4$; (e) Pd/C, NH_4HCO_2; (f) EDCI, phenylacetic acid; (g) LiOH, H_2O; (h) EDCI, HOBt; (i) **6b**, NEt_3; (j) BOP, NEt_3.

Scheme 16: Proposed full synthetic route of belactosin A analog.

This project has accomplished stereoselective synthesis of a cyclopropyl peptidomimetic backbone along with a proposed model to accurately predict the stereoselectivity. Selectivity was only observed with the cyclopropyl keto-esters and not the cyclopropyl Weinreb amides. Unfortunately, this project was unsuccessful in the coupling of the β-lactone warhead to the cyclopropyl peptidomimetic backbone.

REFERENCES FOR ACS

1. Siegel, R. L.; Miller, K. D.; Jemal, A. Cancer statistics, 2019. *CA CANCER J CLIN*. **2019**, *69 (1)*, 7-34.
2. Miller, K.D.; Nogueira, L.; Mariotto, A.B.; Rowland, J.H.; Yabroff, K.R.; Alfano, C.M.; Jemal, A.; Kramer, J.L.; Siegel, R.L. Cancer treatment and survivorship statistics, 2019. *CA A Cancer J Clin*, **2019**, *69*, 363-385.
3. Muthny, T.; *et. al.* The effect of new proteasome inhibitors, belactosin A and C, on protein metabolism in isolated rat skeletal muscle. *J Physiol Biochem*, **2009**, *65 (2)*, 137-146.
4. Thibaudeau, T. A.; Smith, D. M. A Practical Review of Proteasome Pharmacology. *Pharmaco. Rev.* **2019**, *71 (2)*, 170-197.
5. Tanaka K. The Proteasome: Overview of Structure and Function. *Proc. Jpn. Acad. Ser. B. Phys. Biol. Sci.* **2009**, *85 (1)*, 12–36.
6. Myung J.; Kim K. B.; Crews C. M. The Ubiquitin Protease Pathway and Proteasome Inhibitors. *Med. Res. Rev.* **2001**, *21 (4)*, 245-273.
7. Marques, A. J.; Palanimurugan, R.; Matias, A. C.; Ramos, P. C.; Dohmen, R. J. Catalytic Mechanism and Assembly of the Proteasome. *Chem.l Rev.* **2009**, *109 (4)*, 1509-1536.
8. Grigoreva, T. A.; Tribulovich, V. G.; Garabadzhiu, A. V.; Melino, G.; Barlev, N. A. The 26S proteasome is a multifaceted target for anti-cancer therapies. *Oncotarget*. **2015**, *6 (28)*, 24733–24749.
9. Kumartori, A. *et al.* Abnormally high expression of proteasome in human leukemia cells. *Proc. Natl. Acad. Sci.* **1990**, *87*, 7071-7075.

10. Dunlap, N. K.; Huryn, D. M. Medicinal Chemistry, Garland Science: New York, **2018**.
11. Chen, D.; Frezza, M., Schmitt S.; Kanwar, J.; Dou, Q. P. Bortezomib as the first proteasome inhibitor anticancer drug: current status and future perspectives. *Curr. cancer drug targets*. **2011**, *11 (3)*, 239–253.
12. Crawford, L. J.; Walker, B.; Irvine, A. E. Proteasome inhibitors in cancer therapy. *J. Cell Commun. Signal.* **2011**, *5 (2)*, 101–110.
13. Muli, C. S.; Tian, W.; Trader, D. J. Small-Molecule Inhibitors of the Proteasome's Regulatory Particle. *CHEMBIOCHEM.* **2019**, *20 (14)*, 1739-1753.
14. Genin, E.; Rebound-Ravaux, M.; Vidal, Joelle. Proteasome inhibitors: recent advances and new perspectives in medicinal chemistry *Curr. Top. Med. Chem*. **2010**, *10 (30)*, 232-256.
15. Tomaszewski, J. E.; Teicher, B. A. Proteasome Inhibitiors. *Biochem. Pharmacol.* **2015**, *19 (1)*, 1-9.
16. Kim K. B.; Crews C. M. From Epoxomicin to Carfilzomib: Chemistry, Biology, and Medical Outcomes. *Nat. Prod. Rep.* **2013**, *30 (5)*, 600-604.
17. Asai, A.; Hasegawa, A.; Ochiai, K.; Yamashita, Y.; Mizukami, T.; Belactosin A, a novel antitumor antibiotic acting on cyclin/CDK mediated cell cycle regulation, produced by *Streptomyces sp. J. Antibiotics*. **2000**, *53 (1)*, 81-83.
18. Shuto, S. *et. al.* Three-dimensional structure-activity relationship study of belactosin A and its stereo- and regioisomers: development of potent proteasome inhibitors by a stereochemical diversity-oriented strategy. *Org. Biomol. Chem*, **2009**, *7*, 1868-1877.

19. Romo, D.; *et. al.* Mechanistic Investigations of the $ZnCl_2$-Mediated Tandem Mukaiyama Aldol Lactonization: Evidence for Asynchronous, Concerted Transition States and Discovery of 2-Oxopyridyl Ketene Acetal Variants. *J. Am. Chem. Soc*. **2012**, *134*, 3084−3094.
20. de Meijere, A.; *et. al.* Synthesis and biological activity of simplified belactosin C analogues. *Org. Biomol. Chem.* **2012**, *10*, 6363.
21. Vederas, J. C.; *et al.* Serine and Threonine β-Lactones: A New Class of Hepatitis A Virus 3C Cysteine Proteinase Inhibitors. *J. Org. Chem.* **2002**, *67 (5),* 1536-1547.
22. Mor. M.; *et al.* N-(2-Oxo-3-oxetanyl)carbamic Acid Esters as N-Acylethanolamine Acid Amidase Inhibitors: Synthesis and Structure−Activity and Structure−Property Relationships. *J. Med. Chem.* **2012**, *55*, 4824-4836.
23. Inui N.; Kitagawa K.; Miwa S.; Hattori T.; Chida K.; Nakamura H.; Kitagawa M. High expression of Cks1 in human non-small cell lung carcinoma. *Biochem. Biophys. Res. Commun.* **2003**, *303*, 978–984.
24. Tamura D.; *et. al*. Bortezomib potentially inhibits cellular growth of vascular endothelial cells through suppression of G2/M transition. *Cancer Sci.* **2010**, *101*, 1403–1408.
25. Giannis, A.; Kolter, T. Peptidomimetics for Receptor Ligands—Discovery, Development, and Medical Perspectives. *Angew. Chem. Int. Ed.* **1993**, *32 (9)*, 1244–1267.
26. Dunlap, N.; *et al*.; Three- Step Synthesis of Cyclopropyl Peptidomimetics. *Org. Lett.* **2011**, *13 (18)*, 4879-4881.

27. Shuto, S.; et al.; Synthesis of 2,3- and 3,4-Methanoamino Acid Equivalents with Stereochemical Diversity and Their Conversion into the Tripeptide Proteasome Inhibitor Belactosin A and Its Highly Potent Cis-Cyclopropane Stereoisomer. *Org. Lett.* **2008**, *10 (16),* 3571-3574.

28. Martin, S.; *et al.* Cyclopropane-Derived Peptidomimetics. Design, Synthesis, and Evaluation of Novel Ras Farnesyltransferase Inhibitors Michael. *J. Org. Chem*. **2001**, *66,* 1657-1671.

29. Wipf, P.; Xiao, J. Convergent Approach to (*E*)-Alkene and Cyclopropane Peptide Isosteres *Org. Lett.* **2005**, *7 (1),* 103–106.

30. Dunlap, N. K.; Basham, J.; Wright, M.; Smith, K.; Chapa, O.; Huang, J.; Shelton, W.; Yatsky, Y. Synthesis of nitrocyclopropyl peptidomimetics. *Tetrahedron Lett*. **2013**, *54*, 6596-6598.

31. Riches, S.L.; Saha, C.; Filgueira, N.F.; Grange, E.; McGarrigle, E.M.; Aggarwal, V.K. On the mechanism of ylide-mediated cyclopropanations: evidence for a proton-transfer step and its effect on stereoselectivity. *J. Am. Chem. Soc.* **2010**, *132 (22),* 7626-7630.

32. Waschołowski, V.; Hansen, H.M.; Longbottom, D.A.; Ley, S.V. A general organocatalytic enantioselective nitrocyclopropanation reaction. *Synthesis*. **2008**, *8*, 1269-1275.

33. Gaunt, M.J. and Johansson, C.C. Recent developments in the use of catalytic asymmetric ammonium enolates in chemical synthesis. *Chem. Rev.* **2007**, *107 (12),* 5596-5605.

34. Asai, A.; Tsujita, T.; Sharma, S. V.; Yamashita, Y.; Akinaga, S.; Funakoshi, M.; Kobayashi, H.; Mizukami, T. A new structural class of proteasome inhibitors identified by microbial screening using yeast-based assay. *Biochem. Pharmacol*. **2004**, *67*, 227-234.

35. de Meijere, A.; *et.* al Enantioselective Total Syntheses of Belactosin A, Belactosin C, and Its Homoanalogue. *Org. Lett.* **2004**, *6 (13)*, 2153–2156.

36. Romo, D.; Choo, S. Total Synthesis of (−)-Belactosin C and Derivatives via Double Diastereoselective Tandem Mukaiyama Aldol Lactonizations. *Org. Lett.* **2007**, *9 (8)*, 1537–1540.

37. Charette, A. *et. al.* Formal Synthesis of Belactosin A and Hormaomycin via a Diastereoselective Intramolecular Cyclopropanation of an α-Nitro Diazoester. *Org. Lett.* **2010**, *12 (4)*, 672–675.

38. Dijkstra, G.D.; Kellogg, R.M.; Wynberg, H.; Svendsen, J.S.; Marko, I.; Sharpless, K.B., Conformational study of cinchona alkaloids. A combined NMR, molecular mechanics and x-ray approach. *J. Am. Chem. Soc.* **1989**, *111* (*21*), 8069-8076.

39. Caner, H.; Biedermann, P.U.; Agranat, I. Conformational spaces of Cinchona alkaloids. *Chirality*. **2003**, *15 (7)*, 637-645.

40. Papageorgiou, C. D.; Cubillo de Dios, M. A.; Ley, S. V; Gaunt, M. J. Enantioselective organocatalytic cyclopropanation via ammonium ylides. *Angew. Chem. Int.* **2004**, *43 (35)*, 4641-4644.

41. Dawson, K. A. Synthesis of Belactosin A Analogs. M.S Thesis, Middle Tennessee State University: Murfreesboro, TN, **2014**.

42. Sharifzadeh, S.; Boersma, M.J.; Kocaoglu, O.; Shokri, A.; Brown, C.L.; Shirley, J.D.; Winkler, M.E.; Carlson, E.E. Novel electrophilic scaffold for imaging of essential penicillin-binding proteins in Streptococcus pneumoniae. *ACS Chem. Biol.* **2017**, *12 (11)*, 2849-2857.

APPENDICES

APPENDIX A: NMR DATA

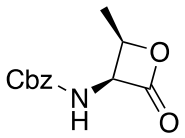

^{1}H-NMR

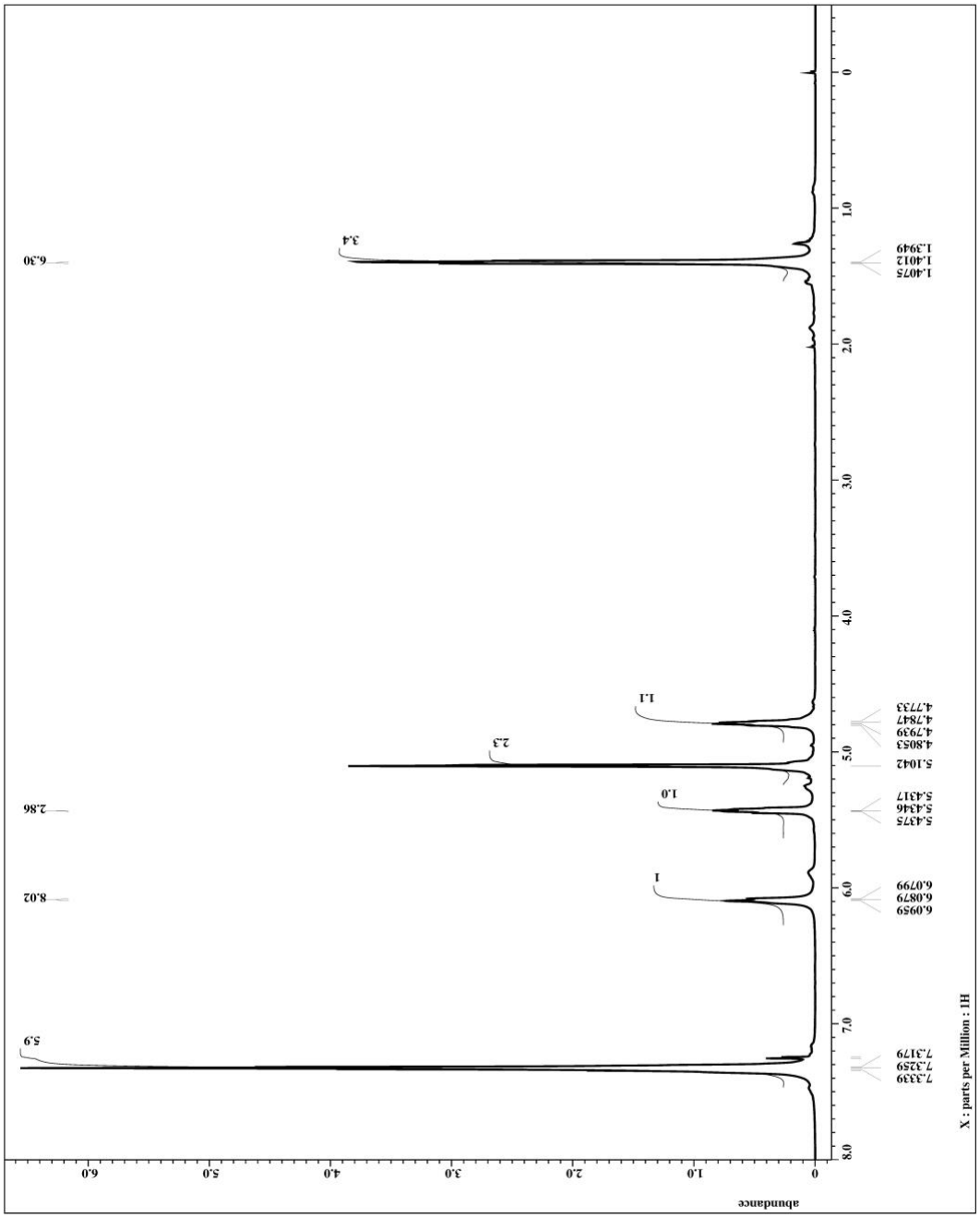

^{13}C-NMR

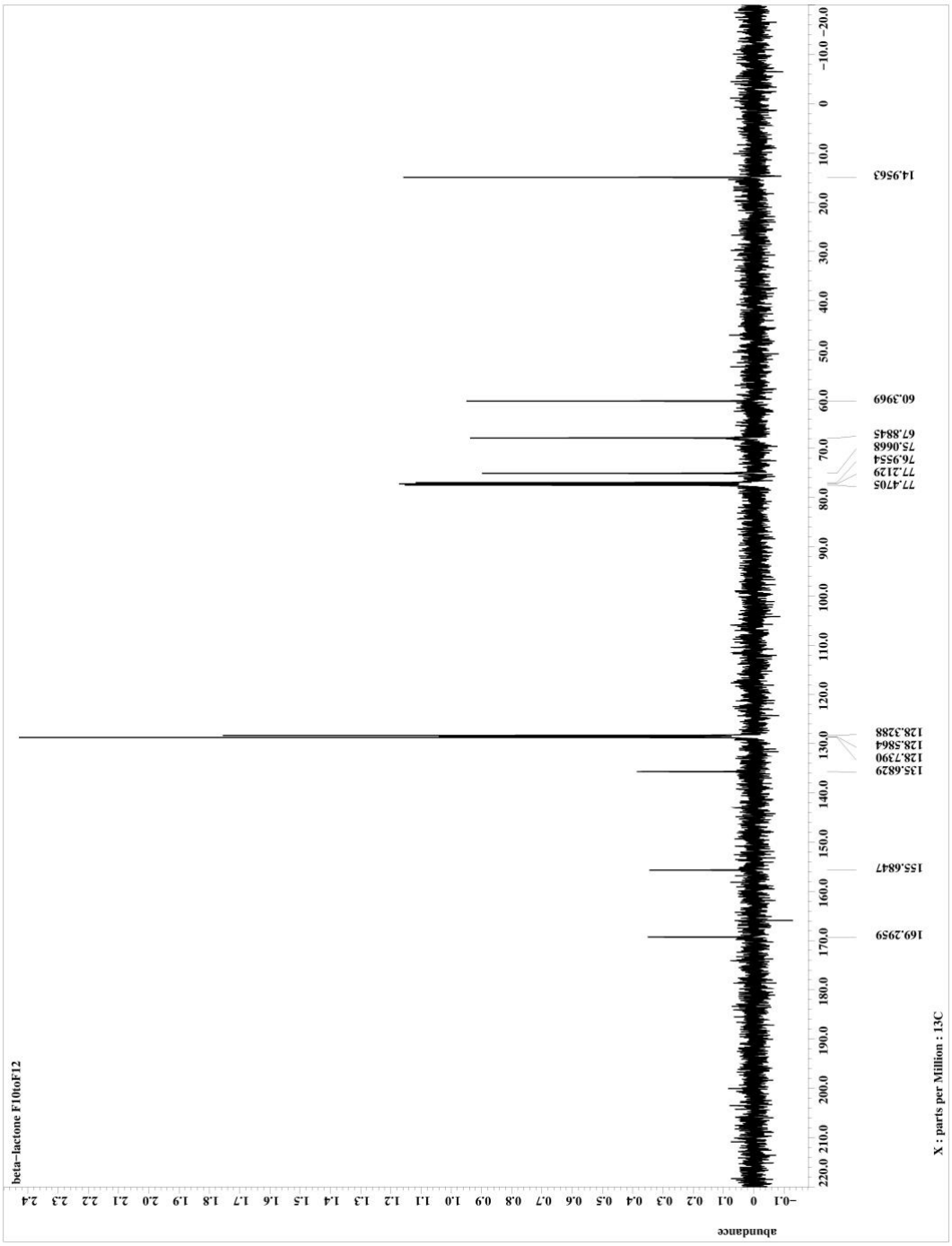
14.9563
60.3969
67.8845
75.0668
76.9554
77.2129
77.4705
128.3288
128.5864
128.7390
135.6829
155.6847
169.2959
X : parts per Million : 13C
beta-lactone F10toF12
abundance

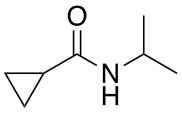
O
N
H

^{1}H-NMR

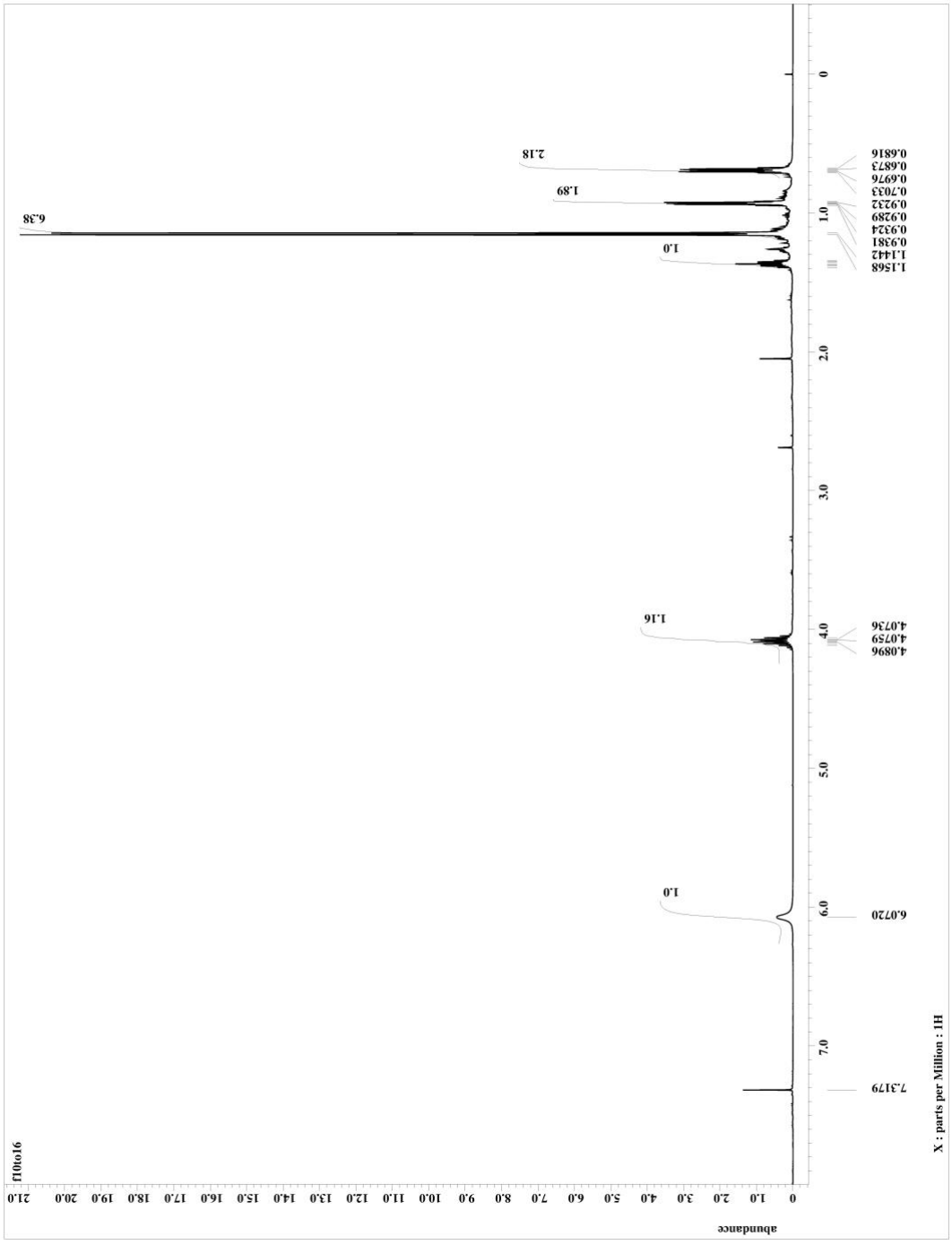
f10to16
abundance
X : parts per Million : 1H
7.3179
6.0720
4.0896
4.0759
4.0736
1.1568
1.1442
0.9381
0.9324
0.9289
0.9232
0.7033
0.6976
0.6873
0.6816
6.38
2.18
1.89
1.16
1.0
1.0

^{13}C-NMR

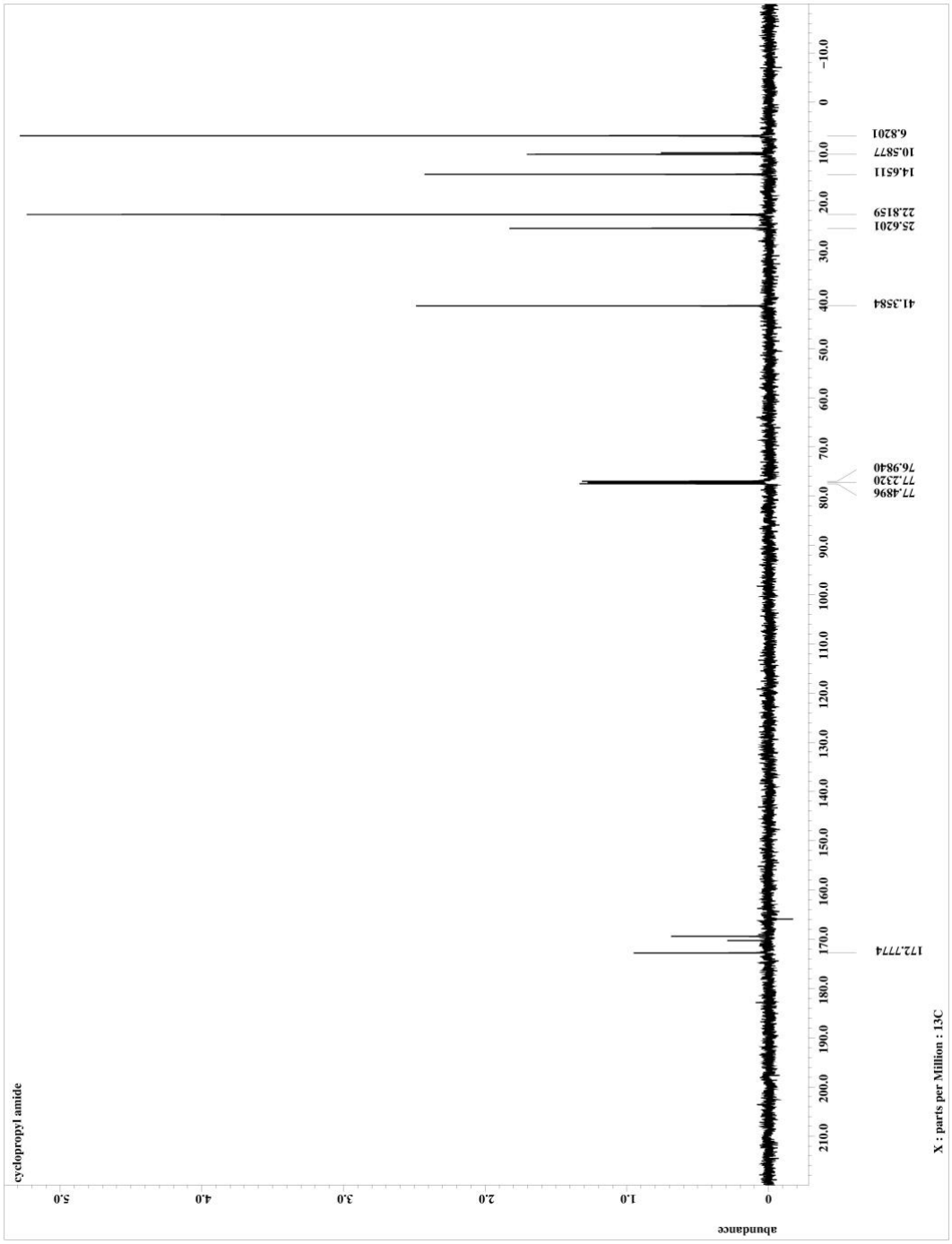
cyclopropyl amide
abundance
X : parts per Million : 13C
172.7714
77.4896
77.2320
76.9840
41.3584
25.6201
22.8159
14.6511
10.5877
6.8201

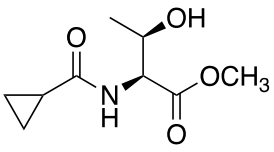
OH
O
N
H
OCH3
O

^{1}H-NMR

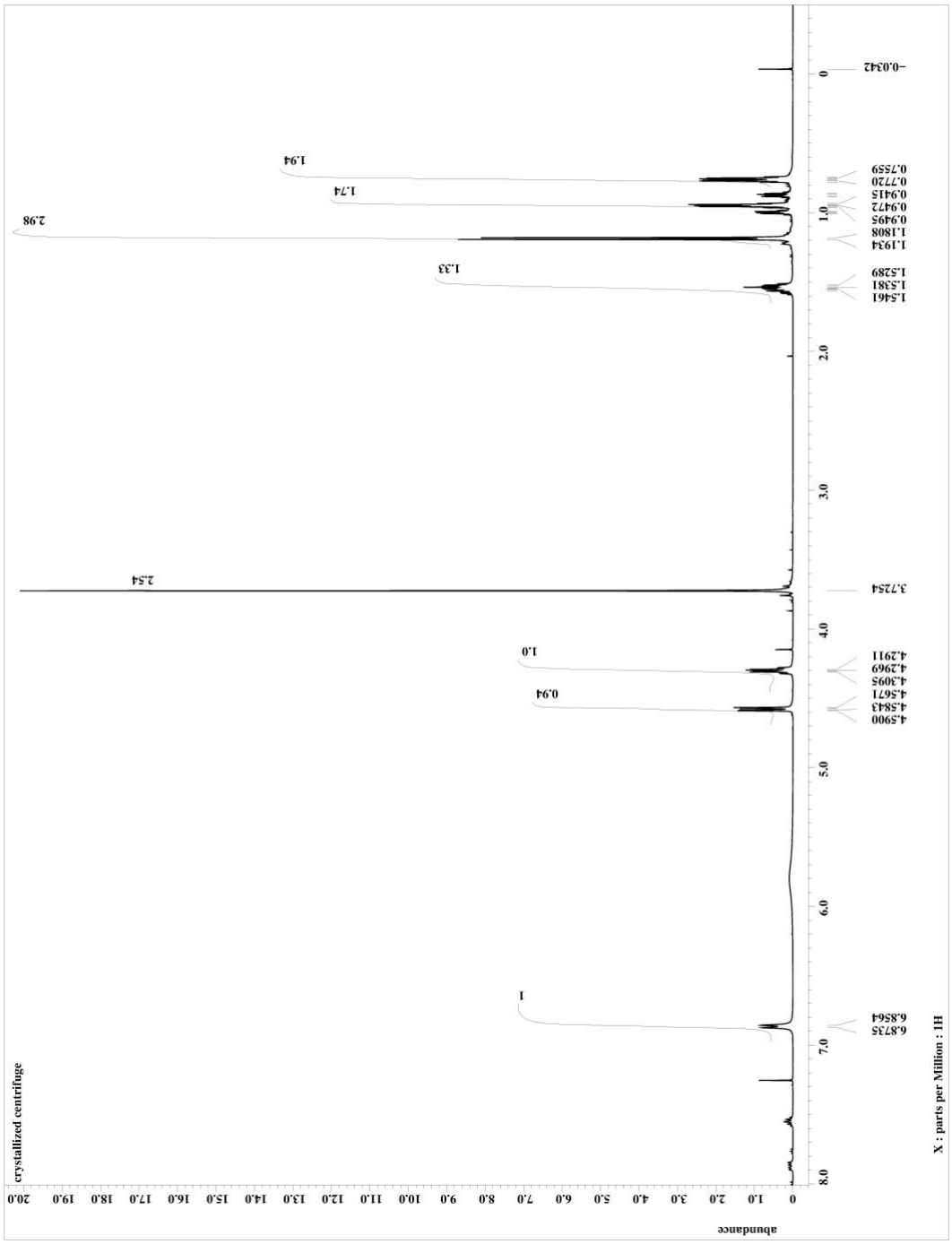
crystallized centrifuge
abundance
X : parts per Million : 1H
6.8735
6.8564
4.5900
4.5843
4.5671
4.3095
4.2969
4.2911
3.7254
1.5461
1.5381
1.5289
1.1934
1.1808
0.9495
0.9472
0.9415
0.7720
0.7559
-0.0342
2.54
2.98
1.33
1.94
1.74
1.0
0.94
1

^{13}C-NMR

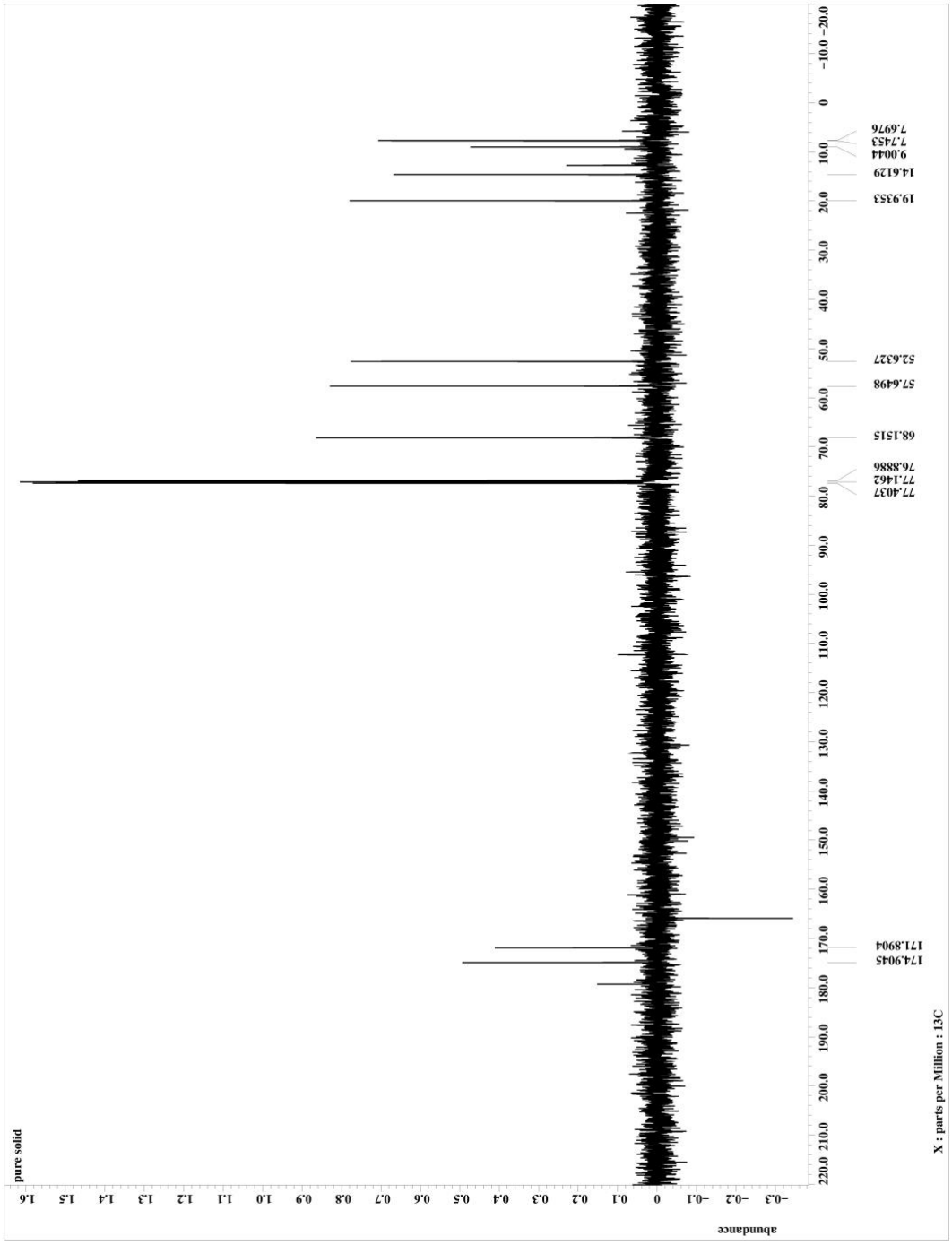
pure solid
abundance
X : parts per Million : 13C
174.9045
171.8904
77.4037
77.1462
76.8886
68.1515
57.6498
52.6327
19.9353
14.6129
9.0044
7.7453
7.6976

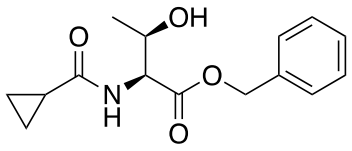
OH
O
N
H
O
O

^{1}H-NMR

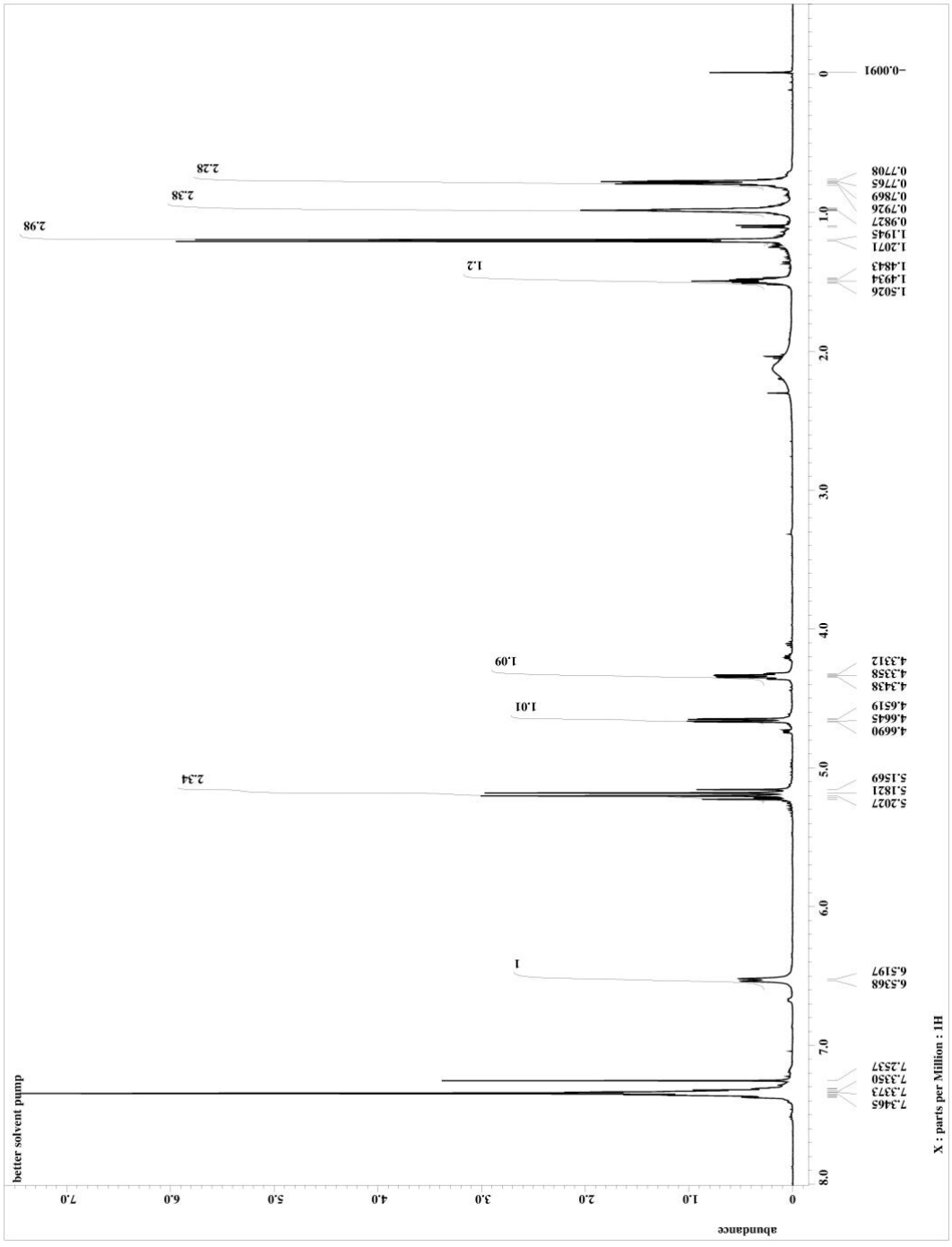
better solvent pump
abundance
X : parts per Million : 1H
-0.0091
7.3465
7.3373
7.3350
7.2537
6.5368
6.5197
5.2027
5.1821
5.1569
4.6690
4.6645
4.6519
4.3438
4.3358
4.3312
1.5026
1.4934
1.4843
1.2071
1.1945
0.9827
0.7926
0.7869
0.7765
0.7708
2.98
2.38
2.28
1.2
1.09
1.01
2.34
1

^{13}C-NMR

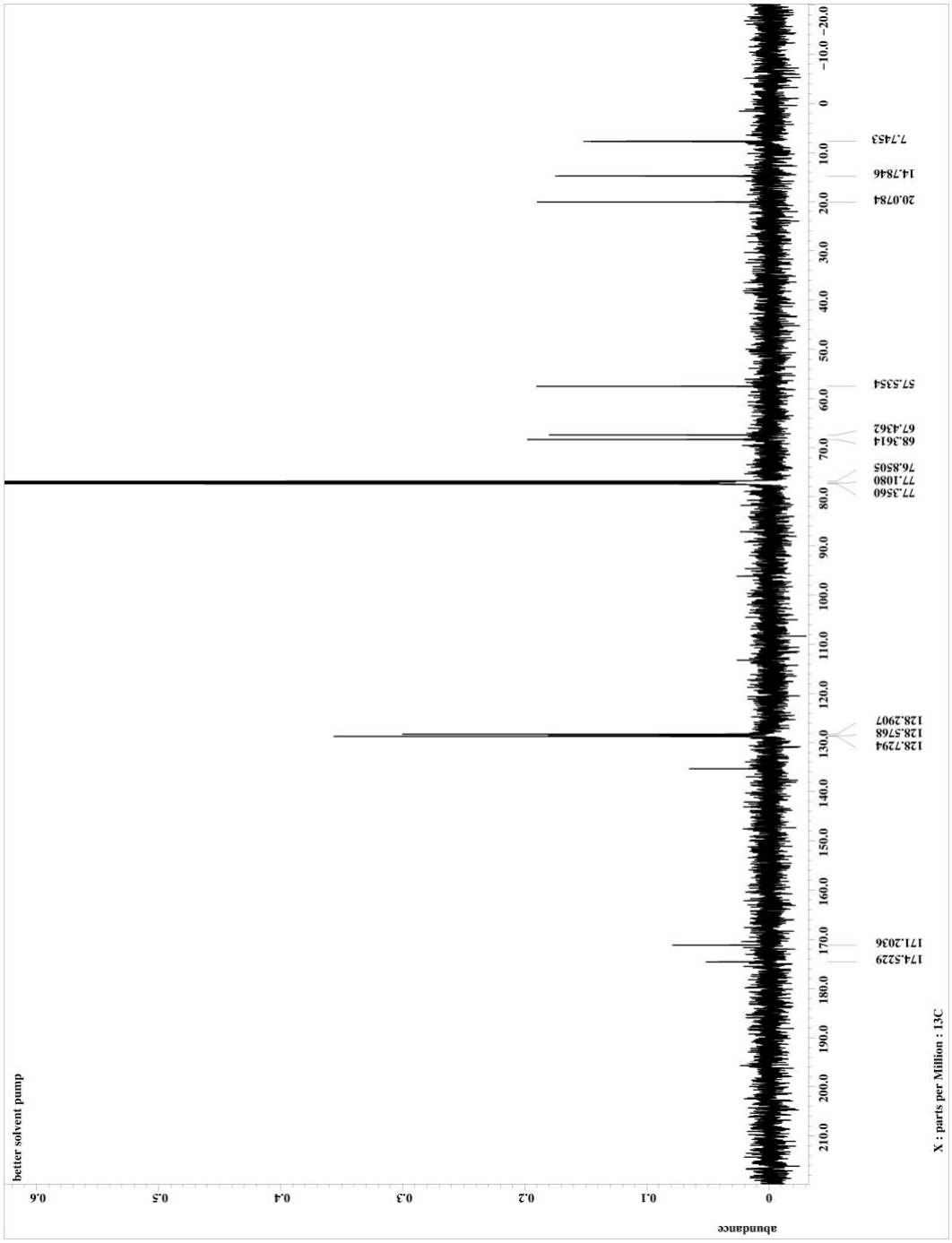
better solvent pump
abundance
X : parts per Million : 13C
174.5229
171.2036
128.7294
128.5768
128.2907
77.3560
77.1080
76.8505
68.3614
67.4362
57.3354
20.0784
14.7846
7.7453

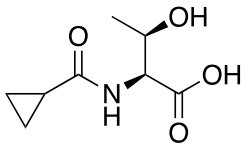
OH
O
N
H
OH
O

^{1}H-NMR

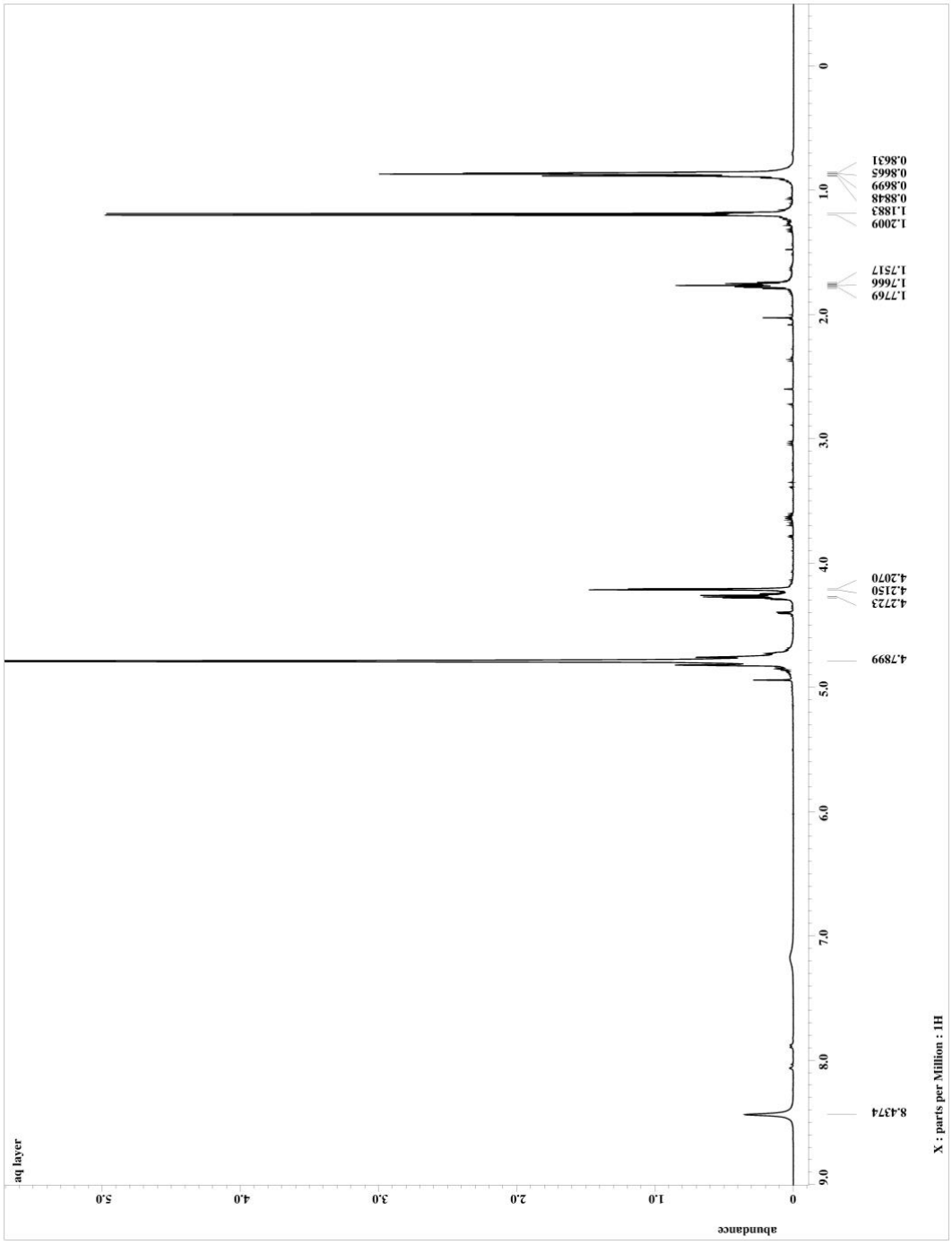
aq layer
abundance
X : parts per Million : 1H
8.4374
4.7899
4.2723
4.2150
4.2070
1.7769
1.7666
1.7517
1.2009
1.1883
0.8848
0.8699
0.8665
0.8631

^{13}C-NMR

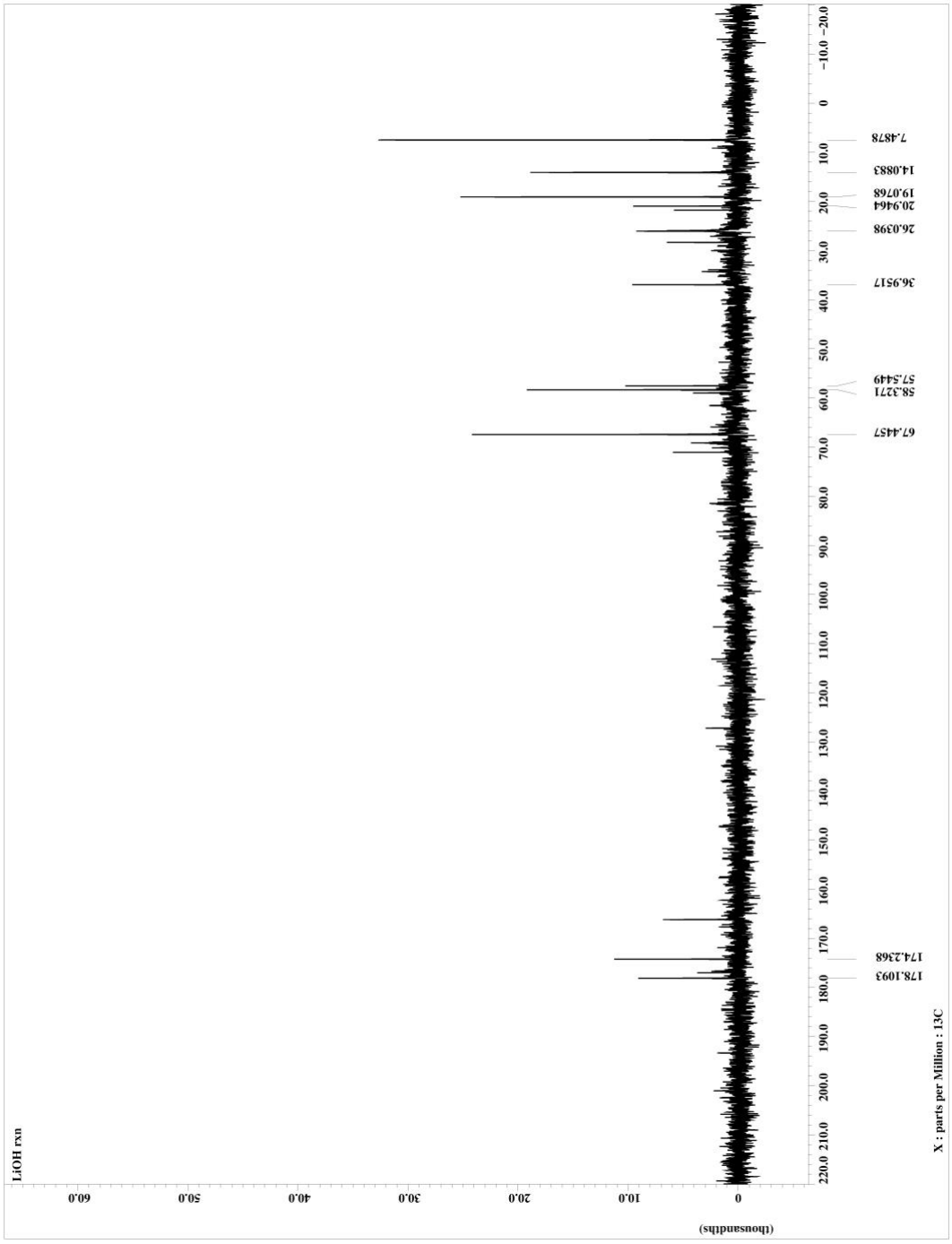
7.4878
14.0883
19.0768
20.9464
26.0398
36.9517
57.5449
58.3271
67.4457
174.2368
178.1093
X : parts per Million : 13C
(thousandths)
LiOH rxn

^{1}H-NMR

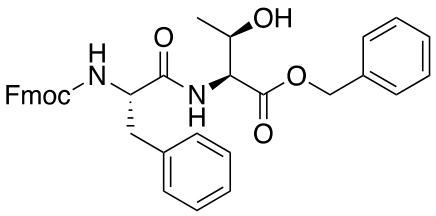
OH
O
H
N
Fmoc
N
H
O
O

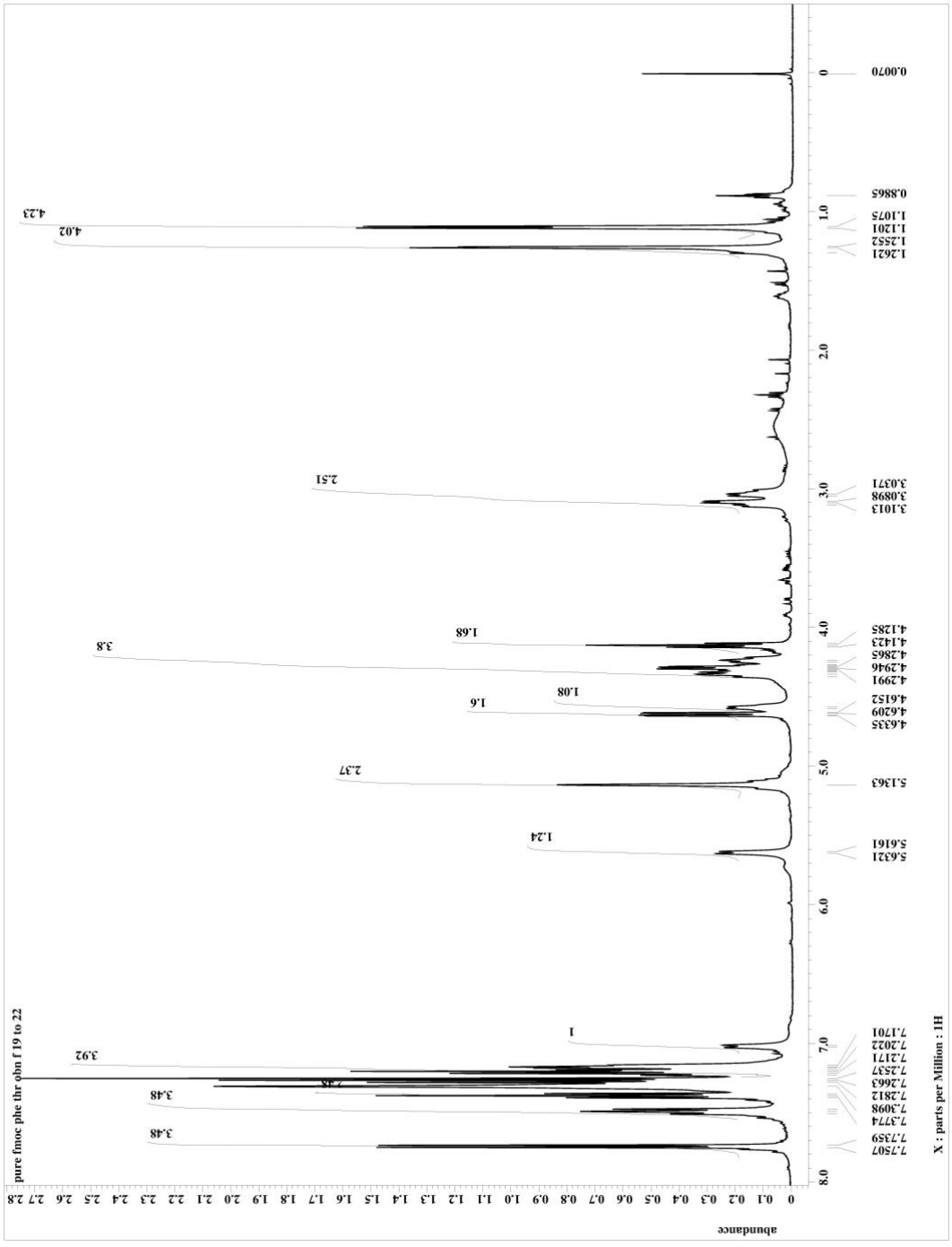
pure fmoc phe thr obn f 19 to 22
abundance
X : parts per Million : 1H
7.7507
7.7359
7.3774
7.3098
7.2812
7.2663
7.2537
7.2171
7.2022
7.1701
5.6321
5.6161
5.1363
4.6335
4.6209
4.6152
4.2991
4.2946
4.2865
4.1423
4.1285
3.1013
3.0898
3.0371
1.2621
1.2552
1.1201
1.1075
0.8865
0.0070
3.92
3.48
3.48
3.48
1
1.24
2.37
1.6
1.08
3.8
1.68
2.51
4.02
4.23

^{13}C-NMR

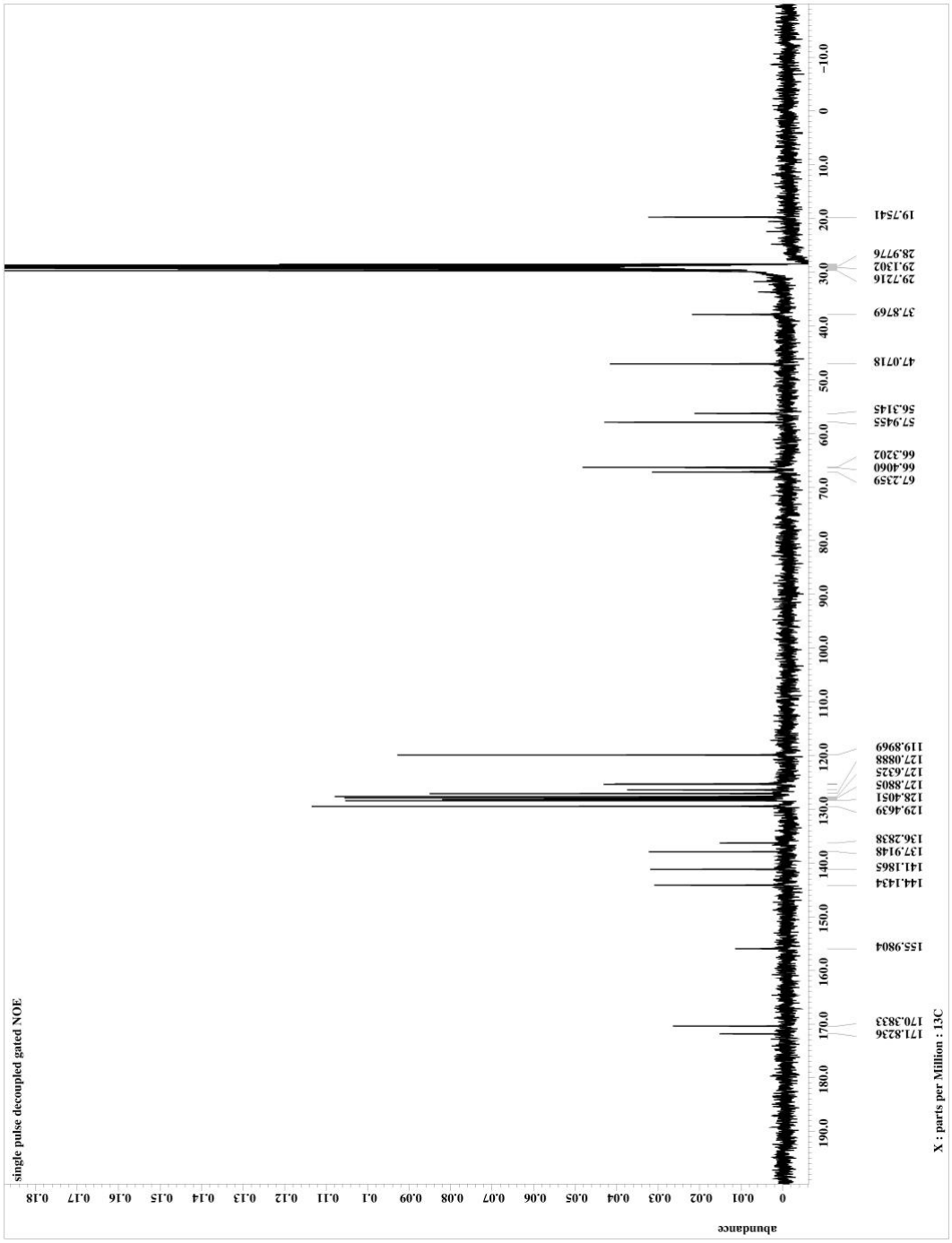
19.7541
28.9776
29.7216
29.1302
37.8769
47.0718
56.3145
57.9455
66.3202
66.4060
67.2359
119.8969
127.0888
127.6325
127.8805
128.4051
129.4639
136.2838
137.9148
141.1865
144.1434
155.9804
170.3833
171.8236
X : parts per Million : 13C
single pulse decoupled gated NOE
abundance

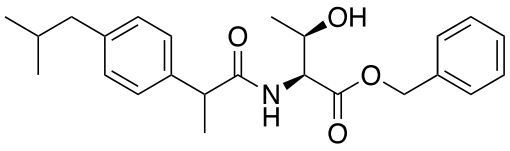
OH
O
N
H
O
O

^{1}H-NMR

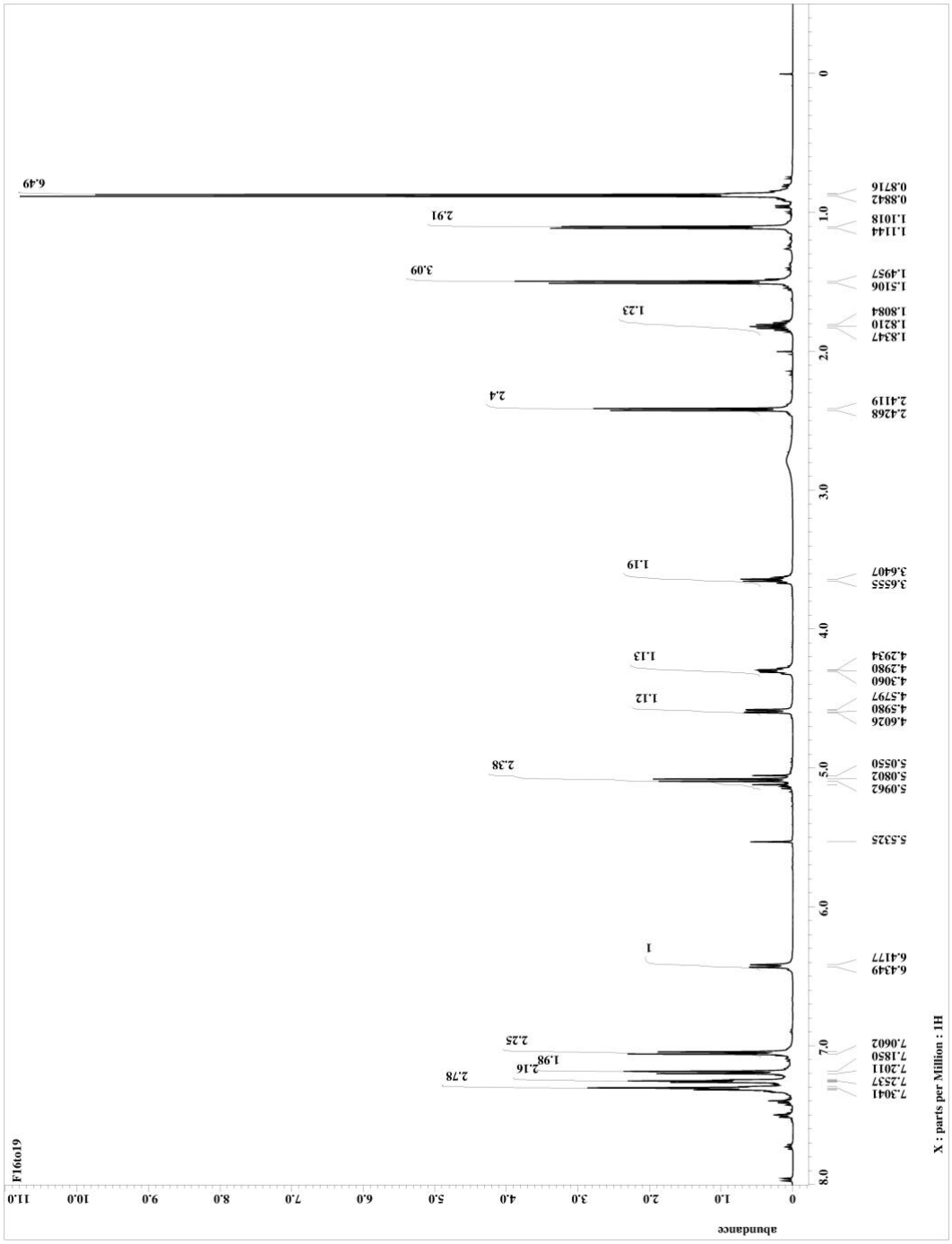
F16o19
abundance
X : parts per Million : 1H
6.49
2.91
3.09
1.23
2.4
1.19
1.13
1.12
2.38
1
2.78
2.16
1.98
2.25
7.3041
7.2537
7.2011
7.1850
7.0602
6.4349
6.4177
5.5325
5.0962
5.0802
5.0550
4.6026
4.5980
4.5797
4.3060
4.2980
4.2934
3.6555
3.6407
2.4268
2.4119
1.8347
1.8210
1.8084
1.5106
1.4957
1.1144
1.1018
0.8842
0.8716

^{13}C-NMR

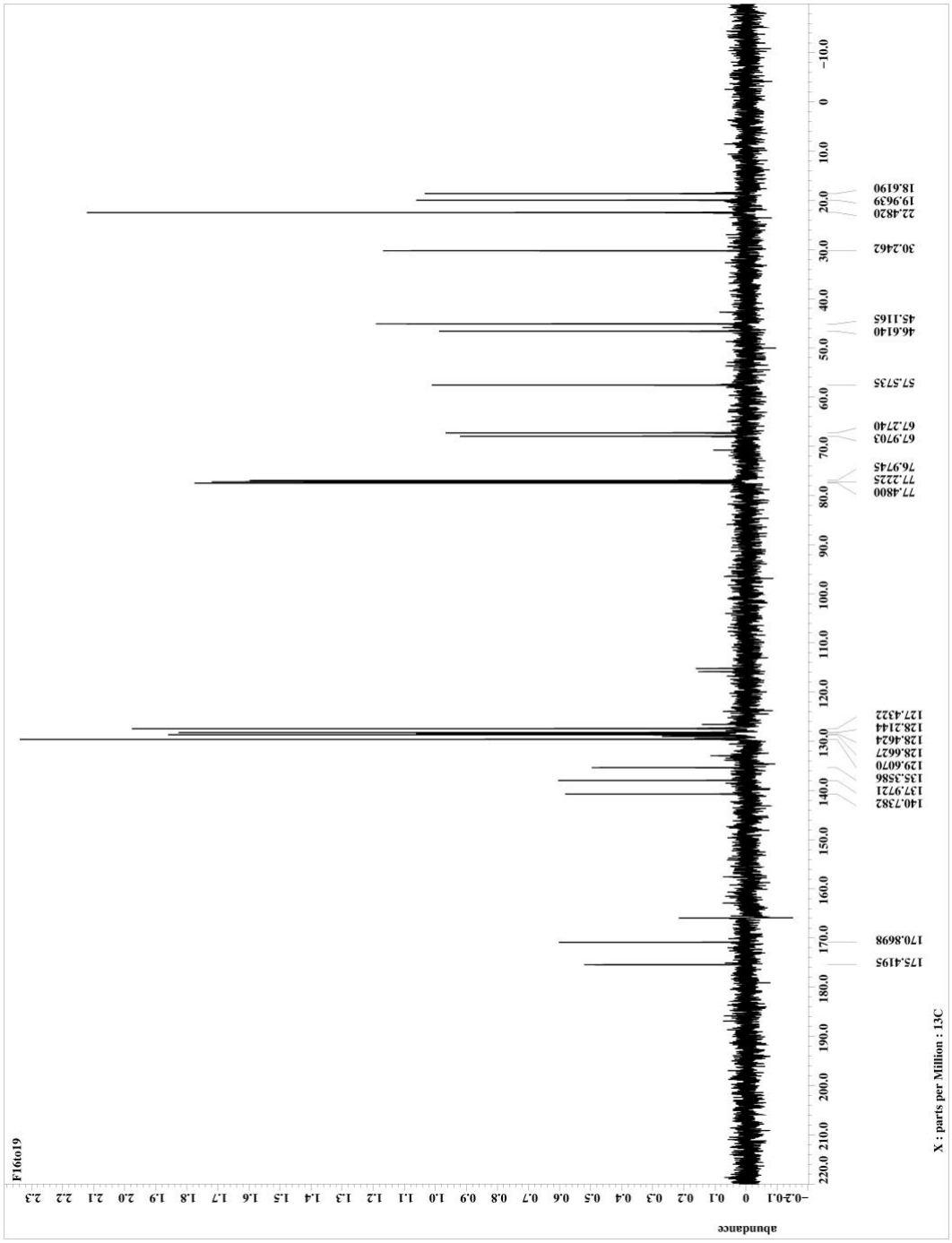
F16to19
abundance
X : parts per Million : 13C
175.4195
170.8698
140.7382
137.9721
135.3586
129.6070
128.6627
128.4624
128.2144
127.4322
77.4800
77.2225
76.9745
67.9703
67.2740
57.5735
46.6140
45.1165
30.2462
22.4820
19.9639
18.6190

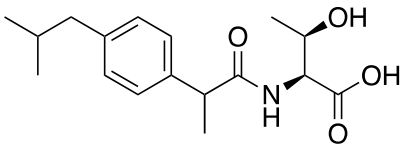
OH
O
N
H
OH
O

^{1}H-NMR

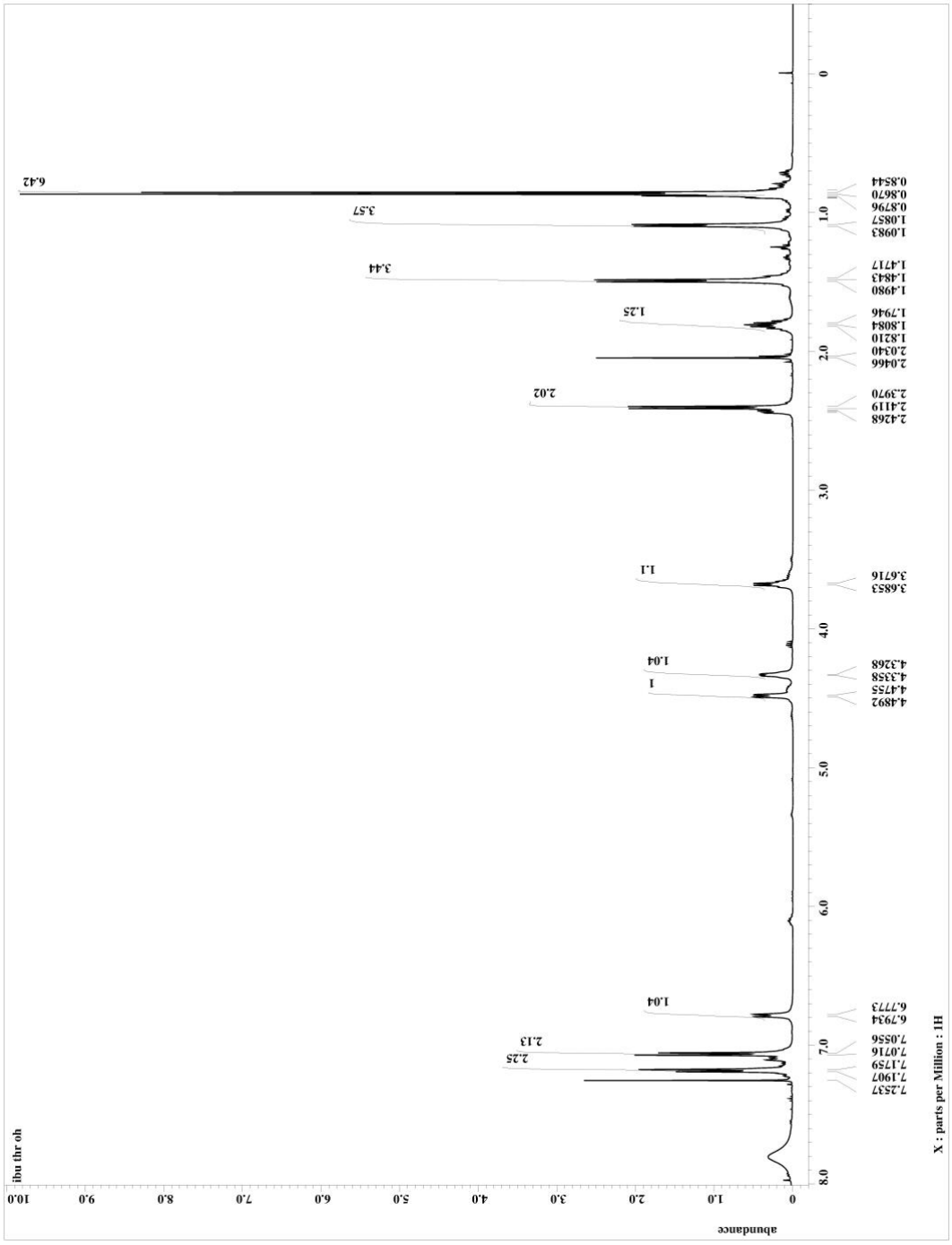
ibu thr oh
abundance
X : parts per Million : 1H
6.42
3.57
3.44
2.25
2.13
2.02
1.25
1.1
1.04
1.04
1
6.7773
6.7934
7.0556
7.0716
7.1759
7.1907
7.2537
4.3268
4.3358
4.4755
4.4892
3.6716
3.6853
2.3970
2.4119
2.4268
1.7946
1.8084
1.8210
2.0340
2.0466
1.4717
1.4843
1.4980
0.8544
0.8670
0.8796
1.0857
1.0983

^{13}C-NMR

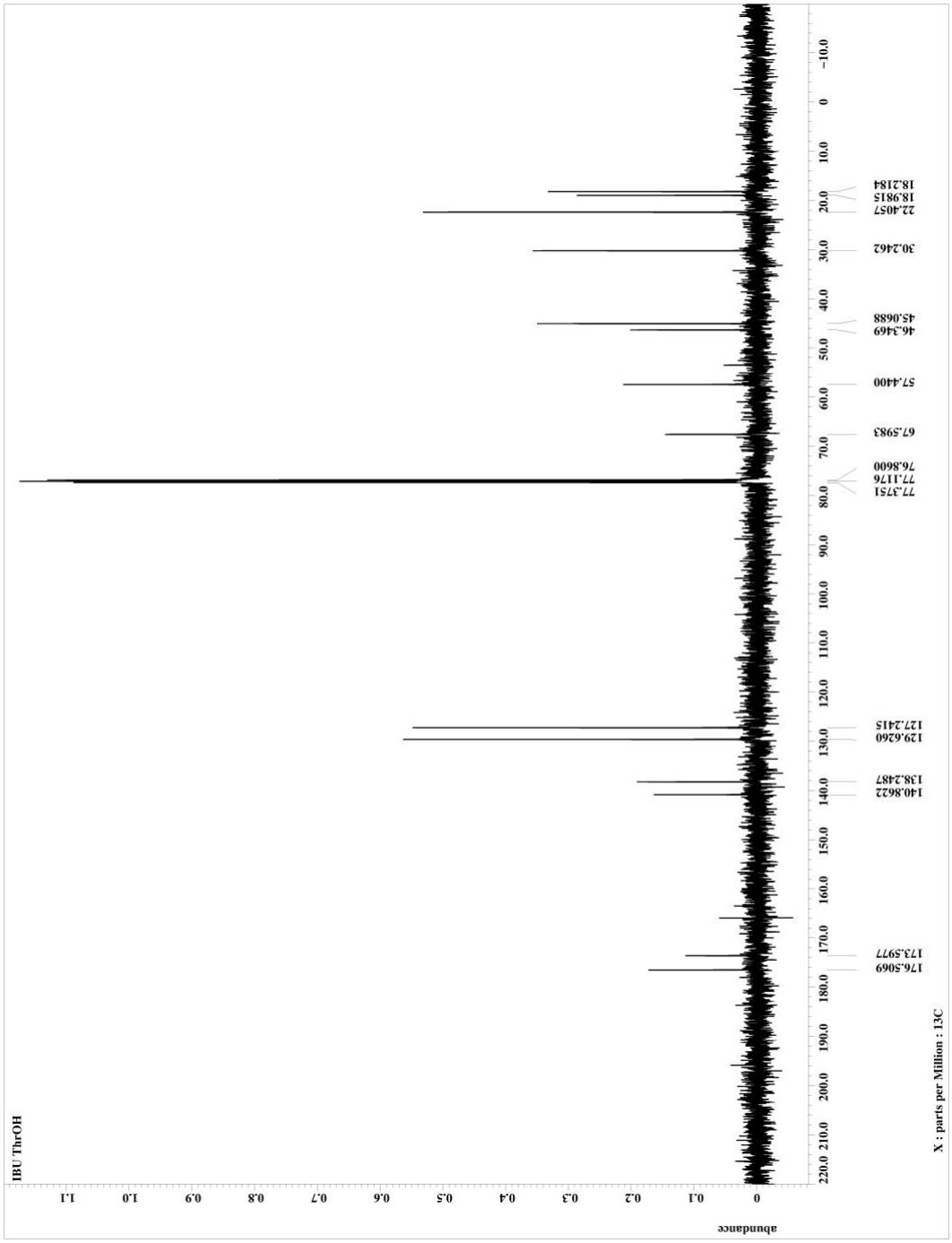
IBU ThrOH
abundance
X : parts per Million : 13C
176.5069
173.5977
140.8622
138.2487
129.6260
127.2415
77.3751
77.1176
76.8600
67.5983
57.4400
46.3469
45.0688
30.2462
22.4057
18.9815
18.2184

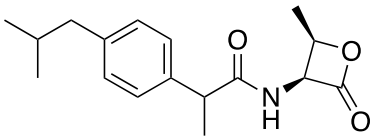

^{1}H-NMR

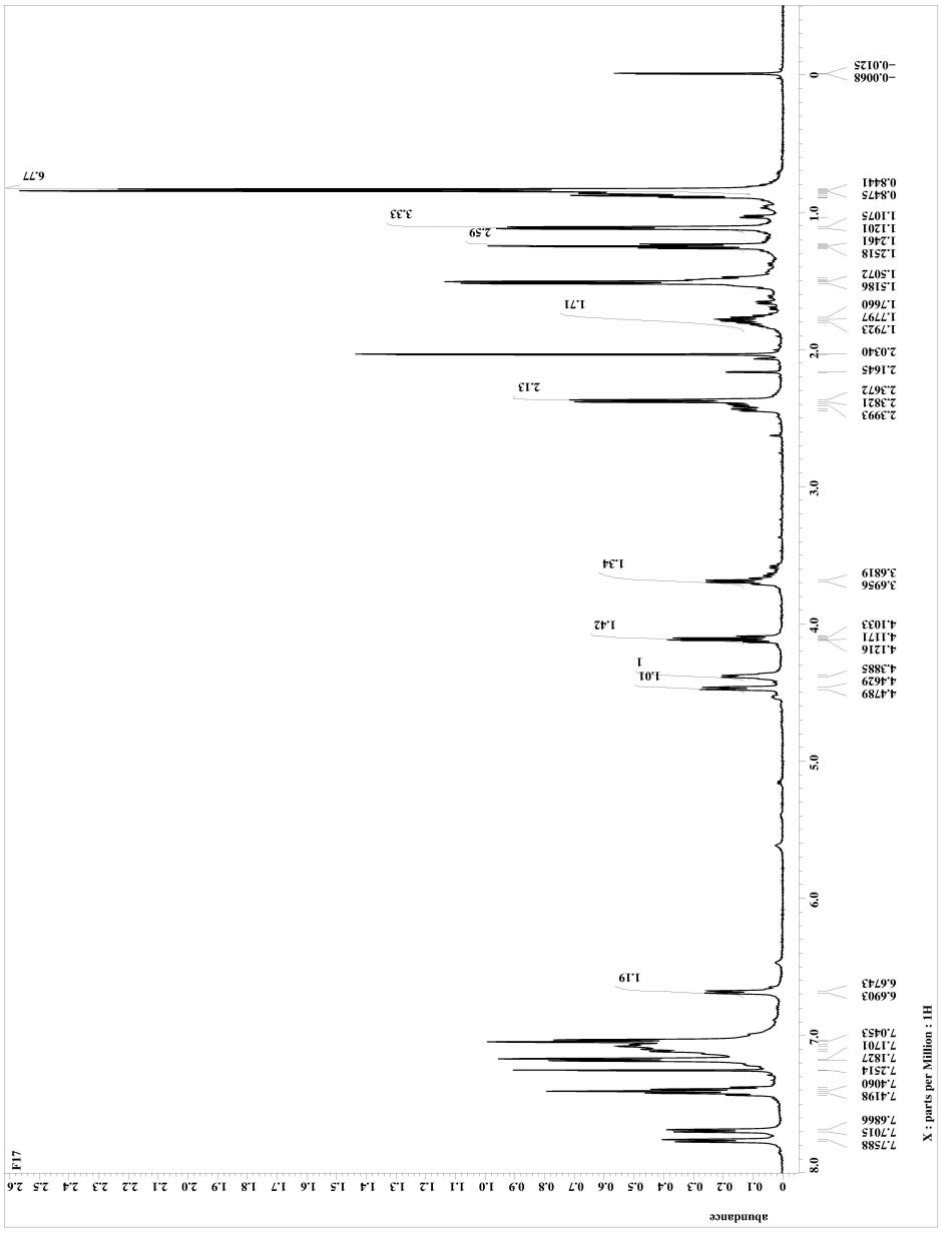
F17
abundance
X : parts per Million : 1H
6.77
3.33
2.59
1.71
2.13
1.34
1.42
1.01
1.19

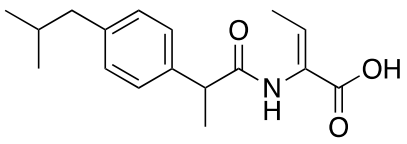
O
N
H
OH
O

^{1}H-NMR

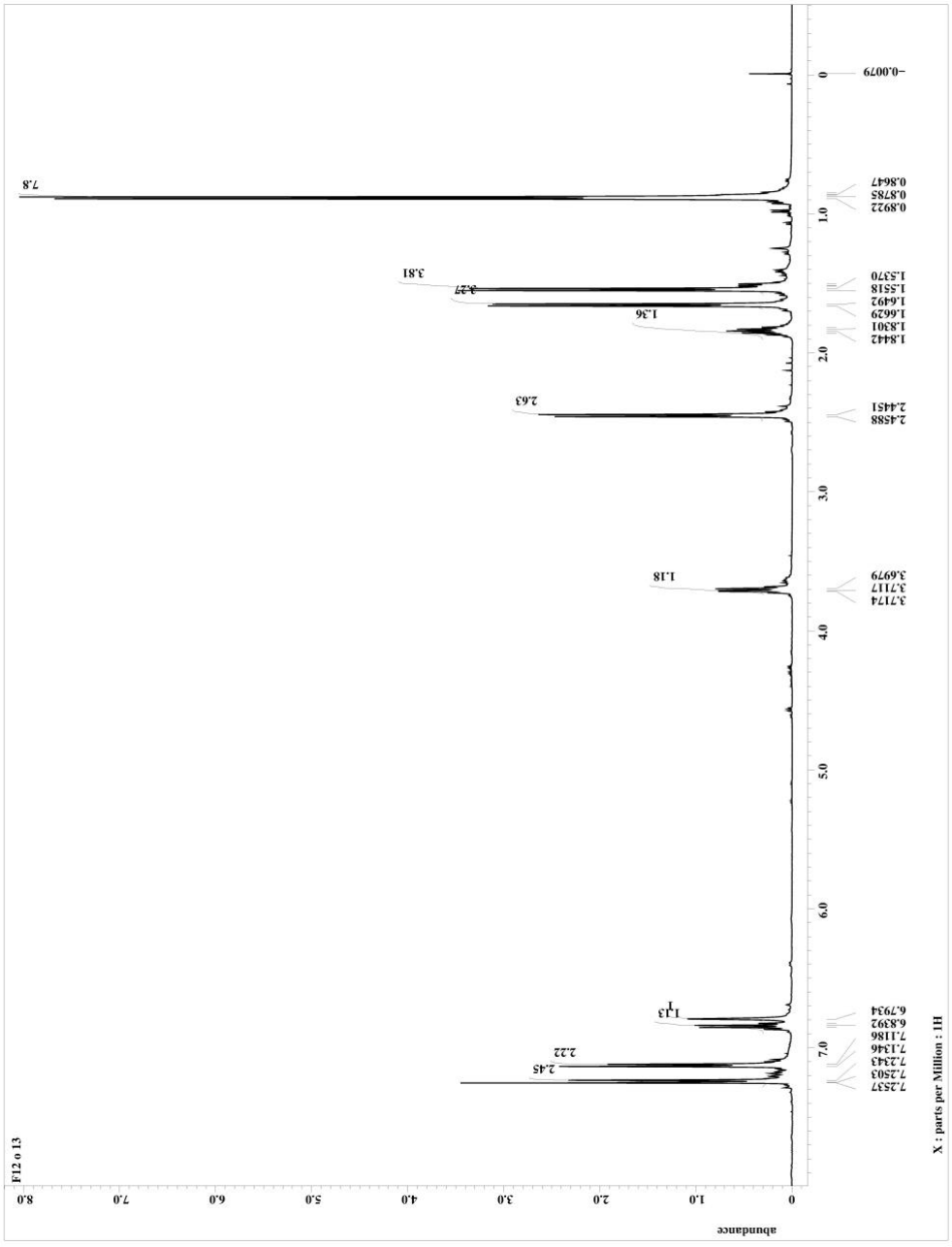
abundance
F12 o 13
X : parts per Million : 1H
7.8
3.81
3.27
2.63
2.45
2.22
1.36
1.18
1.13
-0.0079

^{13}C-NMR

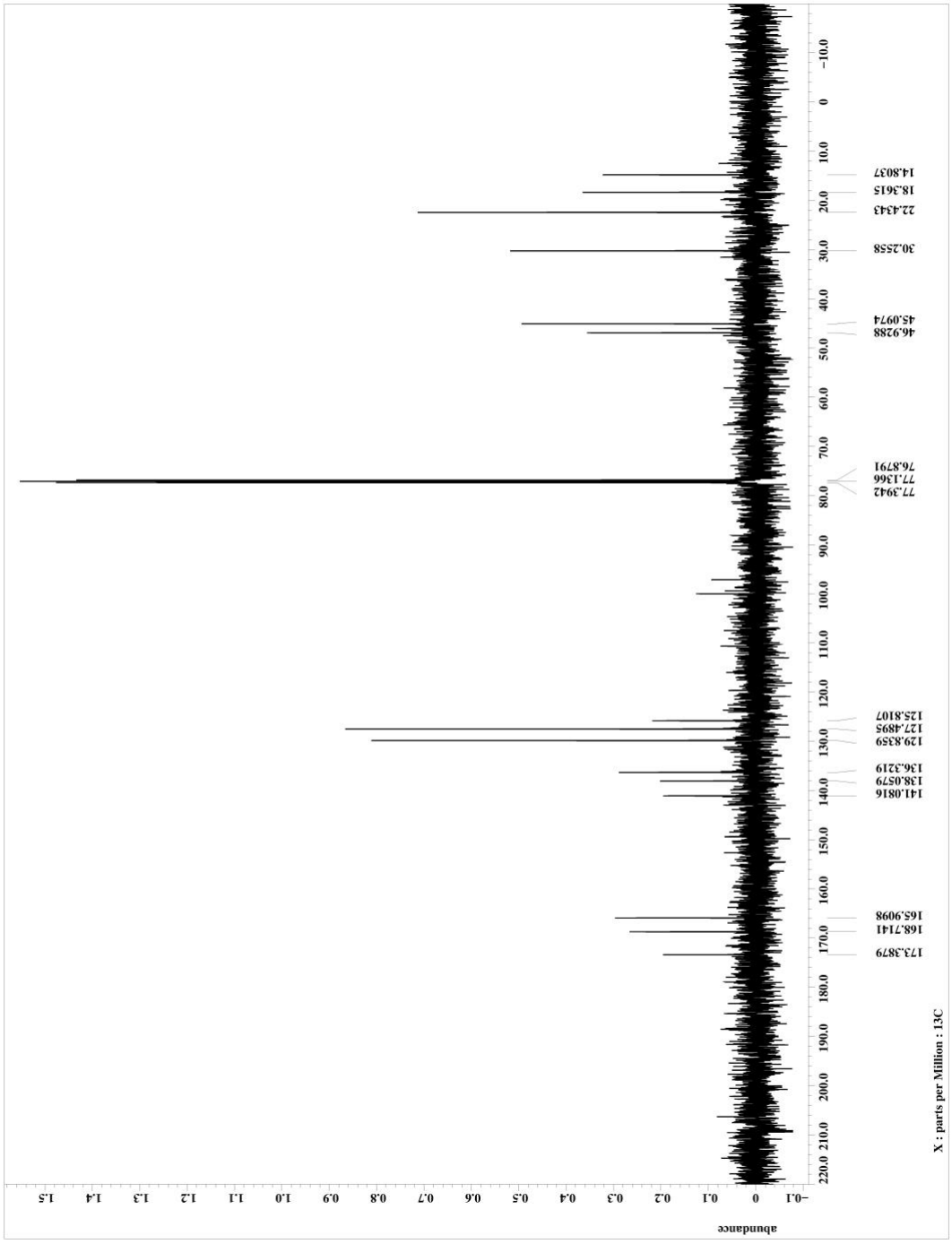
173.3879
168.7141
165.9098
141.0816
138.0579
136.3219
129.8359
127.4895
125.8107
77.3942
77.1366
76.8791
46.9288
45.0974
30.2558
22.4343
18.3615
14.8037
X : parts per Million : 13C
abundance

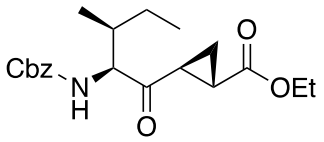
Cbz
N
H
O
O
OEt

^{1}H-NMR

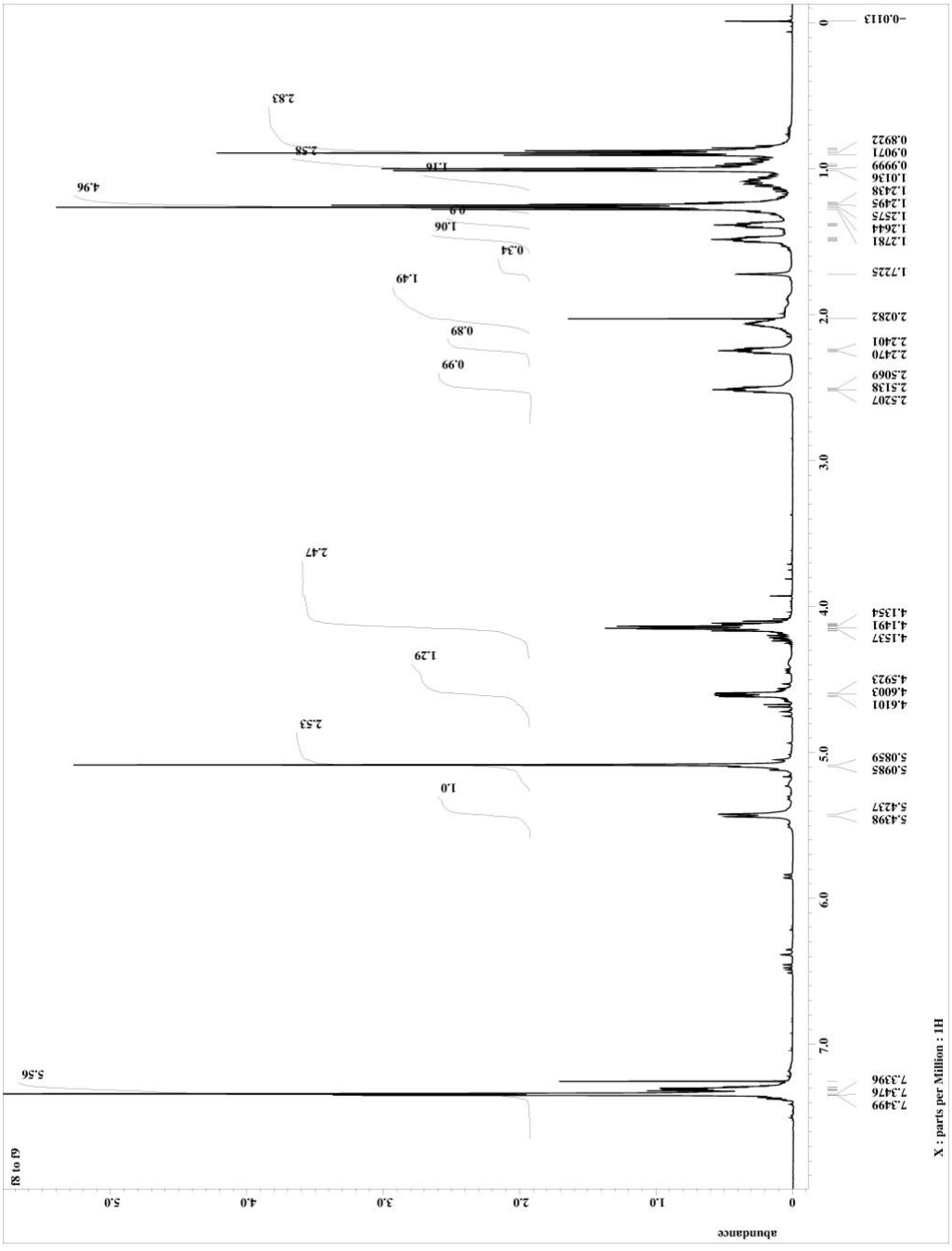
-0.0113
0
0.8922
0.9071
0.9999
1.0136
1.2438
1.2495
1.2575
1.2644
1.2781
1.7225
2.0282
2.2401
2.2470
2.5069
2.5138
2.5207
4.1354
4.1491
4.1537
4.5923
4.6003
4.6101
5.0859
5.0985
5.4247
5.4398
7.3396
7.3476
7.3499
2.83
2.58
1.16
4.96
0.9
1.06
0.34
1.49
0.89
0.99
2.47
1.29
2.53
1.0
5.56
abundance
X : parts per Million : 1H

^{13}C-NMR

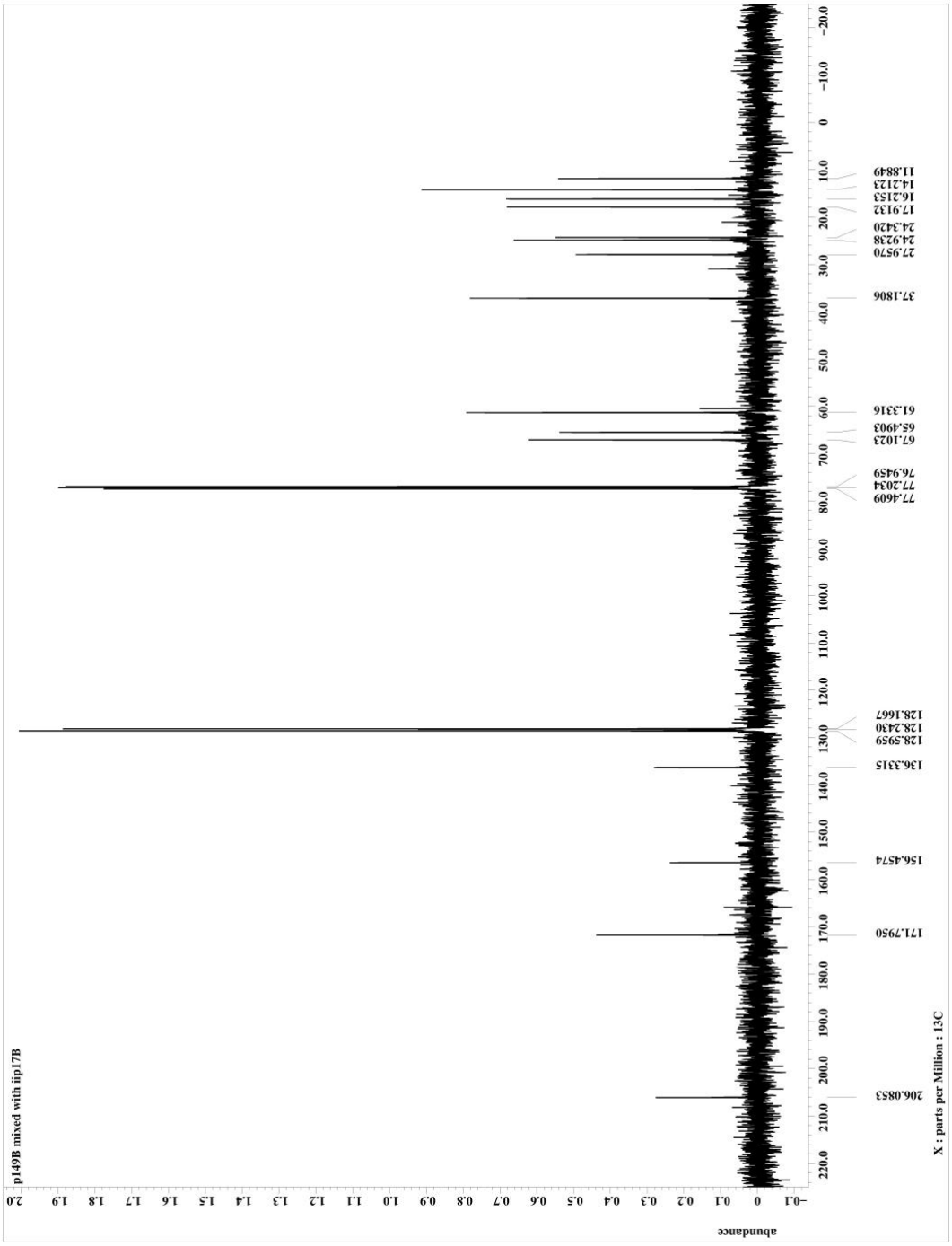
p149B mixed with iip17B
abundance
X : parts per Million : 13C
206.0853
171.7950
156.4574
136.3315
128.5959
128.2430
128.1667
77.4609
77.2034
76.9459
67.1023
65.4903
61.3316
37.1806
27.9570
24.9238
24.3420
17.9132
16.2153
14.2123
11.8849

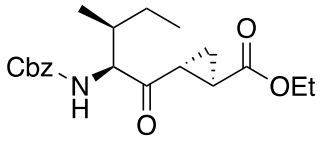
Cbz
N
H
O
O
OEt

^{1}H-NMR

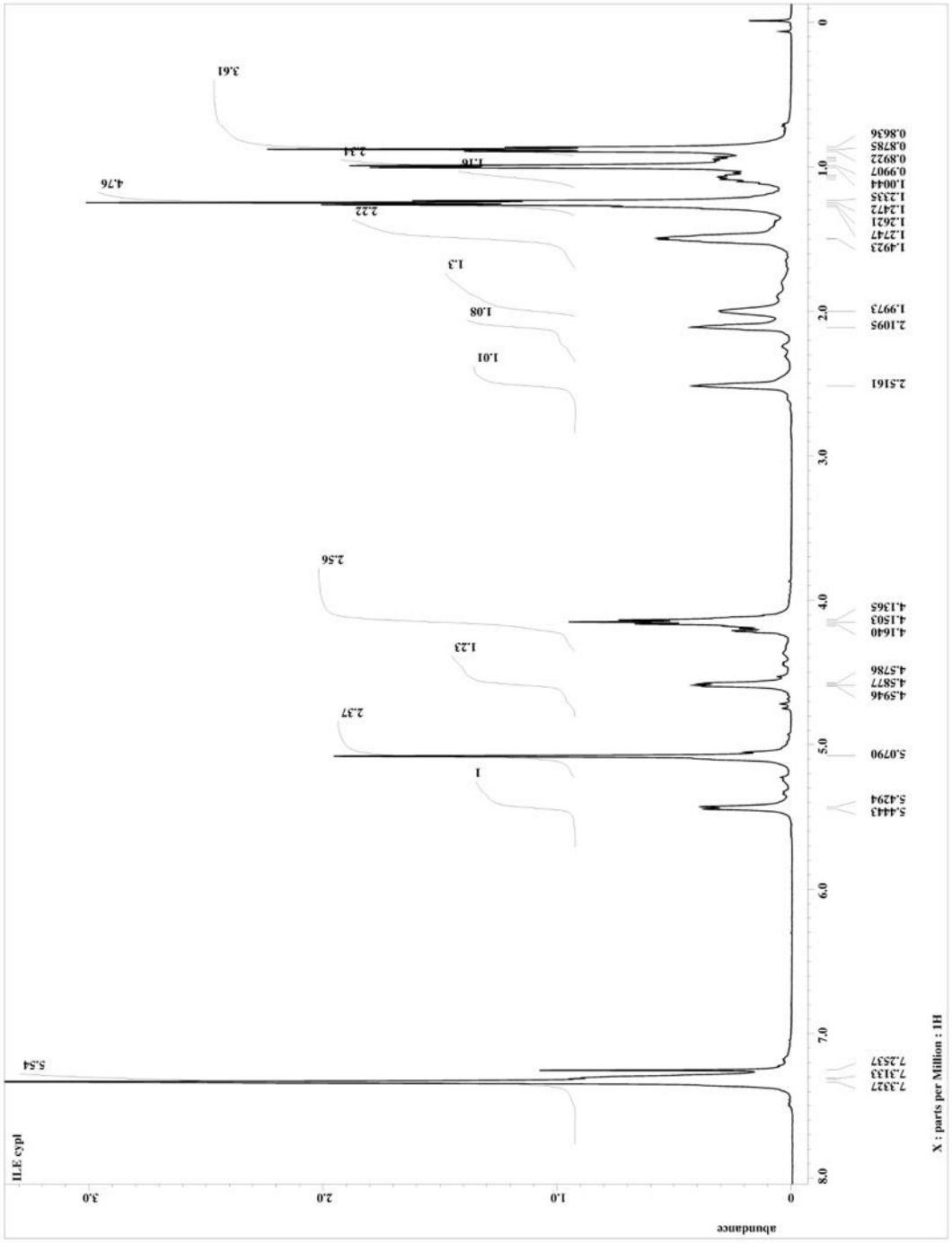
abundance
ILE cypl
X : parts per Million : 1H
5.54
3.61
2.37
4.76
2.22
1.3
1.08
1.01
2.56
1.23
1
2.11
1.16
7.3327
7.3133
7.2537
5.4443
5.4294
5.0790
4.5946
4.5877
4.5786
4.1640
4.1503
4.1365
2.5161
2.1095
1.9973
1.4923
1.2747
1.2621
1.2472
1.2335
1.0044
0.9907
0.8922
0.8785
0.8636

^{13}C-NMR

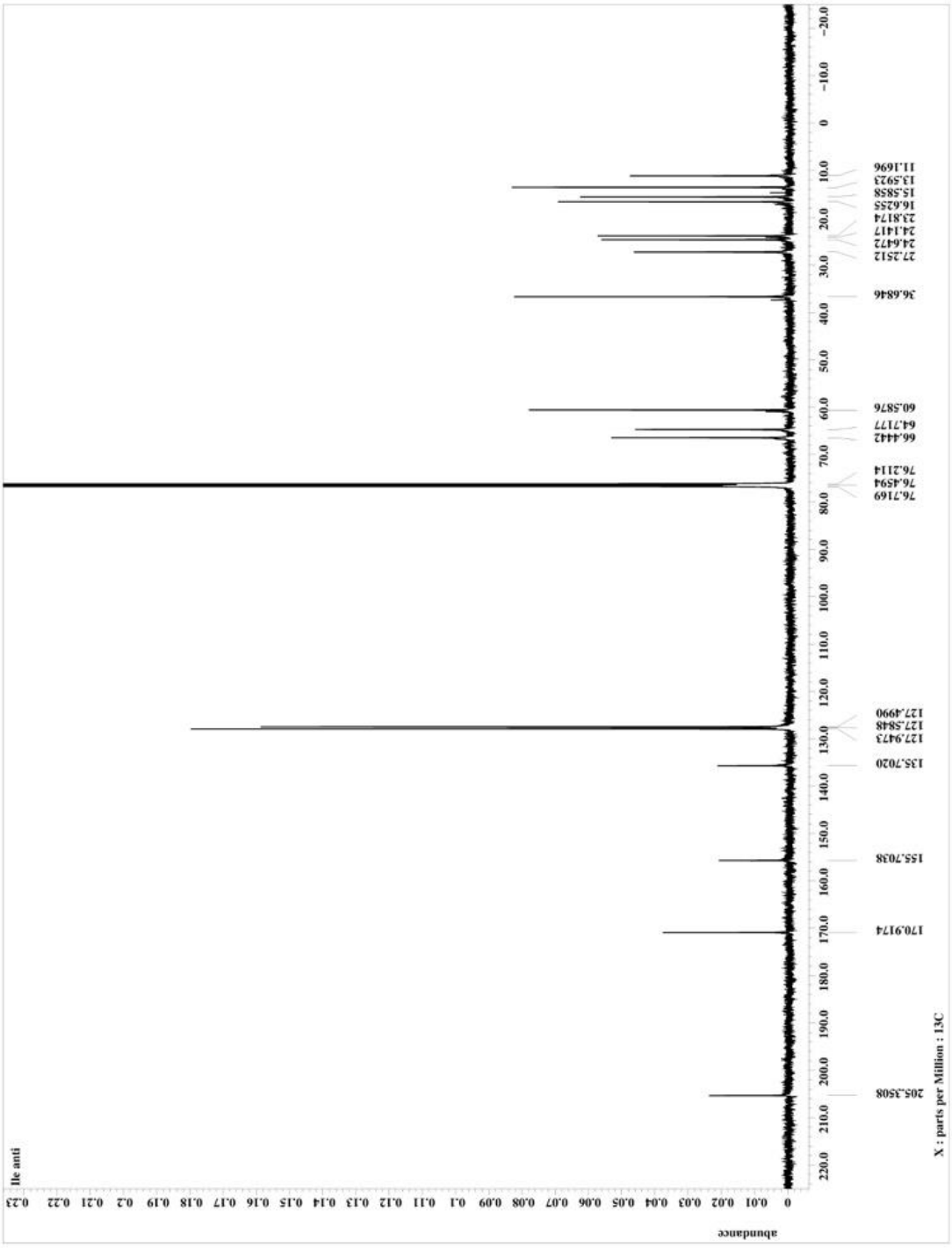
abundance
0 0.01 0.02 0.03 0.04 0.05 0.06 0.07 0.08 0.09 0.1 0.11 0.12 0.13 0.14 0.15 0.16 0.17 0.18 0.19 0.2 0.21 0.22 0.23
Ile anti
220.0 210.0 200.0 190.0 180.0 170.0 160.0 150.0 140.0 130.0 120.0 110.0 100.0 90.0 80.0 70.0 60.0 50.0 40.0 30.0 20.0 10.0 0 -10.0 -20.0
X : parts per Million : 13C
205.3508
170.9174
155.7038
135.7020
127.4990
127.5848
127.9473
76.7169
76.4594
76.2114
66.4442
64.7177
60.5876
36.6846
27.2512
24.6472
24.1417
23.8174
16.6255
15.5858
13.5923
11.1696

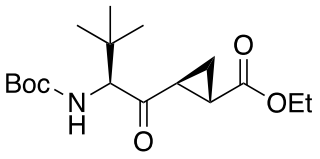
Boc
N
H
O
O
OEt

^{1}H-NMR

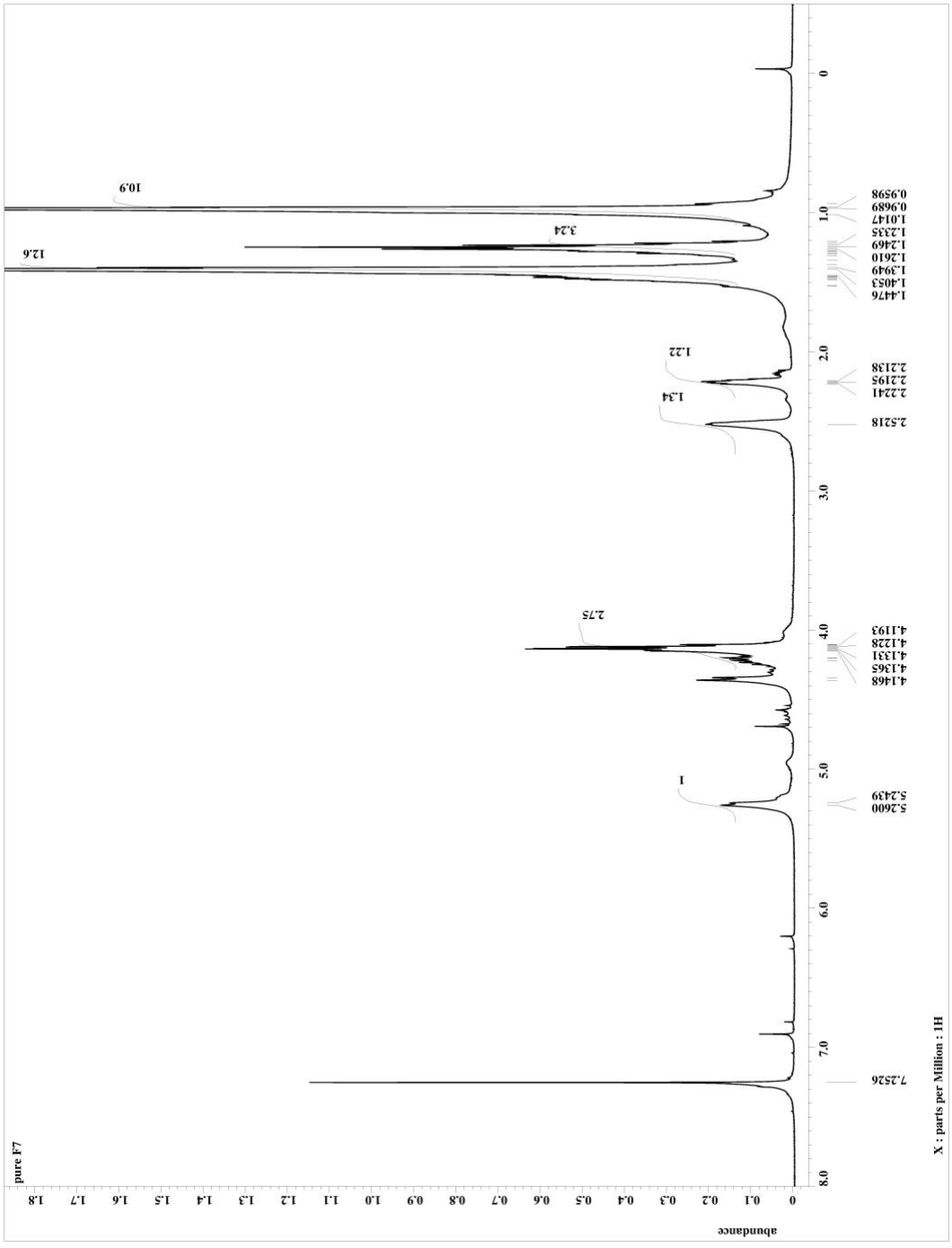
pure F7
abundance
X : parts per Million : 1H
10.9
12.6
3.24
2.75
1.22
1.34
1
7.2526
5.2600
5.2439
4.1468
4.1365
4.1331
4.1228
4.1193
2.5218
2.2241
2.2195
2.2138
1.4476
1.4053
1.3949
1.2610
1.2469
1.2335
1.0147
0.9689
0.9598

^{13}C-NMR

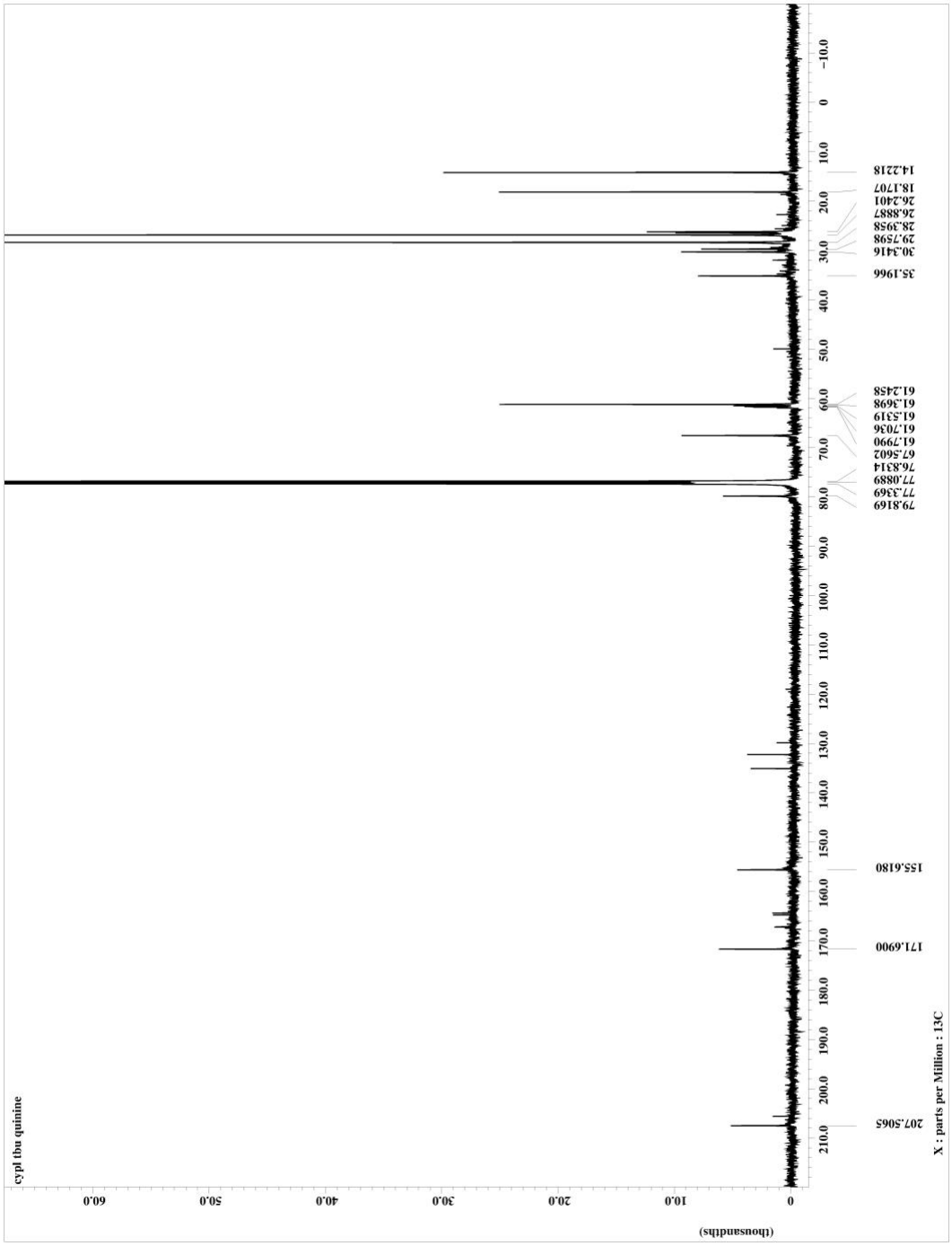
cypl tbu quinine
(thousandths)
X : parts per Million : 13C
207.5065
171.6900
155.6180
79.8169
77.3369
77.0889
76.8314
67.5602
61.7990
61.7036
61.5319
61.3698
61.2458
35.1966
30.3416
29.7598
28.3958
26.8887
26.2401
18.1707
14.2218

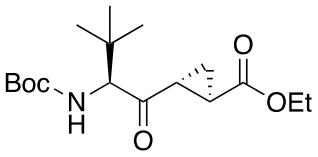
Boc
N
H
O
O
OEt

^{1}H-NMR

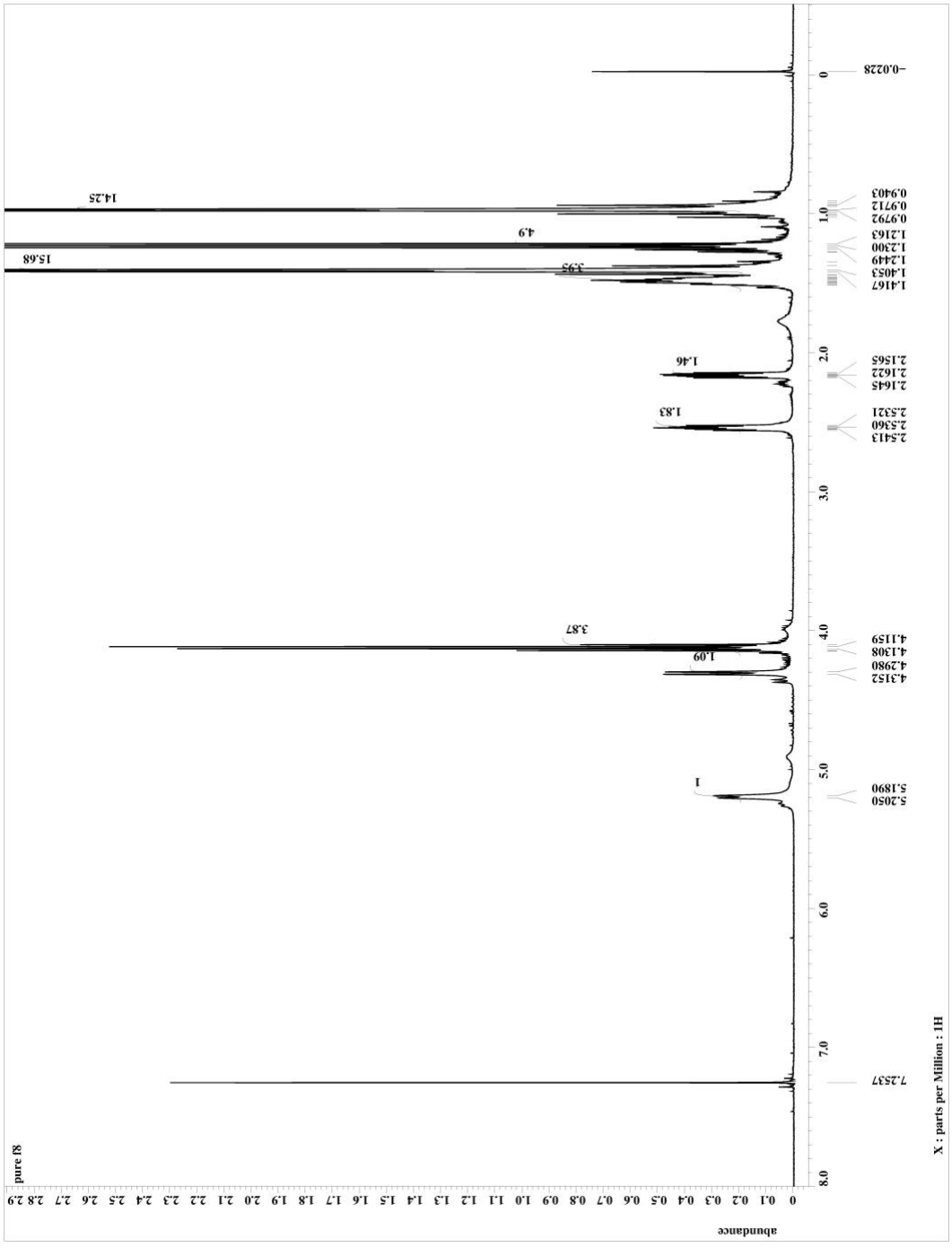
pure f8
abundance
X : parts per Million : 1H
7.2537
5.2050
5.1890
4.3152
4.2980
4.1308
4.1159
2.5413
2.5360
2.5321
2.1645
2.1622
2.1565
1.4167
1.4053
1.2449
1.2300
1.2163
0.9792
0.9712
0.9403
-0.0228
14.25
4.9
15.68
3.95
1.46
1.83
3.87
1.09
1

^{13}C-NMR

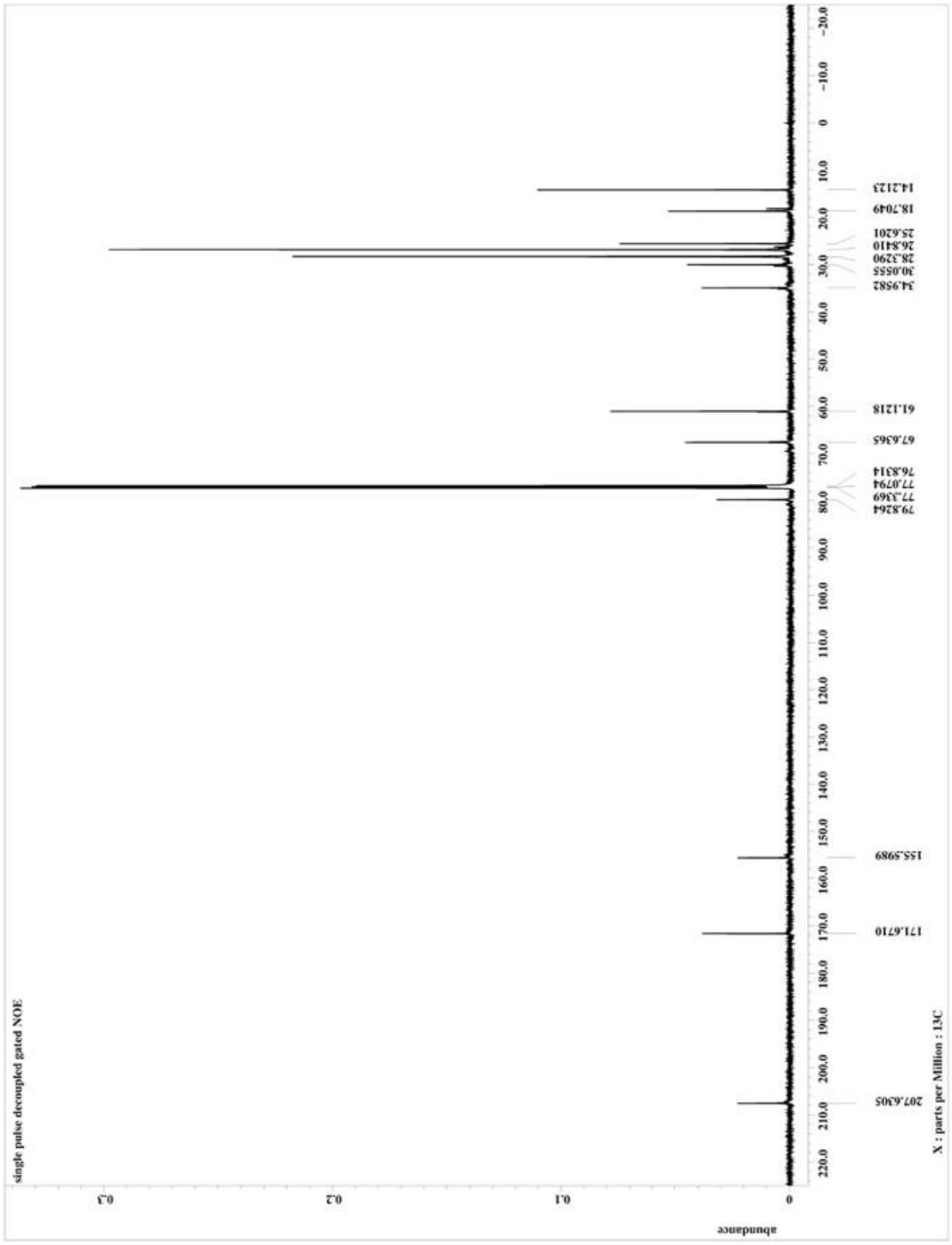
14.2123
18.7049
25.6201
26.3410
28.3290
30.0555
34.9582
61.1218
67.6365
76.8314
77.0794
77.3369
79.8264
155.5989
171.6710
207.6305
X : parts per Million : 13C
single pulse decoupled gated NOE
abundance

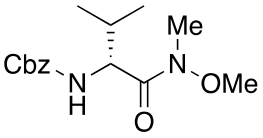
Me
Cbz
N
H
N
OMe
O

^{1}H-NMR

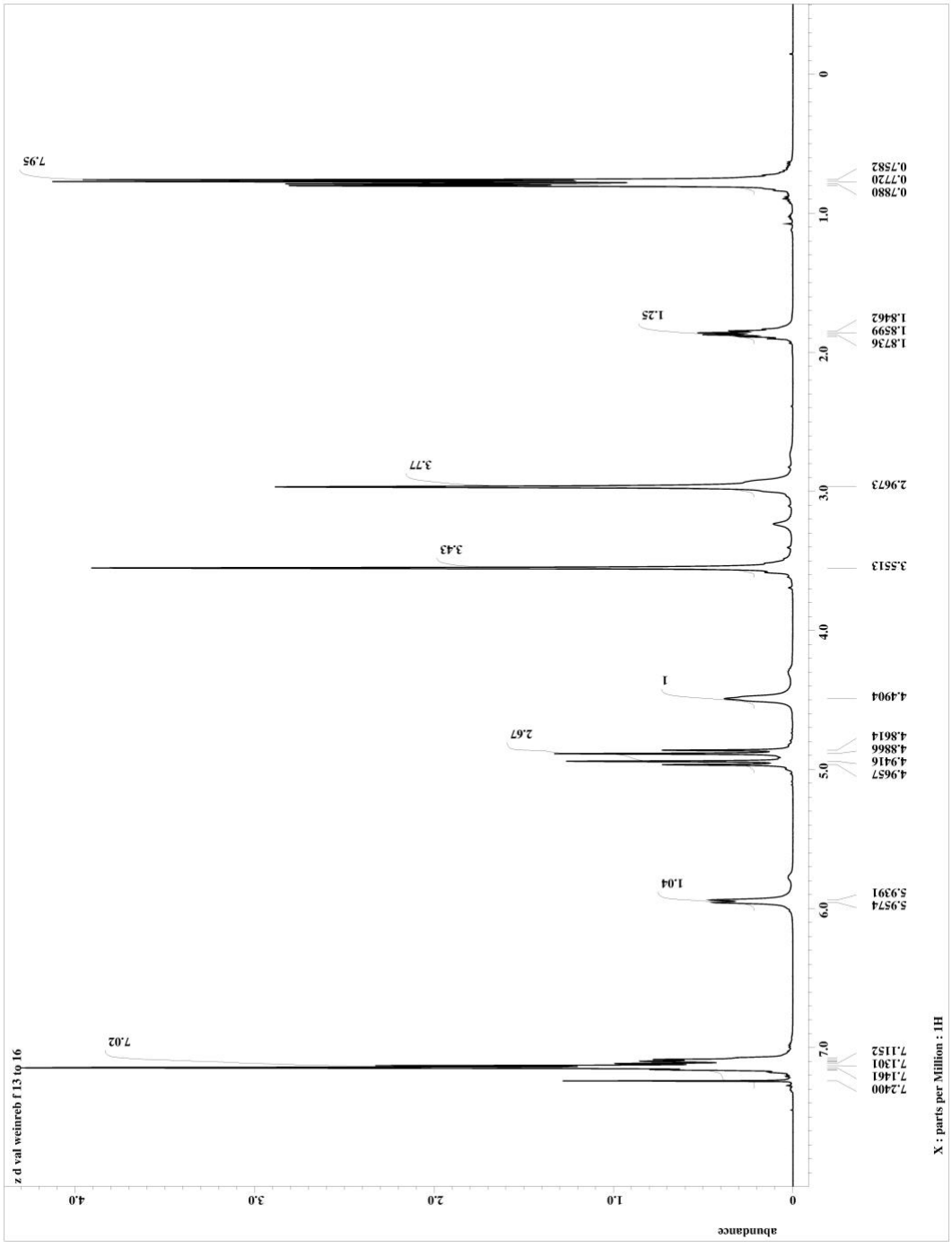
z d val weinreb f 13 to 16
abundance
X : parts per Million : 1H
7.95
7.02
3.77
3.43
2.67
1.25
1.04
1
0.7880
0.7720
0.7582
1.8736
1.8599
1.8462
2.9673
3.5513
4.4904
4.9657
4.9416
4.8866
4.8614
5.9574
5.9391
7.2400
7.1461
7.1301
7.1152

^{13}C-NMR

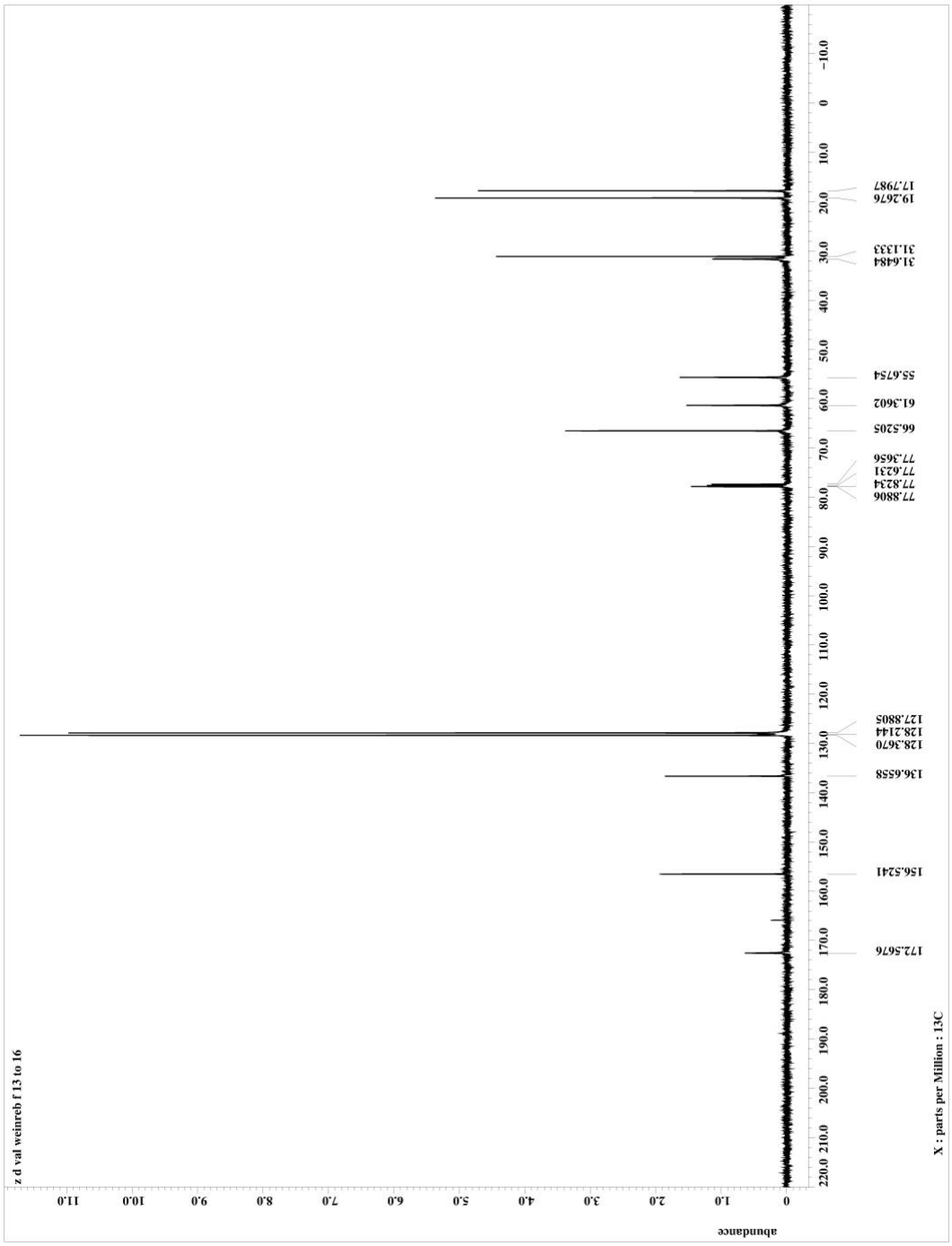
z d val weinreb f13 to 16
abundance
X : parts per Million : 13C
172.5676
156.5241
136.6558
128.3670
128.2144
127.8805
77.8806
77.8234
77.6231
77.3656
66.5205
61.3602
55.6754
31.6484
31.1333
19.2676
17.7987

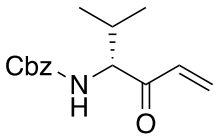
Cbz
N
H
O

^{1}H-NMR

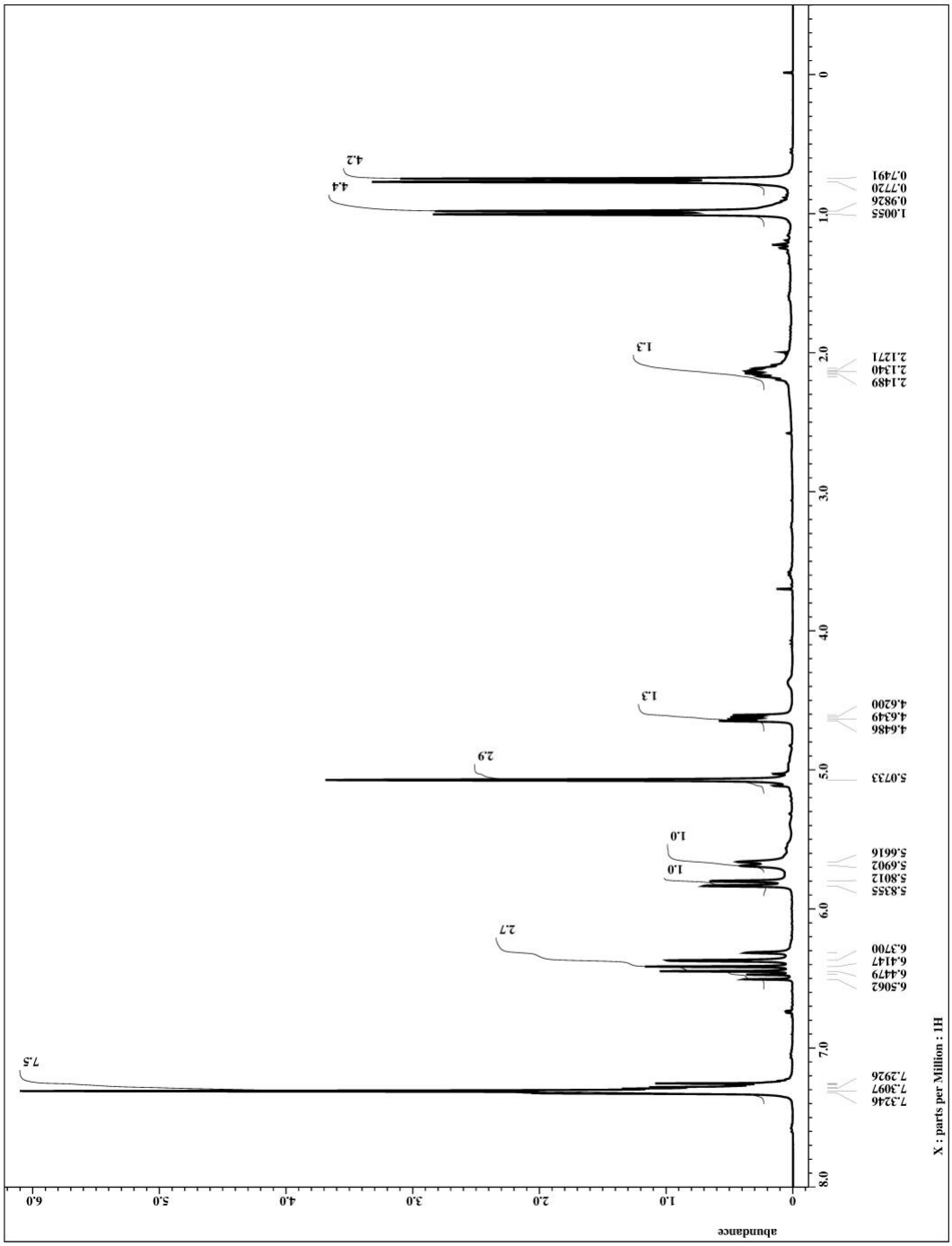
abundance
X : parts per Million : 1H
7.3246
7.3097
7.2926
6.5062
6.4479
6.4147
6.3700
5.8355
5.8012
5.6902
5.6616
5.0733
4.6486
4.6349
4.6200
2.1489
2.1340
2.1271
1.0055
0.9826
0.7720
0.7491
7.5
2.7
1.0
1.0
2.9
1.3
1.3
4.4
4.2

^{13}C-NMR

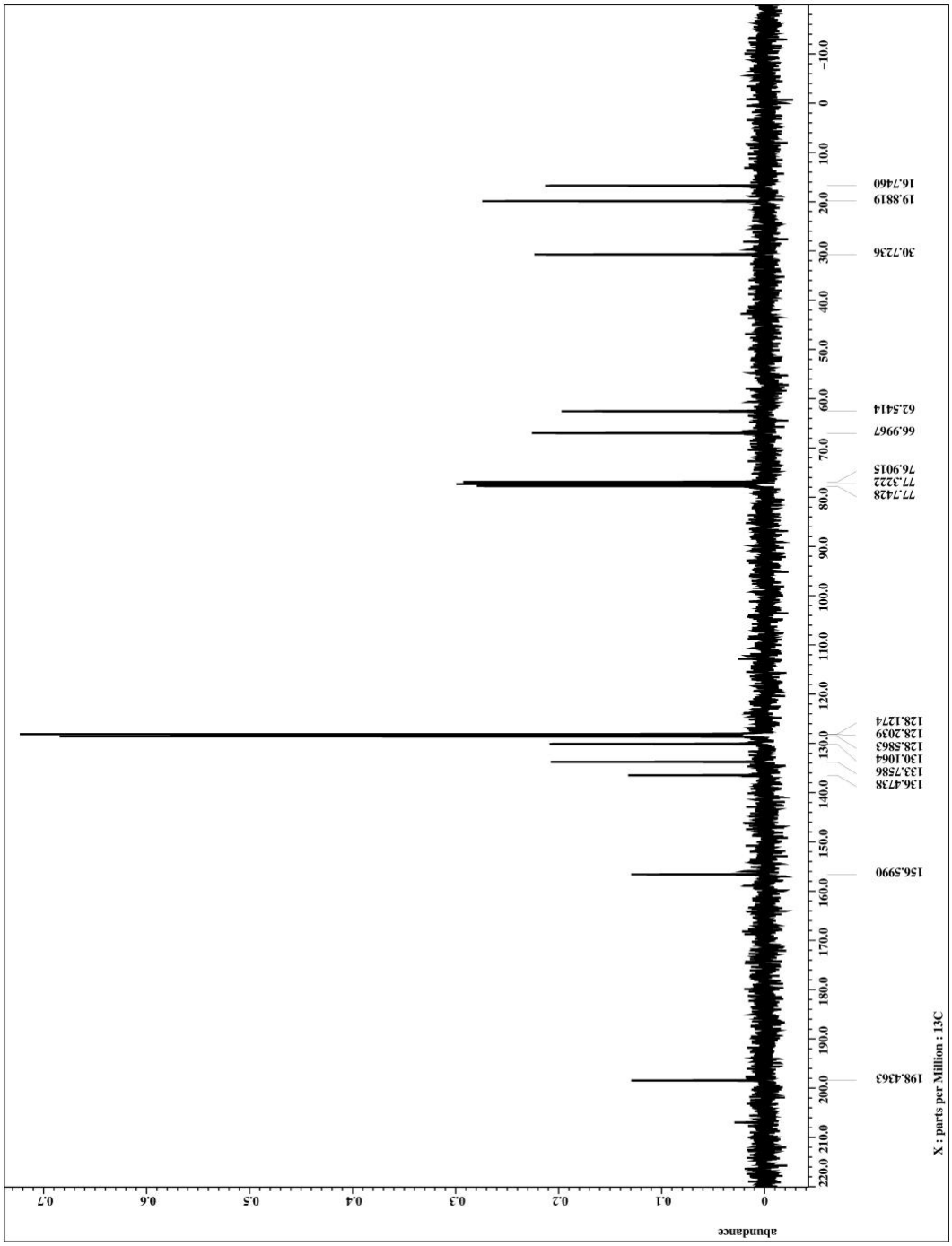
198,4363
156,5990
136,4738
133,7586
130,1064
128,5863
128,2039
128,1274
77,7428
77,3222
76,9015
66,9967
62,5414
30,7236
19,8819
16,7460
X : parts per Million : 13C
abundance

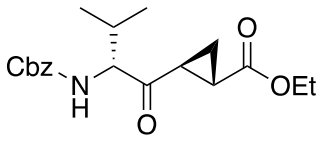
Cbz
N
H
O
O
OEt

^{1}H-NMR

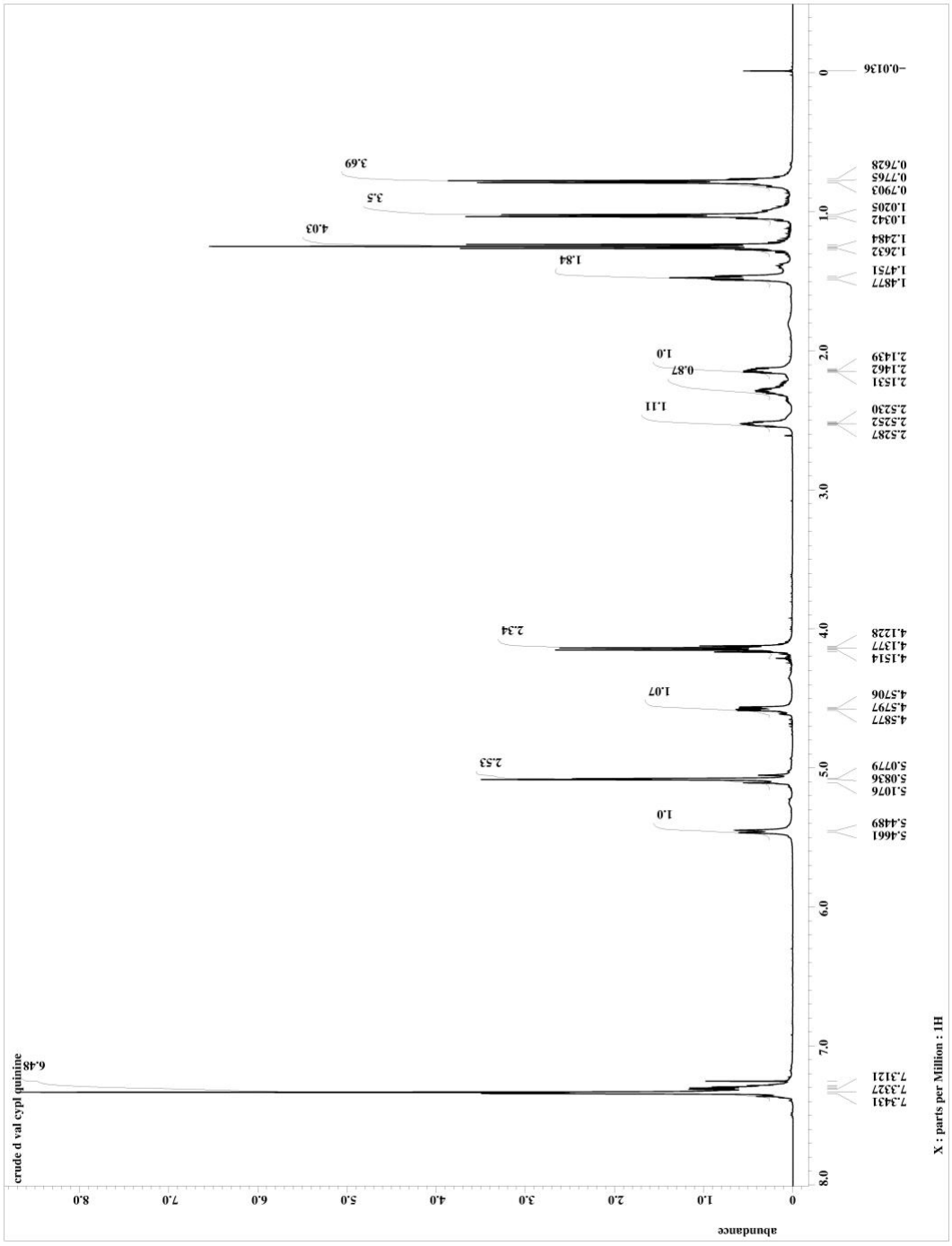
crude d val cypl quinine
abundance
X : parts per Million : 1H
6.48
7.3431
7.3327
7.3121
5.4661
5.4489
1.0
5.1076
5.0836
5.0779
2.53
4.5877
4.5797
4.5706
1.07
4.1514
4.1377
4.1228
2.34
2.5287
2.5252
2.5230
1.11
2.1531
2.1462
2.1439
0.87
1.0
1.4877
1.4751
1.2632
1.2484
1.0342
1.0205
0.7903
0.7765
0.7628
1.84
4.03
3.5
3.69
-0.0136

^{13}C-NMR

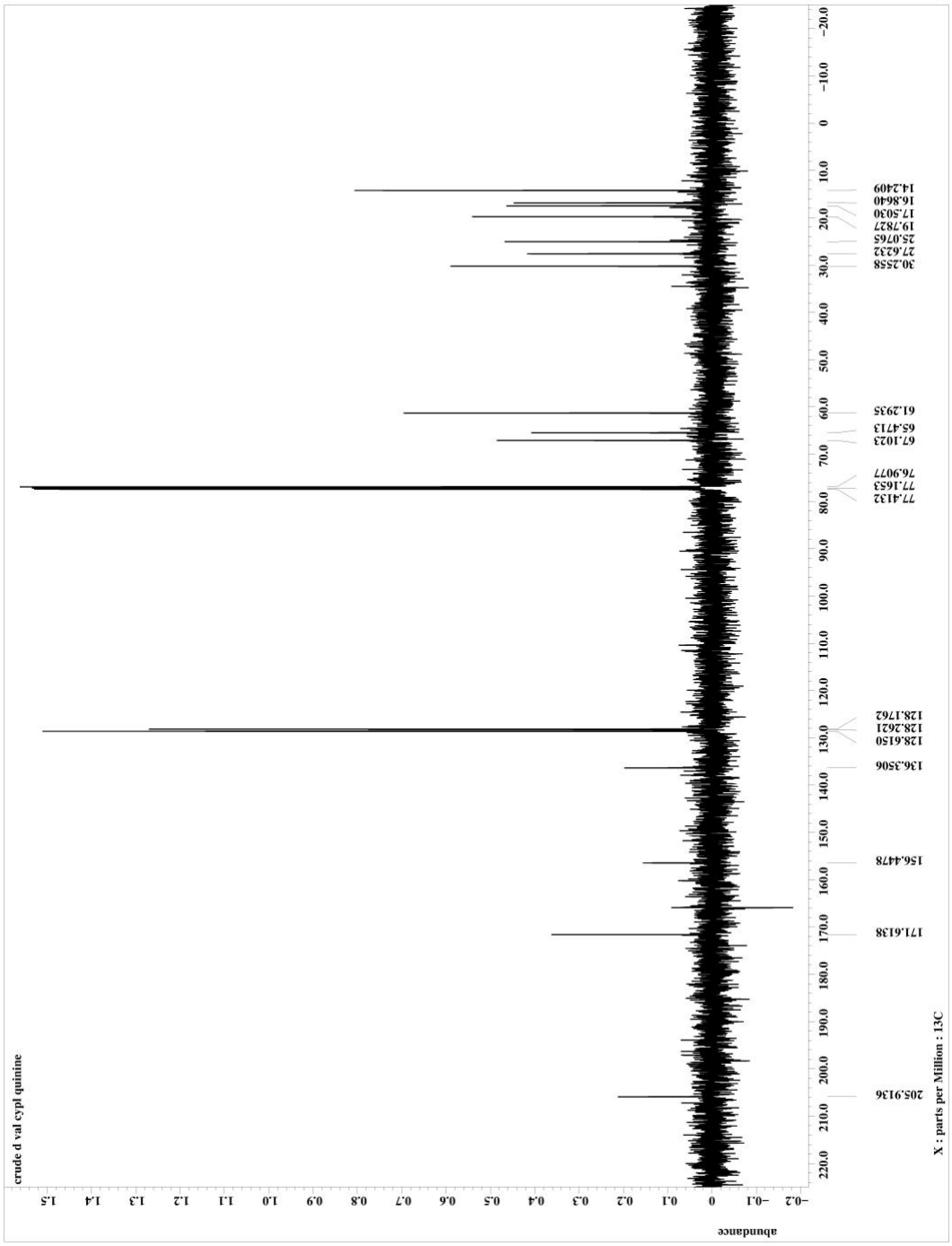
crude d val cypl quinine
abundance
X : parts per Million : 13C
205.9136
171.6138
156.4478
136.3506
128.6150
128.2621
128.1762
77.4132
77.1653
76.9077
67.1023
65.4713
61.2935
30.2558
27.6232
25.0765
19.7827
17.5030
16.8640
14.2409

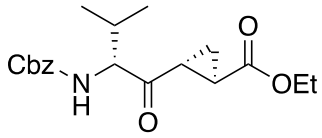
Cbz
N
H
O
O
OEt

^{1}H-NMR

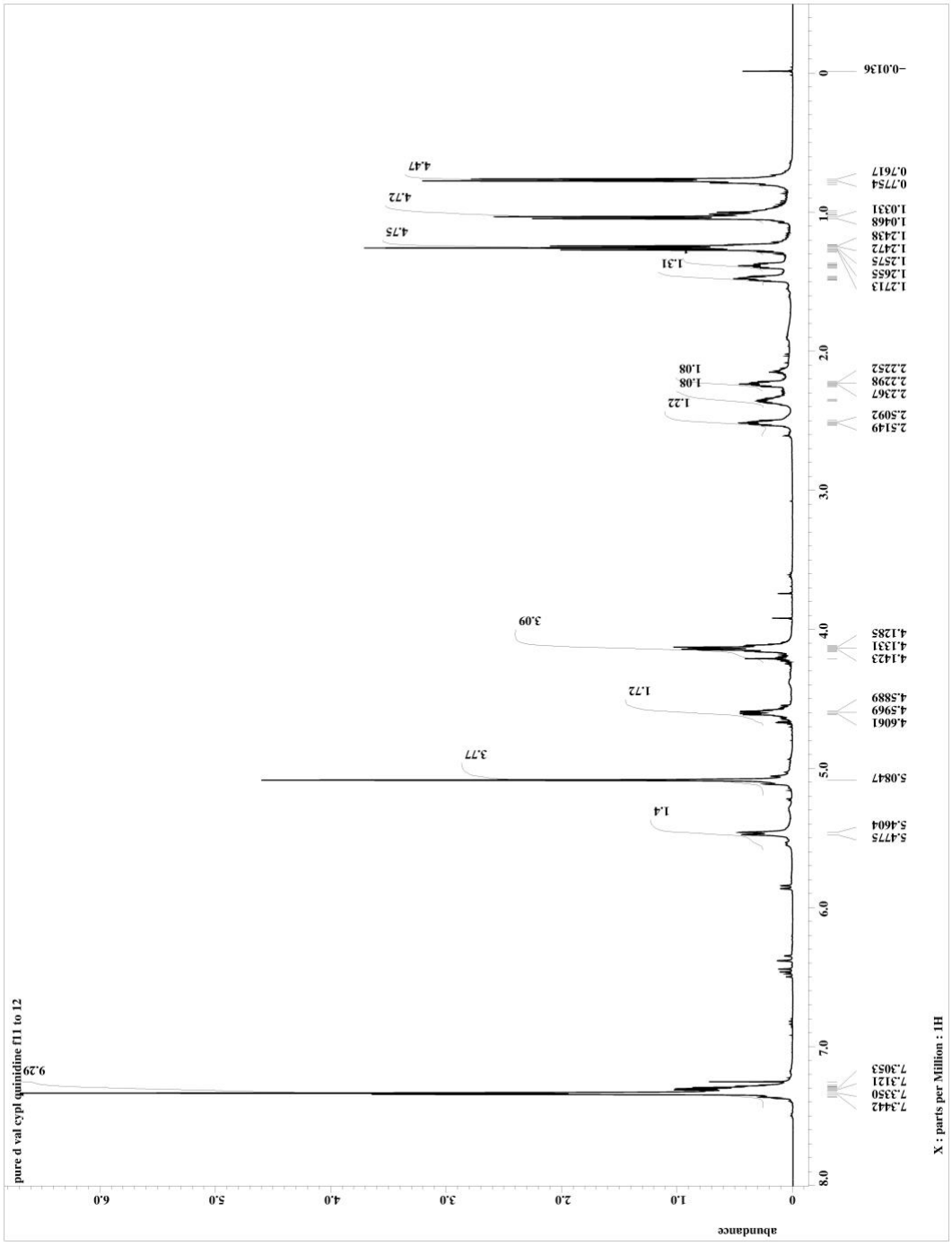
pure d val cypl quinidine f11 to 12
abundance
X : parts per Million : 1H
9.29
7.3442
7.3350
7.3121
7.3053
5.4775
5.4604
5.0847
4.6061
4.5969
4.5889
4.1423
4.1331
4.1285
2.5149
2.5092
2.3367
2.2998
2.2252
1.2713
1.2655
1.2575
1.2472
1.2438
1.0468
1.0331
0.7754
0.7617
-0.0136
4.47
4.72
4.75
1.31
1.08
1.08
1.22
3.09
1.72
3.77
1.4

^{13}C-NMR

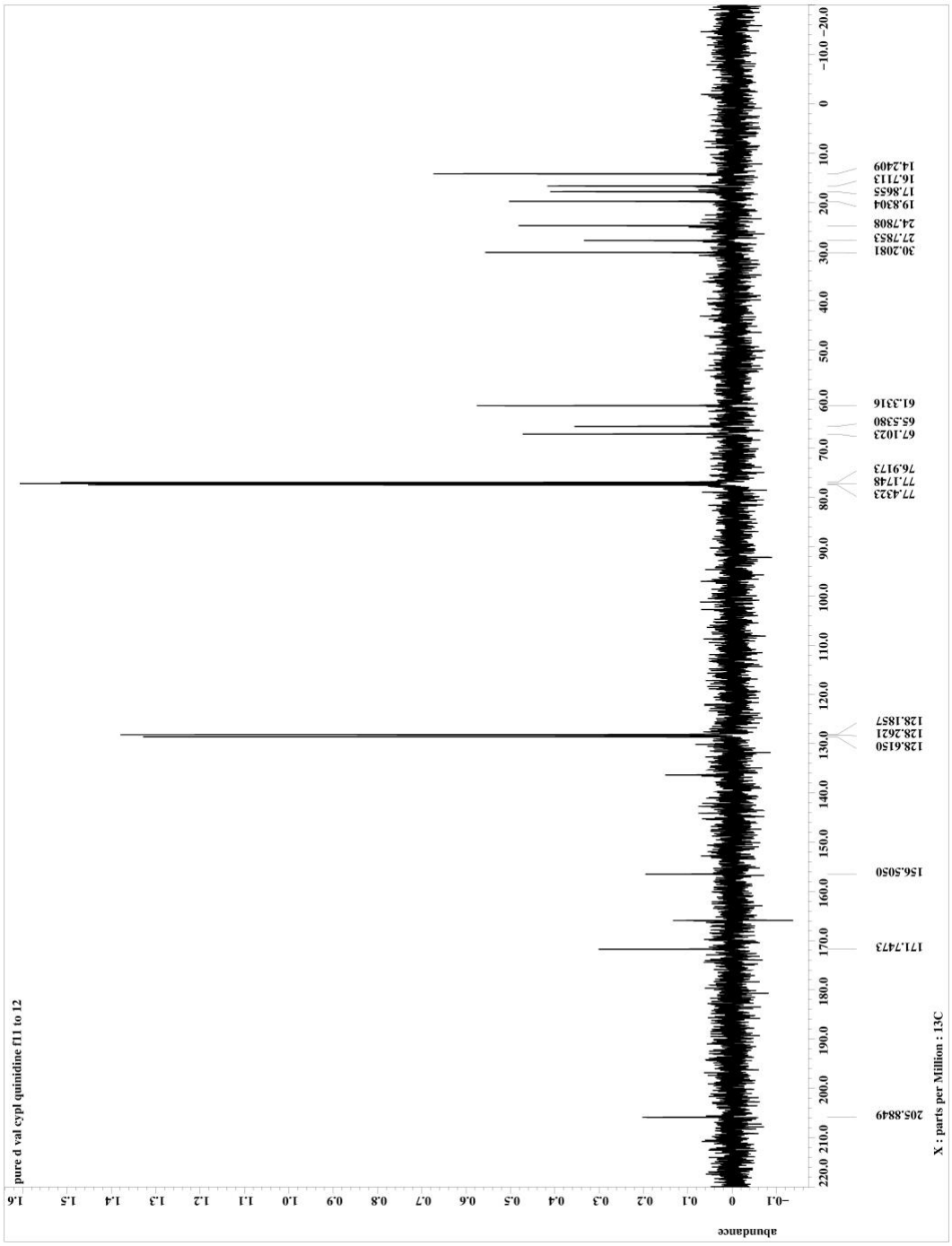
pure d val cypl quinidine f11 to 12
X : parts per Million : 13C
abundance
205.8849
171.7473
156.5050
128.6150
128.2621
128.1857
77.4323
77.1748
76.9173
67.1023
65.5380
61.3316
30.2081
27.7853
24.7808
19.8304
17.8655
16.7113
14.2409